Exploring the biosynthetic pathways of glutamate and benzoate in *Syntrophus aciditrophicus*

Dissertation

zur

Erlangung des Doktorgrades

der Naturwissenschaften

(Dr. rer. nat.)

dem

Fachbereich Biologie

der Philipps-Universität Marburg

Vorgelegt von

Marie Kim

aus Daegu, Republic of Korea

Marburg/Lahn, Germany 2011

Die Untersuchungen zur vorliegenden Arbeit wurden von September 2007 bis Juni 2011 im Laboratorium für Mikrobiologie, Fachbereich Biologie, der Philipps-Universität Marburg unter der Leitung von Prof. Dr. W. Buckel durchgeführt.

Vom Fachbereich Biologie

der Philipps-Universität Marburg

als Dissertation am 06. 07. 2011 angenommen.

Erstgutachter: Prof. Dr. Wolfgang Buckel

Zweitgutachter: Prof. Dr. Johann Heider

Tag der mündlichen Prüfung am: 07. 07. 2011

Contents

Abbreviations

DTNB	5,5'-Dithiobis(2-nitrobenzoate)
DTT	Dithiothreitol
DTE	1,4-Dithioerythritol
FAD	Flavin Adenine Dinucleotide
MALDI-TOF	Matrix-Assisted Laser Desorption Ionization – Time of Flight
TEMED	N,N,N',N'-Tetramethylethylenediamine
Rcs	*Re*-citrate synthase
Gcd	Glutaconyl-CoA decarboxylase
Rnf	NAD^+:ferredoxin oxidoreductase (also involved in *Rhodobacter* nitrogen fixation)

Zusammenfassung

In syntrophischer Lebensweise oxidiert *Syntrophus aciditrophicus* Benzoat zu Acetat und CO_2, während axenische Kulturen Crotonat zu Acetat und Cyclohexancarboxylat mit etwas Benzoat fermentieren. Genomische, proteomische und metabolische Analysen lassen vermuten, dass Abbau und Synthese von Benzoat mit Glutaconyl-CoA als zentralem Intermediat den gleichen Weg benutzen. In strikt anaeroben Bakterien wird Glutamat üblicherweise aus zwei Acetyl-CoA über Pyruvat, Oxalacetat, Citrat und 2-Oxoglutarat synthetisiert. Da im Genom von *S. aciditrophicus* kein Gen für *Si*-Citrat-Synthase gefunden wurde, vermuteten wir, dass Glutaconyl-CoA über 2-Hydroxyglutarat der Vorläufer von Glutamat sein könnte.

Kürzlich wurde gezeigt, dass das *rcs*-Gen, das als Isopropylmalat/ Citramalat/ Homocitrat-Synthase annotiert ist, 49% Sequenzidentitäten mit dem *Re*-Citrat-Synthase-Gen aus *Clostridium kluyveri* aufweist. Wir haben deshalb das *rcs*-Gen kloniert und das rekombinante und mit einem C-terminalen Strep-tag versehene Protein in *Escherichia coli* überproduziert. Das Enzym wurde zur Homogenität gereinigt und mittels ^{14}C-Markierung als *Re*-Citrat-Synthase charakterisiert. Die höchste spezifische Aktivität wurde mit Oxalacetat und Acetyl-CoA in Gegenwart von Co^{2+} erzielt. Pyruvat, 2-Oxoglutarat und 2-Oxoisovalerat konnten Oxalacetat nicht ersetzen; mit Propionyl-CoA war das Enzym ebenfalls inaktiv. Das reine Protein enthielt keine Metallionen; Co^{2+} oder auch Mn^{2+} waren nicht nur für die Aktivität notwendig sondern erhöhten auch die Stabilität. Obwohl Thiolreagenzien das Enzym partiell inaktivierten, scheint ein Cysteinrest nicht an der Katalyse beteiligt zu sein. Mit [$^2H_3$]Acetyl-CoA wurde ein geringer intermolekularer Isotopeneffekt (k_H/k_D = 1.4) gemessen. Vorläufige Versuche mit nativer Gelelektrophorese zeigen, dass das Enzym eine homodimere Struktur besitzt.

Isotop-markierte Glutamate und Aspartate wurden aus *S. aciditrophicus*-Zellen isoliert, die axenisch auf unmarkiertem Crotonat mit [1-^{14}C]Acetat oder $^{13}CO_2$ gewachsen waren. Die Aminosäuren wurden entweder oxidativ decarboxyliert und über ihre Radioaktivität oder mittels ^{13}C-NMR analysiert. Zusammen mit GC-MS-Daten der Universitäten Oklahoma und Washington, die [1-^{13}C]Acetat benutzten, unterstützen unsere Ergebnisse eine Beteiligung der *Re*-Citrat-Synthase, obwohl eine unvollständige Äquilibrierung zwischen markiertem Acetat und ummarkiertem Crotonat in Betracht gezogen werden muss. Leider können die Wege über *Re*-Citrat-Synthase und Glutaconyl-CoA nicht allein durch Isotopenmarkierung unterschieden werden.

Um die postulierte Reversibilität der Energie-konservierenden Glutaconyl-CoA-Decarboxylase (Gcd) zu untersuchen, insbesondere ob die Carboxylierung von Crotonyl-CoA durch einen elektrochemischen Na^+-Gradienten getrieben wird, klonierten wir die im Genom von *S. aciditrophicus* vorhanden Gene *gcdA*, *gcdB* und *gcdC*. Die abgeleiteten Aminosäuresequenzen zeigen 52%, 51%, 46% und 42% Identitäten zu GcdA, B, C1 und C2 von *Clostridium symbiosum*, obwohl die (A+P) reiche Domäne von GcdC und *gcdD* fehlen. Die *S. aciditrophicus*-Gene wurden einzeln oder in den Kombinationen *gcdAC* und *gcdABC* in *E. coli* exprimiert. Nur GcdA, GcdC, und GcdAC konnten erfolgreich produziert werden. GcdA wurde als Carboxytransferase charakterisiert (2 mU/mg mit 5 mM Biotin als artifiziellem Akzeptor). Die Reinigung des Decarboxylase-Komplexes mittels Avidin-Affinitätschromatographie aus *S. aciditrophicus*-Zellen, die von einem Fermenter aus Leipzig stammten, war nicht erfolgreich. Zur Untersuchung der Mechanismus des durch Decarboxylierung getriebenen Na^+-Transports, wären systematische Expressionsstudien von *gcdB* und eine Kristallisation des Komplexes erforderlich. Möglicherweise erleichtert das Fehlen der Aggregate verursachenden (A+P)-reichen Domäne von GcdC diese Aufgabe.

Summary

Syntrophus aciditrophicus thrives syntrophically on benzoate and axenically on crotonate, which is oxidized to acetate and reduced to cyclohexane carboxylate and some benzoate. Genomic, proteomic, and metabolic analyses suggested that degradation and synthesis of benzoate use the same pathway, whereby glutaconyl-CoA serves as central intermediate. In strictly anaerobic bacteria, glutamate is usually synthesized from two acetyl-CoA via pyruvate, oxaloacetate, citrate, and 2-oxoglutarate. As no gene for *Si*-citrate synthase has been detected in the genome of *S. aciditrophicus*, we speculated that glutaconyl-CoA via 2-hydroxyglutarate could be the precursor of 2-oxoglutarate for glutamate biosynthesis.

Recently, the gene *rcs*, which is annotated as isopropylmalate/citratemalate/homocitrate synthase in *S. aciditrophicus*, has been shown to exhibit 49% sequence identity with that coding for *Re*-citrate from *Clostridium kluyveri*. We cloned *rcs* and overproduced the recombinant protein in *Escherichia coli*. The enzyme was purified aerobically and characterized biochemically as *Re*-citrate synthase. The highest achieved specific activity was 1.6 U/mg using oxaloacetate and acetyl-CoA as substrates in the presence of Co^{2+}. Pyruvate, 2-oxoglutarate and 2-oxoisovalerate could not replace oxaloacetate; with propionyl-CoA also no activity was observed. No metal was detected in the recombinant protein. Besides Co^{2+} also Mn^{2+} stimulates the activity and stabilizes the enzyme. Sulfhydryl reagents partially inactivate the enzyme, but a cysteine residue seems not to be involved in the catalytic site. With [$^2H_3$]acetyl-CoA a low intermolecular deuterium isotope effect (k_H/k_D = 1.4) was measured. Preliminary native PAGE data indicate a homodimeric structure of the enzyme.

Labeled glutamate and aspartate were extracted from *S. aciditrophicus* cells grown on unlabeled crotonate with [1-^{14}C]acetate or $^{13}CO_2$ and analyzed by oxidative decarboxylation and its radioactivity or by ^{13}C-NMR, respectively. Together with GC-MS data from the universities of Oklahoma and Washington using [1-^{13}C]acetate, the present results support the idea that *Re*-citrate synthase participates in glutamate biosynthesis, although an incomplete equilibration between labeled acetate and unlabeled crotonate must be considered. Unfortunately, the labeling pattern of glutamate derived from acetate via pyruvate, oxaloacetate and citrate cannot solely be distinguished from that via glutaconyl-CoA and 2-hydroxyglutarate.

To study the proposed reversibility of the energy conserving glutaconyl-CoA decarboxylase (Gcd), especially whether the carboxylation of crotonyl-CoA is driven by an electrochemical Na^+ gradient, we cloned the genes *gcdA*, *gcdB*, and *gcdC* detected in the genome of *S. aciditrophicus*. The deduced amino acid sequences show 52%, 51%, 46% and 42% identity to GcdA, B, C1 and C2 from *Clostridium symbiosum*, respectively, though the (A+P) rich domain of GcdC is missing and a gene for GcdD could not be detected. The *S. aciditrophicus* genes were expressed individually and in the combinations of *gcdAC* and *gcdABC* in *E. coli*, whereby only the productions of GcdA, GcdC, and GcdAC were successful. GcdA was characterized as carboxytranserase (2 mU/mg with 5 mM D-biotin as artificial acceptor). Purification of the decarboxylase complex by avidin affinity chromatography from *S. aciditrophicus* cells, grown in a fermenter in Leipzig, was not successful. To uncover the mechanism of transferring Na^+ and CO_2 in Gcd, a systematic approach of membrane protein overproduction and crystallization should be attempted. Perhaps the lack of the aggregate-forming (A+P) rich domain of GcdC facilitates crystallization.

Introduction

1. Anaerobic food chain and syntrophic metabolism

1.1 Anaerobic food chain

The diversity of metabolic pathways is one of the most fascinating aspects of microbiology. Anaerobic bacteria of the orders Clostridiales (Firmicutes, phylum Bacteria XIII) and Fusobacteriales (Fusobacteria, phylum Bacteria XXI) (Garrity, 2001) and few other anaerobes are able to use amino acids as energy substrates (Barker, 1961; Boone et al, 2001; Jackins & Barker, 1951). They occur in soil, sewage sludge, marine and freshwater sediments and in the gastrointestinal tract of animals. In these anoxic environments, the bacteria participate in the anaerobic food chain, in which polymers such as proteins are degraded to methane and CO_2. The proteins are hydrolyzed by exogenous proteases to small peptides and single amino acids. These are consecutively fermented to ammonia, CO_2, acetate, short chain fatty acids and molecular hydrogen. Acetogenic organisms use the CO_2 and H_2 for the synthesis of acetate. Syntrophic bacteria oxidize the short chain fatty acids and aromatic compounds to acetate, CO_2 and H_2. This process is thermodynamically possible only if methanogenic archaea keep the partial pressure of H_2 at very low values, by reducing CO_2 to methane.

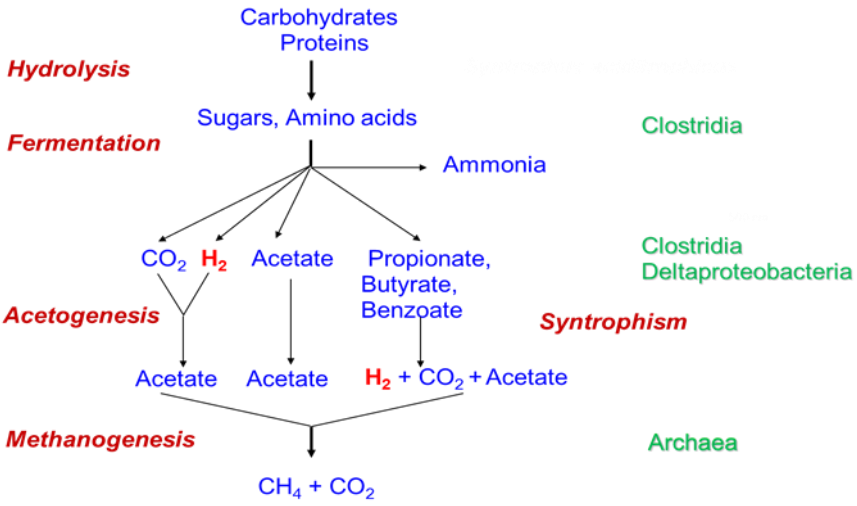

Fig. 1. Anaerobic food chain – fermentation of sugars and amino acids.

1.2 Syntrophism and the global carbon cycle

Fermentative anaerobes conserve energy from glutamate via five different pathways (Buckel, 2001b). Besides these pathways, there are two more catabolic routes leading to ammonia, hydrogen, CO_2 and either acetate or propionate. These routes can only occur in syntrophic cocultures with methanogens to maintain the very low partial pressure of molecular hydrogen of about 1 Pa. Bacteria capable of syntrophic metabolism exist on minimal energy budgets using reactions that proceed close to thermodynamic limits. Syntrophic metabolism requires interspecies interactions, where the degradation of a substrate by one species is made thermodynamically possible by end product (hydrogen or formate) removal by another species.

The term, 'syntrophism' is different from 'commensalism' and 'metabiosis' and should be restricted to those cooperations in which both partners depend entirely on each other in their metabolic activity. This mutual dependence on each other cannot be overcome by simply adding a cosubstrate or nutrient. The commensalism means the minimal cooperation between two partners. For example, aerobic and anaerobic bacteria live in the same habit. The anaerobes profit from the activities of the aerobes, but the aerobes obtain no significant advantage or disadvantage. If such a commensalistic cooperation occurs in the food chain, it is called 'metabiosis'.

The discovery of a syntrophic interaction was *Methanobacillus omelianskii* which ferments ethanol to methane (Barker, 1939). Bryant et al. showed, however, that the *M. omelianskii* culture was in fact a coculture of two organisms, the S organism and *Methanobacterium bryantti* strain M.O.H (Bryant et al, 1967). The S organism fermented ethanol to acetate and hydrogen: $2\ CH_3CH_2OH + 2\ H_2O \rightarrow 2\ CH_3COOH + 4\ H_2$ ($\Delta G^{\circ\prime} = +19$ kJ per 2 mol ethanol). The methanogen could not use ethanol but H_2 made by the S organism to reduce CO_2 to CH_4: $4\ H_2 + CO_2 \rightarrow CH_4 + 2\ H_2O$ ($\Delta G^{\circ\prime} = -131$ kJ per mol of CH_4). When the two reactions are combined, the degradation of ethanol becomes favorable: $2\ CH_3CH_2OH + CO_2 \rightarrow 2\ CH_3COOH + CH_4$ ($\Delta G^{\circ\prime} = -112$ kJ per mol of CH_4).

By comparing the 16S rRNA gene sequences of bacteria capable of syntrophic metabolism it reveals that many of these microorganisms belong to the Deltaproteobacteria and the low G+C Gram-positive bacteria, the Firmicutes. Another syntrophic relationship has been suggested to exist between methane-oxidizing Archaea and sulfate-reducing bacteria, which are in close physical association (Boetius et al, 2000; McInerney et al, 2008).

Ecologically, syntrophic bacteria are key links in the anoxic part of the carbon cycle. Syntrophs use the fermentation products of primary fermenters such as clostridia, and release a key product for methanogens, acetogens, and other H_2 consumers. Without syntrophs, a bottleneck would develop in anoxic environments in which alternative electron acceptors other than CO_2 were limiting. On the other hand, when conditions are oxic or alternative electron acceptors abundant, for example O_2 or NO_3^-, syntrophic relationships are not necessary. Because these electron acceptors create the energetics of the oxidation of a fatty acid so favorable, syntrophic cooperation is not needed. Therefore, syntrophy is characterized in anoxic processes in which (1) the energy available is only very small, (2) one or more products are continually removed, and (3) the organisms are highly specialized for exploiting energetically marginal reactions.

1.3 *Syntrophus aciditrophicus* SB

S. aciditrophicus strain SB^T (ATCC 700169^T) was isolated from a benzoate-degrading enrichment culture obtained from a secondary anaerobic digester sludge from the municipal sewage treatment plant in Norman, Oklahoma, USA (Hopkins et al, 1995). The name "a.ci.di.tro'phi.cus." is derived from the Latin *acidum* as acid; *trephein* in Greek as to feed*; trophicus* in Latin as suffix relating to feeding. Thus, the name means that one feeds on acids, acid feeding. The strain is a strictly anaerobic, Gram-negative, non-motile, non-sporeforming, rod-shaped bacterium which degrades benzoate and certain fatty acids in syntrophic association with hydrogen/formate-using microorganisms. This strain produced approximately 3 mol of acetate and 0.6 mol of methane per mol of benzoate in coculture with *Methanospirillum hungatei* strain JF1. In coculture with *Desulfovibrio* strain G11, saturated fatty acids, some unsaturated fatty acids, and methyl esters of butyrate and hexanoate also support growth of the strain. Crotonate is a substrate in pure axenic culture producing acetate, butyrate, caproate, and hydrogen. The generation time has been reported as 24 – 50 h with low yield. The analysis of the 16S rRNA gene sequence placed the strain in the δ-subdivision of the Proteobacteria, together with sulfate reducing bacteria (Jackson et al, 1999).

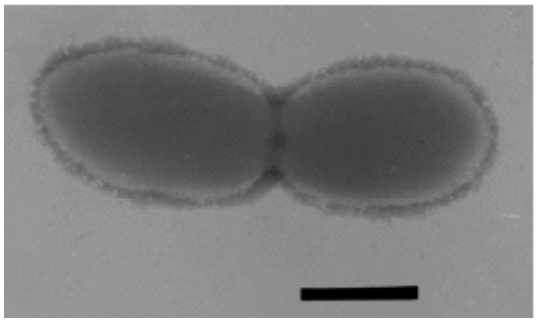

Fig. 2. Transmission electron micrograph of negatively stained whole cells of *S. aciditrophicus* strain SB^T (Bar 500 nm) (Jackson et al, 1999)**.**

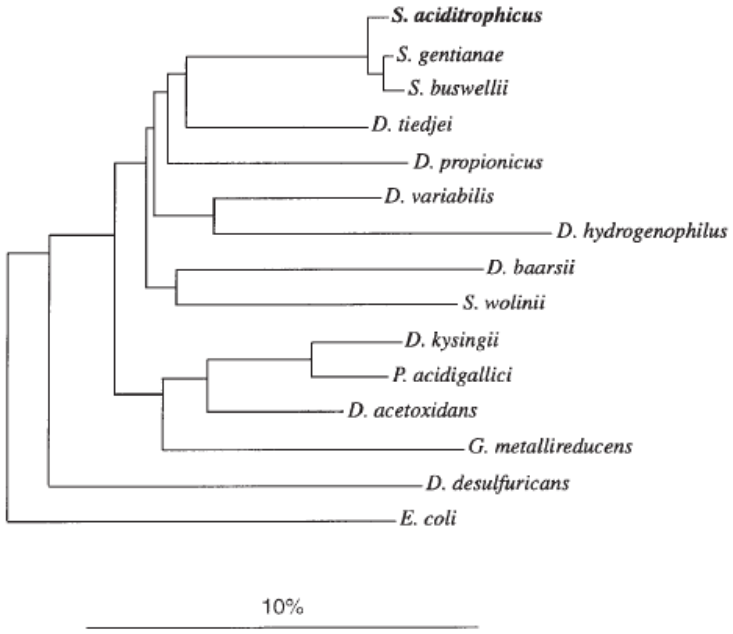

Fig. 3. Phylogenetic relationship of strain *S. aciditrophicus* strain SB^T to bacteria in the δ-subclass of the Proteobacteria (Jackson et al, 1999)**.** Complete species names are*: Sytrophus gentianae* HQGö1^T (X85132), *Syntrophus buswellii* DM-3^T, *Desulfomonile tiedjei* DCB-1^T, *Desulfobulbus propionicus* Lindhorst^T, *Desulfosarcina variabilis* Montepellier^T, *Desulfobacter hydrogenophilus* AcRS1^T, *Desulfoarculus baarsii* 2st14^T, *Syntrophobacter wolinii* DSM 2805^T, *Desulfuromusa kysingii* Kysw2^T, *Pelobacter acidigallici* MaGal2^T, *Desulfuromonas acetoxidans* 11070^T, *Geobacter metallireducens* GS-15^T, *Desulfovibrio desulfuricans* ATCC 27774, and *Escherichia coli* K-12. The bar represents 10% estimated sequence divergence.

The genome of *S. aciditrophicus* has been sequenced (McInerney et al, 2007). The genome contains 3,179,300 base pairs and 3,169 genes where 1,618 genes were assigned putative functions. Metabolic reconstruction of the gene revealed that most biosynthetic pathways of a typical Gram-negative microorganism were present. The presence of a unique

Rnf-type ion-translocating electron transfer complex, menaquinone, and membrane-bound Fe-S proteins associated with heterodisulfide reductase domains suggest the reverse electron transport which is needed for syntrophic metabolism. Although the genomic analysis provides insights of metabolic and regulatory commitment to a nonconventional mode of life, still biochemical and metabolic approaches are required to understand the carbon and energy flow of the organism. For example, the genomes revealed unexpected features of metabolism such as multiple gene copies for many of the key enzymes for pathways leading to acetate formation from fatty and aromatic acids such as acetyl-CoA synthetase (AMP-forming) genes and genes for β-oxidation (acyl-CoA dehydrogenase and acetyl-CoA acetyltransferase (thiolase) genes) dispersed throughout the chromosome.

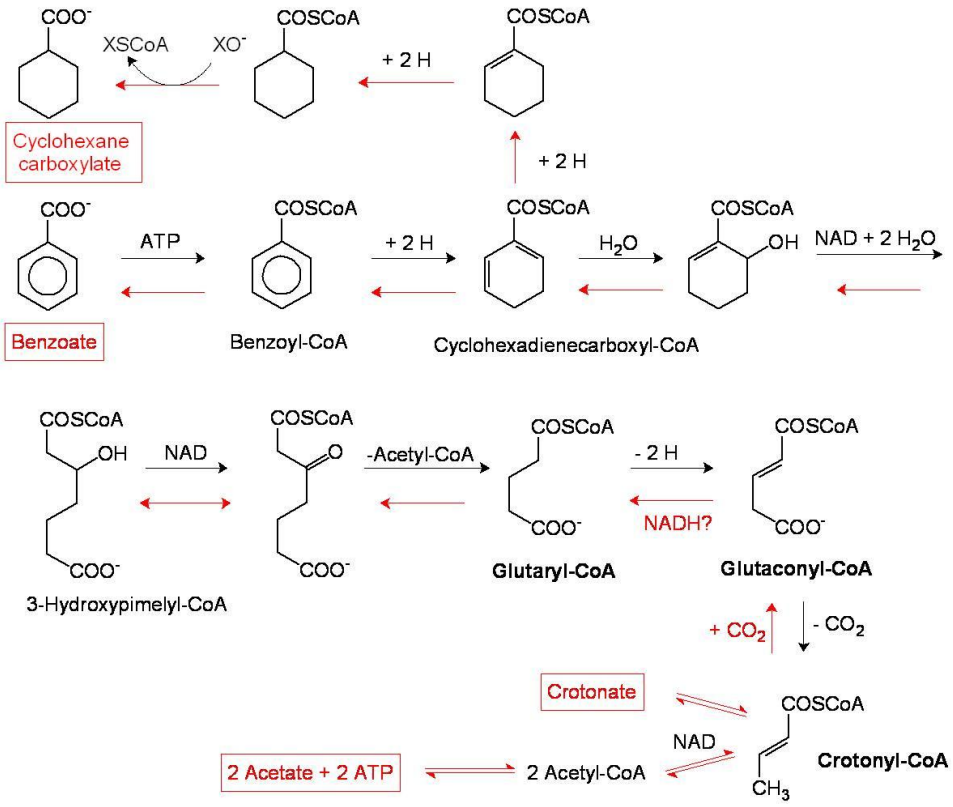

Fig. 4. Benzoate fermentation in *S. aciditrophicus*. The depicted scheme is based on physiological genomic analyses

The benzoate metabolism in *S. aciditrophicus* is not fully understood. It is not clear why cyclohex-1-ene-1-carboxylate and cyclohexane carboxylate are accumulated during syntrophic benzoate metabolism (Elshahed et al, 2001). Genes similar to those discovered in

Geobacter metallireducens, which probably code for a ATP-independent benzoyl-CoA reductase, also are found in denitrifiers and photosynthetic bacteria (Wischgoll et al, 2005). *S. aciditrophicus* contains enzymes needed to convert cyclohex-1,5-diene carboxyl-CoA to 6-hydroxycyclohex-1-ene carboxyl-CoA, and for 6-oxocyclohex-1-ene carboxyl-CoA to 3-hydroxypimelyl-CoA (Kuntze et al, 2008; Peters et al, 2007). In pure culture, *S. aciditrophicus* can ferment benzoate either alone to acetate and cyclohexane carboxylate (Elshahed & McInerney, 2001) as well as together with crotonate as the electron donor (Mouttaki et al, 2008). Moreover, *S. aciditrophicus* is able to form cyclohexane carboxylate grown on crotonate alone (Mouttaki et al, 2007). At the moment, it is speculated that *S. aciditrophicus* uses a pathway for the synthesis of cyclohexane carboxylate from acetate intermediates derived from crotonate by reversing the route used for anaerobic benzoate oxidation.

2. Fermentation and biosynthesis of glutamate

2.1 Fermentation of glutamate

Eukaryotes and many bacteria are only able to degrade glutamate via 2-oxoglutarate followed by further oxidation in the tricarboxylic acid cycle (TCA cycle). In anoxic habitats, the orders of Clostridiales and Fusobacteriales and some other anaerobes participate in the anaerobic food chain, where finally polymers such as proteins are degraded to methane and carbon dioxide. Among 20 proteinogenic amino acids, glutamate may be degraded to fatty acids by at least five different pathways, most of which contain radical enzymes (Buckel, 2001b). The first two pathways proceed to ammonia, acetate and pyruvate via the coenzyme B_{12}-dependent glutamate mutase. The enzyme catalyzes the re-arrangement of the linear carbon skeleton to the branched-chain amino acid (2*S*,3*S*)-3-methylaspartate, which further degraded to acetate and pyruvate. Then pyruvate disproportionates either to CO_2 and butyrate or to CO_2, acetate and propionate. The third pathway via 2-hydroxyglutarate is described below. The remaining two pathways demand more than one organism for the complete catabolism of glutamate to short chain fatty acids. For example, glutamate is decarboxylated to 4-aminobutyrate, which is fermented by a second organism to acetate and butyrate by an unusual dehydratase that catalyzes the reversible dehydration of 4-hydroxybutyryl-CoA to crotonyl-CoA. The last fifth pathway is the only one without decarboxylation, because the γ-carboxylate of glutamate is

reduced to the amino group of δ-aminovalerate, which is then further fermented to acetate, propionate and valerate.

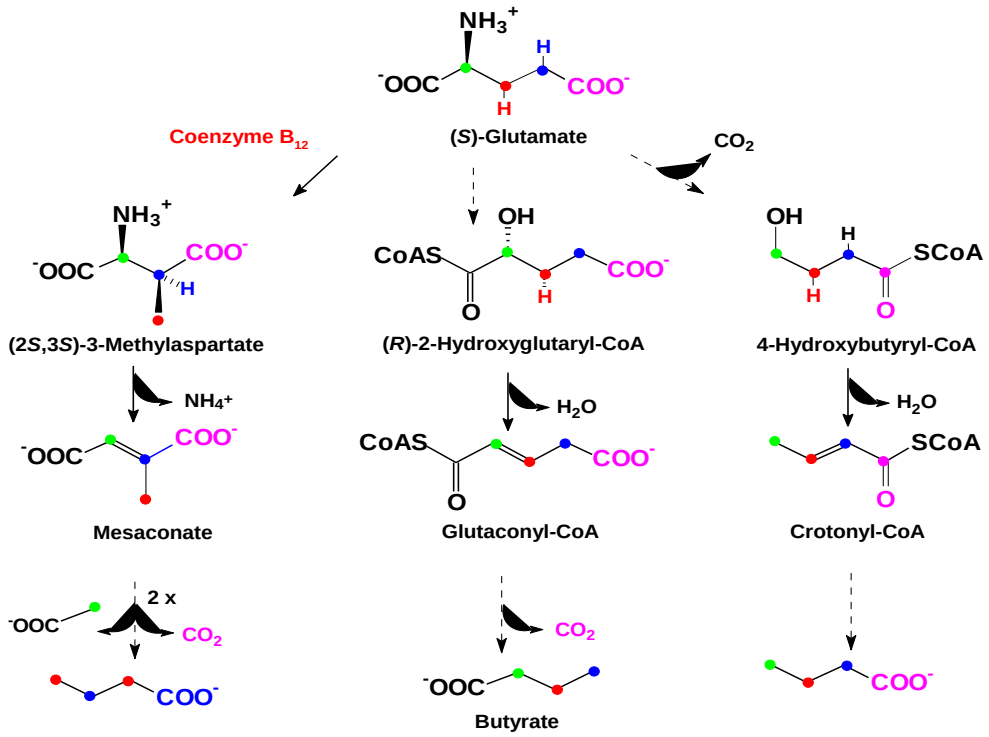

Fig. 5. Three pathways leading from (*S*)-glutamate to butyrate in Clostridiales. They can easily be distinguished by using isotopically labeled glutamates and characterization of enzymes.

2.2 2-Hydroxyglutarate pathway

The 2-hydroxyglutarate pathway is found in organisms living in anoxic environments within humans and animals, for example, *Acidaminococcus fermentans*, *Clostridium sporosphaeroides*, *Clostridium symbiosum*, *Fusobacterium nucleatum* and *Peptostreptococcus asaccharolyticus* (Buckel, 1980a; Buckel & Barker, 1974). These organisms ferment glutamate via (*R*)-2-hydroxyglutaryl-CoA, glutaconyl-CoA and crotonyl-CoA. The latter diproportionates to acetate, butyrate and H_2. In this 2-hydroxyglutarate pathway, the extra energy is conserved via $\Delta\mu Na^+$ generated by decarboxylation of glutaconyl-CoA (Buckel, 2001b).

$$5\ \text{Glutamate-} + 6\ H_2O + 2\ H^+ \rightarrow 5\ NH_4^+ + 5\ CO_2 + 6\ \text{Acetate-} + 2\ \text{Butyrate-} + H_2;$$

$$\Delta G' = -59\ \text{kJ mol}^{-1}\ \text{glutamate};\ 70\ \text{kJ mol}^{-1}\ \text{ATP}$$

One of the interesting points of the pathway is that identical products as in the methylaspartate pathway are formed without use of coenzyme B_{12}. Thus the most complicated coenzyme is avoided, whose biosynthesis via the anaerobic pathway requires about 20 different gene products (Scott et al, 1999). The dehydration of (*R*)-2-hydroxyglutaryl-CoA to (*E*)-glutaconyl-CoA is another step to which attention should be paid. This unusual biochemical transformation is carried out by the (*R*)-2-hydroxyglutaryl-CoA dehydratase together with its activator (Buckel, 1980b; Hans et al, 2000; Schweiger et al, 1987). During this dehydration the 3*Si*-proton has to be removed from the non-activated β-position ($pK_a \approx 40$), whereas the hydroxyl anion is released from the α-position. The activation of this proton is achieved by addition of one high energy electron to the thioester carbonyl, forming a ketyl radical that eliminates the hydroxyl group (Fig. 6). It has been shown that the pK_a of the 3*Si*-proton of the resulting enoxy radical intermediate is lowered by 26 unites (Smith et al, 2003). The radical generator is the ATP dependent activator enzyme, which is initially reduced by ferredoxin or dithionite (Kim et al, 2008). Variations of the remarkable enzyme systems have been found in *C. symbiosum*, *A. fermentans* and *F. nucleatum*. The dehydratase yielded two protein components, the activator (A) and the dehydratase (D). The component D from *C. symbiosum* contains two $[4Fe\text{-}4S]^{2+}$ clusters instead of the one $[4Fe\text{-}4S]^{2+}$ found in *A. fermentans*, even though both component D share 70% sequence identity.

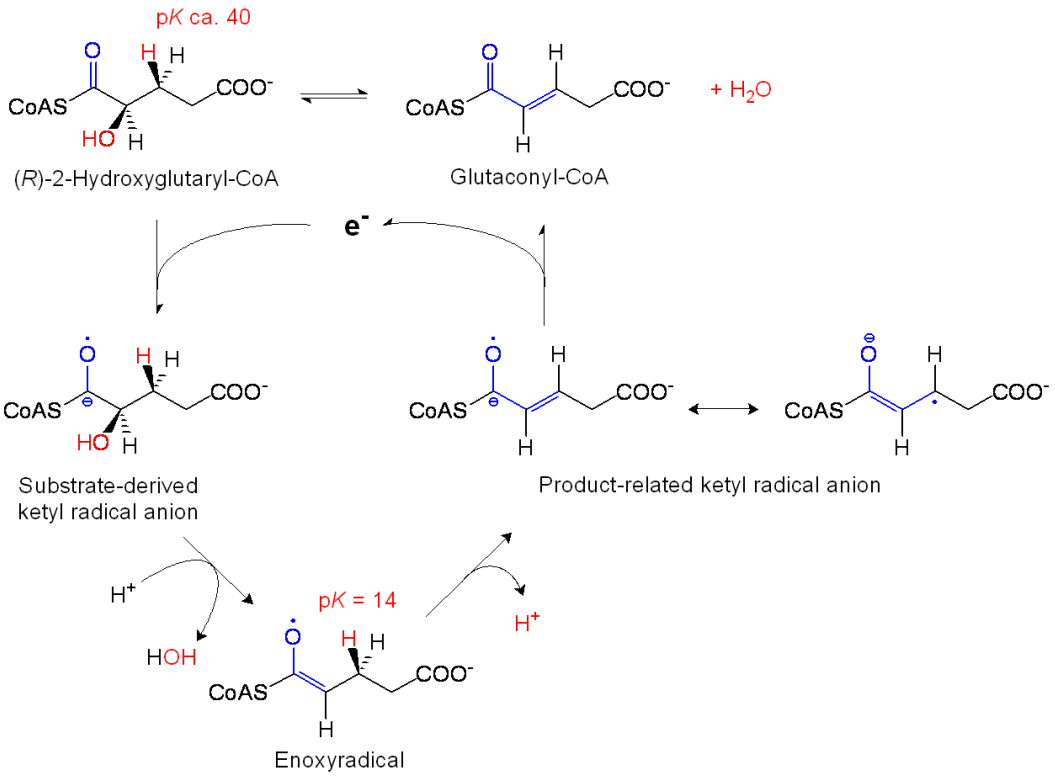

Fig. 6. Proposed mechanism for the dehydration of (*R*)-2-hydroxyacryl-CoA to (*E*)-2-enoyl-CoA by (*R*)-2-hydroxyglutaryl-CoA as an example.

After decarboxylation, the pathway branches in oxidative and reductive parts. Crotonyl-CoA is reduced to butyryl-CoA (E_0´= – 10 mV) by NADH (E_0´= – 320 mV) in the reductive branch. This reduction is highly exergonic and irreversible under physiological conditions ($\Delta G°$´= – 60 kJ mol^{-1}). It is proposed that the reduction is coupled with the exergonic reduction of ferredoxin (E_0´= – 410 mV) with NADH (Herrmann et al, 2008; Li et al, 2008). Two electrons from NADH are bifurcated by the Bcd/Etf complex from anaerobic bacteria. One electron is transferred via butyryl-CoA dehydrogenase to more positive electron acceptor crotonyl-CoA and the other electron is transferred to the more negative acceptor ferredoxin (Fd → Fd^{-}). The next NADH carries the electrons for complete reduction of crotonyl-CoA to butyryl-CoA and Fd^{-} to Fd^{2-}. The reduced ferredoxin can be re-oxidized either by NAD^+ catalyzed by Rnf with generation of $\Delta\mu H/Na^+$ or by protons mediated by a hydrogenase with the formation of molecular hydrogen. Crotonyl-CoA is hydrated to 3-hydroxybutyryl-CoA and oxidized to acetoacetyl-CoA and two acetates together with ATP are produced at the end in the oxidative branch

2.3 Biosynthesis of glutamate and the TCA cycle

Protein, the major cell constituent, is composed of the 20 natural L-amino acids. The pathways for the biosynthesis of these amino acids are diverse. But the important common feature is that their carbon skeletons come from intermediates of glycolysis, the pentose phosphate pathway, or the TCA cycle. Moreover, all amino acids are derived from only a few central precursor metabolites. For example, three α-ketoacids (α-oxoglutarate, oxaloacetate, and pyruvate) can be converted into amino acids in one step through the addition of an amino group (Fig. 7). Alanine and aspartate are synthesized by the transamination of pyruvate and oxaloacetate, respectively. Glutamate is synthesized by the reductive amination of 2-oxoglutarate catalyzed by glutamate dehydrogenase. Glutamine is synthesized from NH_4^+ and glutamate, and asparagine is synthesized similarly. Among these various pathways, in this study we focus mainly on glutamate derived from 2-oxoglutarate which is an intermediate of TCA cycle.

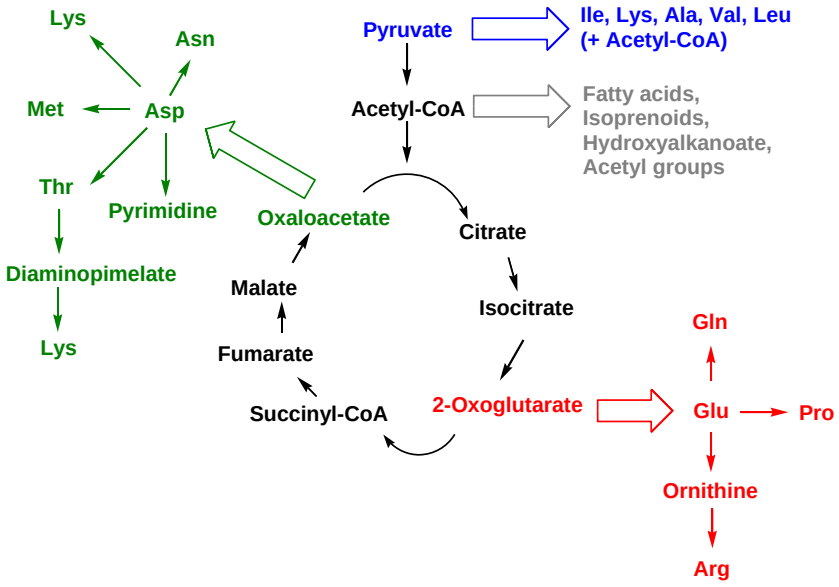

Fig. 7. Formation of building blocks from central intermediates of carbon metabolism around the TCA cycle.

In 1937, Hans Krebs summarized the evidence for a cyclic sequence of reactions in pigeon breast muscle, which he named the citric acid cycle and which could explain the complete oxidation of pyruvate to 3 CO_2 (Krebs & Johnson, 1980; Thauer, 1988). Up to now, it is generally regarded that the TCA cycle is an energy acquisition pathway by oxidation of

carbohydrates that is widely distributed in aerobic organisms. Most of the TCA cycle enzymes are also found in anaerobes where a part of the TCA cycle operates in an oxidative or reductive direction. The reductive TCA cycle is known as one of the CO_2-fixing pathways (Hugler et al, 2005) and has been proposed to be the earliest autotrophic pathway. The genomic perspective of variation of the TCA cycle shows that in incomplete cycles, the last part of the oxidative cycle, leading from succinate to oxaloacetate, is the most highly conserved, whereas the initial steps, from acetyl-CoA to 2-oxoglutarate, show the least conservation (Huynen et al, 1999). The TCA cycle is important for generation of intermediates for anabolic pathways. Specifically, 2-oxoglutarate, oxaloacetate and succinyl-CoA are starting points for the synthesis of glutamate, aspartate and porphyrin, respectively. The autotrophic species, which have incomplete cycles, are still able to generate these three compounds from pyruvate. In autotrophic bacteria, 2-oxoglutarate is generated from pyruvate via the oxidative branch of the TCA cycle, whereas the methanogenic Archaea and *Archaeoglobus fulgidus* generate it via the reductive branch.

2-Oxoglutarate, a direct precursor for glutamate biosynthesis, could be achieved by either via isocitrate dehydrogenase (EC 1.1.1.42) or 2-oxoglutarate synthase (EC 1.2.7.3) in the TCA cycle. Isocitrate dehydrogenase catalyzes the oxidative decarboxylation of isocitrate, producing 2-oxoglutarate and CO_2 by converting $NAD(P)^+$ to NAD(P)H. The 2-oxoglutarate synthase mediates the reaction: 2-oxoglutarate + CoA + 2 Fd_{ox} = succinyl-CoA + CO_2 + 2 Fd_{red}.

There are two different enzymes convert 2-oxoglutarate to glutamate. The glutamate synthase (NADPH) (EC 1.4.1.13) catalyzes the reductive amination of 2-oxoglutarate with the use of glutamine as the nitrogen donor: 2-oxoglutarate + glutamine + NADPH + H^+ = 2 glutamate + $NADP^+$. The glutamate dehydrogenase (EC 1.4.1.2) converts glutamate to 2-oxoglutarate, and vice versa: NH_4^+ + 2-oxoglutarate + NADPH + $2H^+$ = glutamate + $NADP^+$ + H_2O. In genome of *S. aciditrophicus*, the genes for glutamate synthase (SYN_00363, SYN_01629, SYN_01630, SYN_01631, SYN_02385) and glutamate dehydrogenase (SYN_02382, SYN_01242) as well as isocitrate dehydrogenase (SYN_01410) and 2-oxoglutarate synthase subunits (SYN_02498, SYN_02499) are present.

3. Mechanism of citrate synthase and its stereospecificity

Citrate synthase (*Si*-specific EC 2.3.3.1, *Re*-specific EC 2.3.3.3) catalyzes the first step in the oxidative branch of the TCA cycle in which acetyl-CoA and oxaloacetate are condensed and hydrolysed to generate citrate and CoA. Eukarya, Gram-positive bacteria and Archaea possess a homodimeric form of the enzyme, whereas in the majority of Gram-negative bacteria the citrate synthase is homohexamer (Gerike et al, 1998; Wiegand & Remington, 1986). The reaction is a aldol condensation consisting of two half reactions (Kurz et al, 2009; Man et al, 1994; Petterson et al, 1989): the mechanistically intriguing condensation of acetyl-CoA with oxaloacetate to form citryl-CoA and the subsequent hydrolysis of citryl-CoA. The condensation reaction requires the abstraction of a proton from the methyl carbon of acetyl-CoA to generate a reactive enolate intermediate. This proton abstraction step is kinetically challenging because carbon acids are weak and have large activation energy barriers. The carbanion of the intermediate then attacks the oxaloacetate carbonyl either from the *Re* or from the *Si*-side to furnish (*R*)- or (*S*)-citryl-CoA, respectively. Citryl-CoA is hydrolyzed to citrate and CoA.

The involvement of citric acid in the TCA cycle was questioned in 1940s. Harland Wood and Earl Evans showed that 2-oxoglutarate synthesized from pyruvate and $^{14}CO_2$ in pigeon liver was almost exclusively labeled in the carboxyl group adjacent to the carbonyl group (Evans & Slotin, 1940). It was generally assumed that enzymes handled compounds like citric acid as a symmetric molecule, at that time. In 1948, Alexander Ogston proposed that both citrate synthase and aconitase could interact with citric acid so that the two $-CH_2$-COOH groups of citric acid do not react identically (Ogston, 1948). It was later shown that the citrate synthase involved in the TCA cycle incorporates acetyl-CoA only into the (*pro-S*) carboxymethyl group and that the aconitase abstracts a hydrogen only from the (*pro-R*) carboxymethyl group of citrate (Hanson & Rose, 1963; Rose & O'Connell, 1967). The citrate synthase with this stereospecificity has been referred to as *Si*-citrate synthase. The work of Ogston was the start of the branch of stereochemistry of compounds that behave like citrate. (Cornforth, 1976).

Tomlinson demonstrated (Tomlinson, 1954) that the origin of the carbon atoms in glutamate synthesized in *C. kluyveri* grown on ^{14}C-labeled ethanol, acetate, and CO_2 was unusual and was confirmed later (Jungermann et al, 1968). Gottschalk and Barker showed that this anaerobic bacterium contains a *Re*-citrate synthase (EC 2.3.3.3), which explained the

unusual labeling pattern observed in glutamate (Gottschalk & Barker, 1966). A *Re*-citrate synthase was also found in other anaerobic bacteria, such as *Clostridium acidiurici* (Gottschalk, 1969), *Desulfovibrio vulgaris* (Tang et al, 2007), *Clostridium cylindrosporum*, *Desulfovibrio desulfuricans* and *C. kluyveri* (Gottschalk, 1968; Gottschalk & Barker, 1967; Li et al, 2007). By the isotopomer-assisted metabolite analysis, the presence of putative *Re*-citrate synthase has been reported from Heliobacteria (Tang et al, 2010), *Thermoanaerobacter* sp. (Feng et al, 2009), *Dehalococcoides ethenogenes* (Tang et al, 2009) and *Clostridium acetobutylicum* (Crown et al, 2011). The *Re*-citrate synthase from *C. acidiurici* was partially purified and characterized (Gottschalk, 1969; Gottschalk et al, 1972; Wunderwald et al, 1971). In 2007, the gene encoding *Re*-citrate synthase was identified from *C. kluyveri* and characterized by overproducing the recombinant enzyme in *E. coli* (Li et al, 2007). The *Re*-citrate synthase requires Mn^{2+} or Co^{2+} for activity, is O_2 sensitive, and is inactivated by *p*-chloromercuribenzoate (pCMB), properties unusual for most *Si*-citrate synthases. As there is no significant sequence similarity detected, it is believed that *Si*-citrate synthase and *Re*-citrate synthase are not phylogenetically related. For example, *Si*-citrate synthase is related to citrate lyase, methylcitrate synthase, (*S*)-citramalate lyase and malate synthase. On the other hand, *Re*-citrate synthase is related to homocitrate synthase, citramalate synthase, and isopropylmalate synthase. From this enzyme family only the structure of isopropylmalate synthase is known (Koon et al, 2004); that of *Re*-citrate synthase remains to be established.

4. Energy conservation and glutaconyl-CoA decarboxylase

4.1 Energy conservation via electrochemical ion gradients

In living organism, biological redox reactions are important for the synthesis of energy rich compounds such as adenosine triphosphate (ATP), the universal energy carrier. In general, there are two basic mechanisms in which redox reactions are coupled with the energy conservation: (1) substrate level phosphorylation in which a substrate is oxidized to an energy rich phosphate followed by transfer of the phosphate to ADP; (2) electron transport phosphorylation which converts the electrochemical potential between two redox partners into an electrochemical ion gradient that drives ATP synthesis (Decker et al, 1970). The latter mechanism combines an ATP synthase and a multiple-enzyme electron transport chain integrated in the bacterial membrane, where ATP synthesis is linked to the translocation of

ions ($\Delta\mu H^+$ or $\Delta\mu Na^+$). In aerobic heterotrophic organisms, the electron donor is usually an organic compound such as glucose and the electron acceptor is molecular oxygen. But many bacteria are able to thrive under anoxic conditions and oxygen is replaced with various organic or inorganic compounds as electron acceptors. In most cases, the redox potentials of theses acceptors are much less positive than that of oxygen. This causes smaller energy differences that allow the synthesis of much less ATP. In most catabolic pathways 70 – 80 kJ are required for the formation of 1 mol ATP (Thauer et al, 1977). In acetogenesis and methanogenesis, 1 mol substrate sometimes generates only 20 − 30 kJ. Therefore, substrate phosphorylation is not possible. The organisms have to rely on ion gradient phosphorylation, which can use such small energy increments produced by pumping 1 Na^+ or H^+ through the membrane. After accumulation of 3 − 4 ions one ATP can be formed. turnover in these organisms often is much higher than in aerobic organisms (Lengeler et al, 1999). Unlike aerobes, the anaerobes conserve energy even from reactions, which are neither respirations nor fermentations for example decarboxylations.

4.2 Sodium ion-translocating decarboxylases

Carboxylases and decarboxylases catalyse the formation and cleavage of carbon-carbon bonds with retention of configuration, whereby one partner of the reaction is either bicarbonate or CO_2. In 'Enzyme Nomenclature', 90 enzymes of this class are listed as carboxy lyases (EC 4.1.1). Moreover, there are numerous carboxylases and decarboxylases with concomitant redox reactions, which are found under 'oxidoreductases', e.g. isocitrate dehydrogenase (EC 1.1.1.41 and 42) or pyruvate synthase (EC 1.2.7.1). Carboxylases coupled to hydrolysis of ATP form a distinct small group of six biotin-containing 'carbon-carbon ligases' (EC 6.4.1) (Buckel, 2001a).

Among these carboxylases and decarboxylases, here we consider Na^+-dependent biotin-containing decarboxylases, which catalyze the substitution of a carboxylate in β-position to a keto or thioester group by H^+ ($\Delta G°' = -30$ kJ mol^{-1}). At least four enzyme systems of this type are known:

1. Oxaloacetate decarboxylase from enterobacteria: *Klebsiella pneumonia* (Dimroth, 1982), *Salmonella typhimurium* (Wifling & Dimroth, 1989) and *Vibrio chloerae* (Dahinden et al, 2005)

2. Malonate decarboxylase system from *Malonomonas rubra*

3. Methylmalonyl-CoA decarboxylase from *Veillonella parvula*, *Propionigenium modestum* and *Peptostreptococcus sp*.

4. Glutaconyl-CoA decarboxylase from *A. fermentans*, *F. nucleatum*, *P. asaccharolyticus*, *C. symbiosum*, *Pelospora glutaria* and *Syntrophus gentianaea*

In the first catalytic step, the carboxyl group of the substrate is converted to a kinetically activated carboxylate in *N*-carboxybiotin. After swing-over to the decarboxylase *N*-carboxybiotin is decarboxylated, whereby an electrochemical Na^+ gradient is generated. The free energy of the decarboxylation is used to translocate 2 Na^+ from inside to the outside across the cytoplasmic membrane, whereas the proton comes from the outside (Fig. 8).

4.3 Glutaconyl-CoA decarboxylases

Glutaconyl-CoA, the product of the dehydration of (*R*)-2-hydroxyglutaryl-CoA, is decarboxylated to crotonyl-CoA by glutaconyl-CoA decarboxylase (Gcd). In aerobic organisms and respiring anaerobes this decarboxylation represents the irreversible second half-reaction of the FAD-containing homotetrameric enzyme glutaryl-CoA dehydrognease (Härtel et al, 1993; Schaarschmidt et al, 2011). The energy-limited fermentative bacteria, however, conserve the small amount of free energy of decarboxylation ($\Delta G^{\circ\prime} \approx 30$ kJ mol^{-1}) as an electrochemical Na^+ gradient. Because of generation of a sodium motive force, the decarboxylation should be reversible as observed in vitro by the related Na^+-dependent oxaloacetate and methylmalonyl-CoA decarboxylases (Dimroth & Hilpert, 1984). In *S. aciditrophicus*, it probably happens in vivo because the synthesis of benzoate from crotonate requires carboxylation of crotonyl-CoA to glutaconyl-CoA (Mouttaki et al, 2007).

Glutaconyl-CoA decarboxylase (Gcd) shares features such as its integration into the cytoplasmic membrane, biotin content and the Na^+ dependency of the enzymatic reaction (Buckel, 1986a; Buckel, 1986b) with oxaloacetate decarboxylase from Gammaproteobacteria (Dahinden et al, 2005; Dimroth, 1980) and methylmalonyl-CoA decarboxylases from *V. parvula* (Hilpert & Dimroth, 1982) and *P. modestum* (Bott et al, 1997). Gcd has been intensively characterized from *A. fermentans* (Braune et al, 1999; Buckel & Liedtke, 1986; Buckel & Semmler, 1982; Buckel & Semmler, 1983), *F. nucleatum* (Beatrix et al, 1990) and

from *C. symbiosum* (Buckel & Semmler, 1982; Kress et al, 2009). Gcds consist of 4 – 5 functional domains or subunits; a carboxytrasnferase (α), a 9 – 11 transmembrane helix-containing Na^+-dependent carboxybiotin decarboxylase (β), 1 – 2 mobile alanine and proline-rich biotin carriers (γ) and a membrane anchor (δ) (Fig. 8).

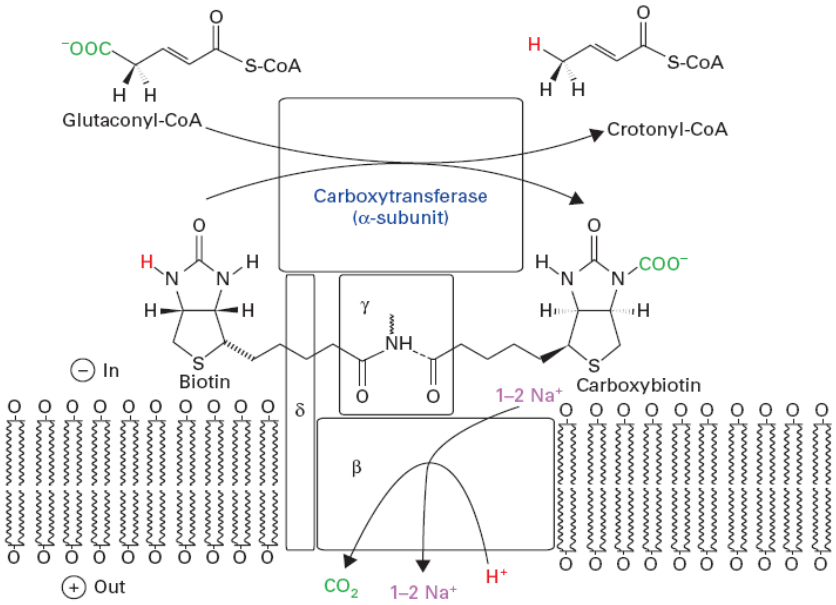

Glutaconyl-CoA + Biotin-GcdC = Crotonyl-CoA + Carboxy-Biotin-GcdC

Carboxy-Biotin-GcdC + H^+ = Biotin-GcdC + CO_2

Fig. 8. Model of glutaconyl-CoA decarboxylase. The array in the lower part of the picture depicts the cytoplasmic membrane, in which the β- and δ-subunits are embedded. This model was adapted from Boiangiu et al, 2005.

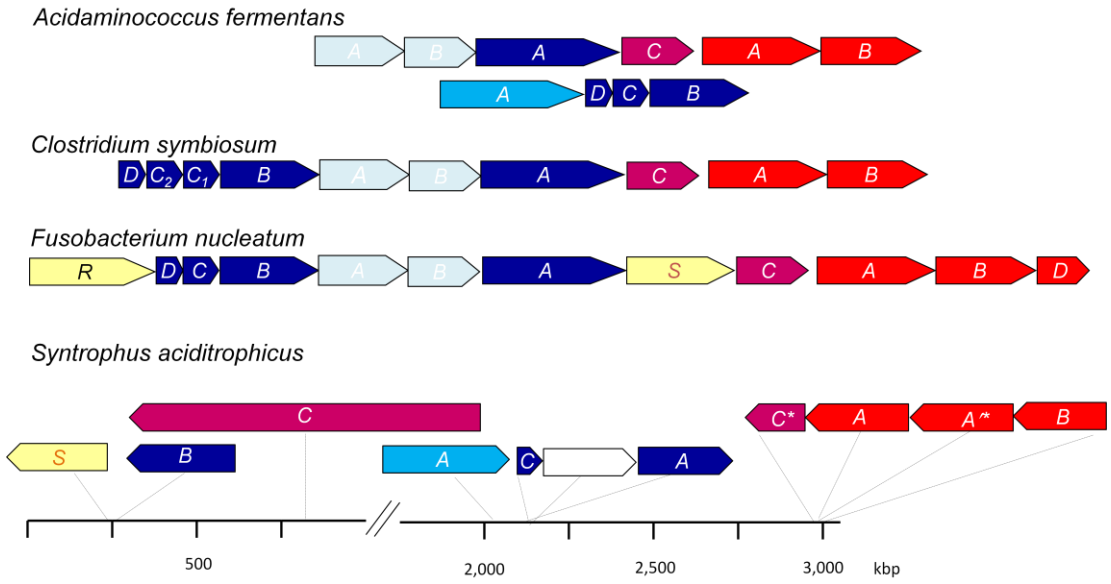

Fig. 9. Arrangement of the genes involved in glutamate fermentation (Kress et al, 2009)**.** Gene cluster of the glutaconyl-CoA decarboxylase genes (*gcd*, dark blue) in *A. fermentans*, *C. symbiosum* and *F. nucleatum*. Further genes encode the glutaconate-CoA transferase (*gct*, pale blue) and 2-hydroxyglutaryl-CoA dehydratase (*hgd*, red) with its activator (*hgdC* or *hgdD*, magenta). Additional genes in *F. nucleatum* code for a regulator *R* and the glutamate/Na^+ symporter S (both in yellow). In *A. fermentans* the *gcdDCB* genes are in a separate locus preceded by the gene of subunit A of methylmalonyl-CoA decarboxylase (*mmdA*, turquoise). In *S. aciditrophicus* the gene of glutaryl-CoA dehydrogenase is depicted as white color.

The gene encoding the α-subunit, *gcdA*, of *A. fermentans* is located in the 2-hydroxyglutarate operon, preceded by *gctAB*, encoding the heterodimeric glutaconate CoA-transferase, and followed by *hgdCAB*, encoding the homodimeric activator protein (HgdC) and the heterodimeric 2-hydroxyglutaryl-CoA dehydratase (HgdAB), respectively. The other three genes *gcdDCB* of the decarboxylase are present in a separate transcription unit preceded by the gene encoding the α-subunit of a methylmalonyl-CoA decarboxylase. In *F. nucleatum* all these genes form one cluster, but are arranged in the same order: *R – gcdDCB – gctAB – gcdA – S – hgdCABD*. *R* encodes a putative regulatory protein and *S* for a glutamate-Na^+-symporter. A similar arrangement of the *gcd* genes involved in glutamate fermentation via 2-hydroxyglutarate pathway is found in *C. symbiosum* (Fig. 9) (Hans et al, 1999; Kress et al, 2009). In *S. aciditrophicus*, genes coding for the decarboxylase are located separately across the chromosome. The *gcdA* is in the downstream of *gcdC* and the gene encoding glutaryl-CoA dehydrogenase which is involved in the subsequent reduction of glutaconyl-CoA to glutaryl-CoA. No gene annotated as glutaconate CoA-transferase was found. The gene encoding the activator of 2-hydroxyglutaryl-CoA dehydratase is located far from the three genes annotated

as benzoyl-CoA reductase/2-hydroxyglutaryl-CoA dehydratase. The size of the monomer (160 kDa) is much bigger than one of the known activators (ca. 22 – 26 kDa). The three genes annotated as benzoyl-CoA reductase/2-hydroxyglutaryl-CoA dehydratase show ca. 35% amino acid sequence identities with 2-hydroxyglutaryl-CoA dehydratase from *Clostridium difficile*. Regarding to homology studies and conserved cystein residues for the iron-sulfur cluster with subunit A and B of 2-hydroxyglutaryl-CoA from *C. difficile*, *C. symbiosum*, *A. fermentans*, *F. nucleatum* and *A. fulgidus*, only two genes (Fig. 9, A and A* in red) might contain iron-sulfur cluster, whereas another gene (Fig. 9, B in red) might not. In the same transcription unit of these three genes, a gene annotated as activator of 2-hydroxyacyl-CoA dehydrtase is present. The deduced amino acid sequence of the gene reveals that 2 cysteins for iron-sulfur cluster of the activator of 2-hydroxyglutaryl-CoA dehydratase are conserved. The gene of the α-subunit of methylmalonyl-CoA decarboxylase is present downstream of *gcdC*, but in a separate transcription unit. Interestingly, as the operon found in *F. nucleatum*, the gene encoding H^+/Na^+-glutamate symport chain is at the upstream of *gcdB*, but the distance between these two genes in the genome is not close.

The carboxyltrasnferase α subunits of Gcd from *A. fermentans* and *C. symbiosum* have been overproduced in *E. coli* and its structures have been solved by X-ray crystallography (Bendrat & Buckel, 1993; Braune et al, 1999; Kress et al, 2009). The GcdA from *A. fermentans* is a homodimer and the N-terminal of domain provides the binding site of glutaconyl-CoA and the C-terminal domain for biotin attached to the carrier. As the CO_2 is transferred from glutaconyl-CoA to subunit 1 to biotin bound on subunit 2, the dimer is a functional unit. Based on these structural evidences, a symmetric model was proposed (Fig. 10, A). GcdA from *A. fermentans* catalyses the transfer of CO_2 from glutaconyl-CoA to GcdC that subsequently is decarboxylated by the carboxybiotin decarboxylation site within the actual Na^+ pump, GcdB. The GcdA from *C. symbiosum* is a homotetramer. This tetrameric assembly was also supported by size exclusion chromatography. The stability of the GcdA tetramer and the presence of the two different biotin-carrier subunits, $GcdC_1$ and $GcdC_2$ led to the asymmetric model (Fig. 10, B). Attempts to crystallize the whole decarboxylase from *A. fermentans* as well as $GcdAC_1$ from *C. symbiosum* failed. Due to the following reasons: (1) the recombinant $GcdAC_1$ subcomplex was not pure enough and (2) the instability and aggregation of GcdC impeded its crystallization.

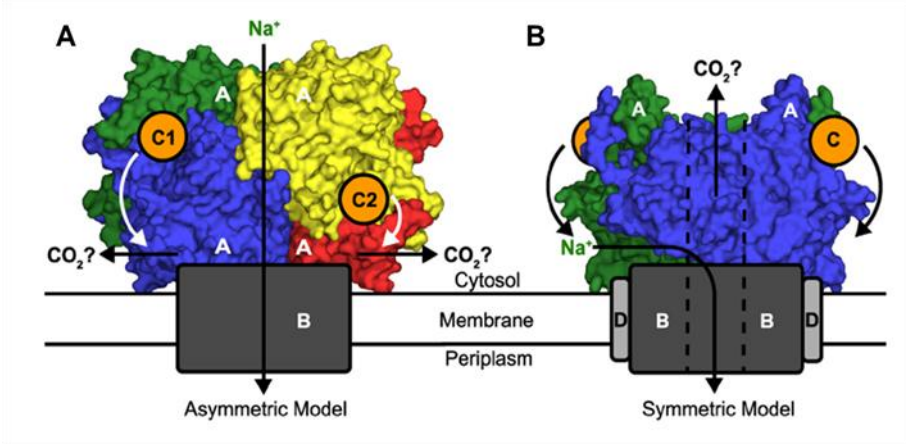

Fig. 10. Hypothetical model of the Gcd complex (Kress et al, 2009)**.** A, Asymmetric model of Gcd from *C. symbiosum*; B, symmetric model from *A. fermentans*. The GcdA subunits are shown in surface representation. The subunit B, C, and D are colored dark gray, orange, and light gray. The hypothetical movement of the GcdC subunits is indicated by bended arrows.

Amino acid sequences of GcdC from *A. fermentans* show an interesting feature that it contains 35 alanines and 14 prolines at the center of the sequence, mainly as AAP and AAAP. Unlikely, the fusobacterial GcdC only has 9 alanines and 4 prolines. Similar (A+P) rich domain was found in the biotin-carrier subunit of methylmalonyl-CoA decarboxylase from *P. modestum* (Bott et al, 1997) and *V. parvula* (Huder & Dimroth, 1993). The specific function of the (A+P) rich domain is not reported yet. In case of the acetyltrasnferase component of pyruvate dehydrogenase from *E. coli*, ^{1}H-NMR spectroscopy of the alanine methyl groups revealed a higher mobility than the surrounding peptides. Deletion of the region did not affect the enzymatic activity (Boiangiu et al, 2005; Miles et al, 1987; Texter et al, 1988). Two different GcdCs (14 and 15 kDa, respectively) were characterized from *C. symbiosum*. Both GcdCs also contain an (A+P) rich domain. The main difference between the two GcdCs is the shortening of the one of the GcdCs linker by 10 amino acids (Kress et al, 2009).

Another noticeable point of GcdC is M**K**M biotin binding motif. The biotin is attached via an amide bond to the ε-amino group of the lysine residue in the MKM motif of the C-terminus. This motif is conserved not only in the biotin-carrier protein of Gcds but also in all biotin containing enzymes.

5. Proposed pathways of glutamate and benzoate biosyntheses

5.1 Glutamate biosynthesis via glutaconyl-CoA

Glutamate is usually synthesized from acetyl-CoA via citrate, isocitrate and 2-oxoglutarate. But in the genome of *S. aciditrophicus*, no gene for *Si*-citrate synthase has been detected. Therefore, it was proposed that glutaconyl-CoA could be the precursor of 2-oxoglutarate. Glutaconyl-CoA is an intermediate in the anaerobic benzoyl-CoA degradation pathway or obtained by carboxylation of crotonyl-CoA depending on the carbon source of the organisms, either benzoate or crotonate. Glutaconyl-CoA can be hydrated to 2-hydroxyglutaryl-CoA. CoA-transfer and oxidation would lead to 2-oxoglutarate, the direct precursor of glutamate (Buckel, 2001b).

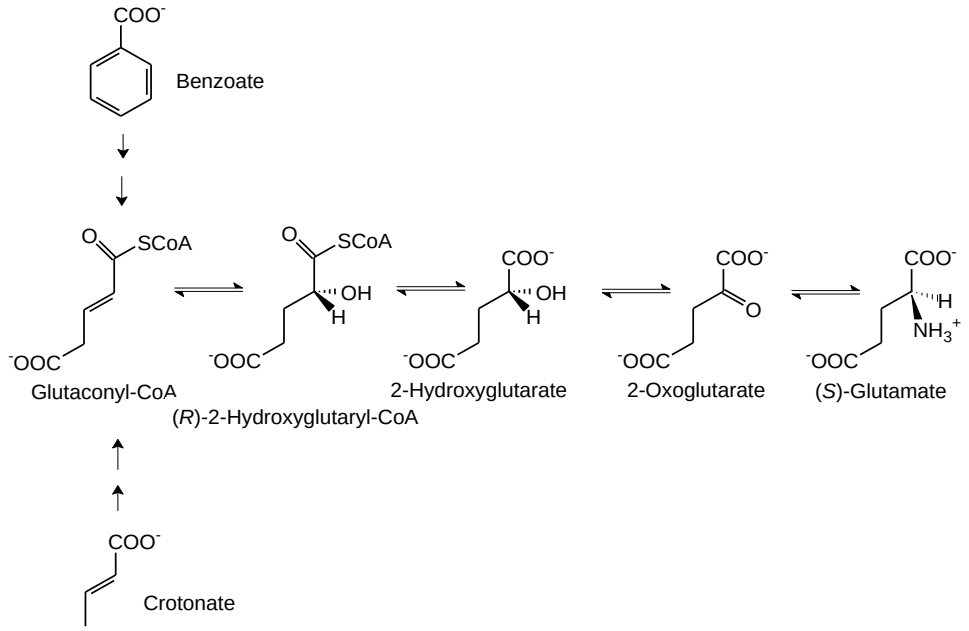

Scheme 1. Biosynthesis of glutamate via glutaconyl-CoA

5.2 Glutamate biosynthesis via the TCA cycle

Recently, the gene encoding *Re*-citrate synthase from *C. kluyveri* has been identified and a homologue has been detected in *S. aciditrophicus* (Li et al, 2007). As shown in Scheme 2, *Re*-citrate synthase catalyzes the attack of acetyl-CoA at oxaloacetate from the *Re*-side (from the front in Scheme 2) and *Si*-citrate synthase from the *Si*-side (from back in Scheme 2).

Therefore, both enzymes must have different active sites and are most likely phylogenetically unrelated.

Both *Re*- and *Si*-citrate synthases catalyze the formation of the identical product citrate from acetyl-CoA and oxaloacetate. If, however, isotopically labeled acetyl-CoA is used, the resulting citrates can be distinguished (Scheme 2). Starting with [1-^{14}C]acetyl-CoA *Si*-citrate synthase yields [5-^{14}C]citrate, whereas *Re*-citrate synthase gives [1-^{14}C]citrate. Cleavage of [5-^{14}C]citrate with the *Si*-specific citrate-lyase regenerates [1-^{14}C]acetate and unlabeled oxaloacetate; with [1-^{14}C]citrate the oxaloacetate will be labeled. In the pathway of glutamate synthesis, *Si*-citrate synthase yields [5-^{14}C]glutamate, whereas with *Re*-citrate synthase [1-^{14}C]glutamate is formed.

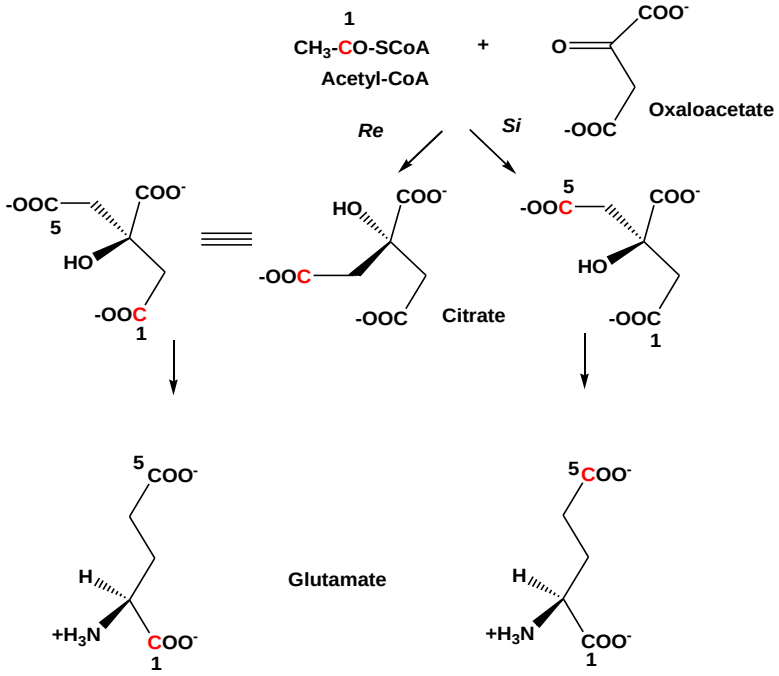

Scheme 2. Stereospecific pathway of glutamate biosynthesis by *Re*/*Si*-citrate synthases.

5.3 Benzoate biosynthesis by glutaconyl-CoA decarboxylase

Anaerobic bacteria degrade aromatic compounds mainly via benzoyl-CoA, glutaryl-CoA and acetyl-CoA, finally to CO_2. Crotonyl-CoA is the common intermediate of the oxidative decarboxylation of glutaryl-CoA. In nitrate-reducing bacteria such as *Thauera aromatica*, which are not energy-limited, the oxidative decarboxylation of glutaryl-CoA is catalysed by the glutaryl-CoA dehydrogenase (Härtel et al, 1993). The prosthetic group FAD of this

homotetrameric enzyme is reduced by glutaryl-CoA to yield $FADH_2$, crotonyl-CoA and CO_2. Re-oxidation of $FADH_2$ is achieved by the heterodimeric FAD-containing electron transferring flavoprotein (Etf), which transfers the electrons to the respiratory chain and finally to nitrate. The energy-limited *S. aciditrophicus* contains two separate enzymes for this process, a glutaconyl-CoA forming glutaryl-CoA dehydrogenase and Na^+-translocating glutaconyl-CoA decarboxylase. This allows the organism to conserve the free energy of decarboxylation as an electrochemical Na^+-gradient ($\Delta\mu Na^+$), equivalent to about ¼ ATP (Buckel, 2001a). On the other hand, *S. aciditrophicus* grows non-syntrophically on crotonate, which is oxidized to acetate with formation of ATP and reduced mainly to cyclohexane-carboxylate, but also to benzoate (Mouttaki et al, 2007). Therefore, glutaconyl-CoA decarboxylase must act in the reverse direction, which has not been observed in vivo before. The subsequent reduction of glutaconyl-CoA to glutaryl-CoA, most likely by NAD(P)H (Djurdjevic, 2010), is probably catalysed by an enzyme similar to the clostridial Etf/butyryl-CoA dehydrogenase complex concomitantly with the reduction of ferredoxin. The reduced ferredoxin may regenerate NAD(P)H mediated by the Rnf-like NAD^+-ferredoxin reductase, whereby $\Delta\mu Na^+/H^+$ is formed. The *rnf* genes have been detected in the genome of *S. aciditrophicus* and the enzymatic activity was detected with NADH and ferricyanide (unpublished data, J. Sieber, University of Oklahoma). The Rnf complex showed a higher specific activity in cells grown syntrophically on benzoate (2.7 U/mg) than in pure culture on crotonate (1.6 U/mg). Thus the reductive synthesis of glutaryl-CoA from crotonyl-CoA consumes and produces $\Delta\mu Na^+/H^+$. It suggests that the oxidation of glutaryl-CoA by NAD^+ should be driven by reduced ferredoxin under syntrophic conditions (Herrmann et al, 2008).

6. Aims of the work

To investigate the glutamate biosynthetic pathway in *S. aciditrophicus*, a gene for the putative *Re*-citrate synthase has to be cloned and expressed as well as the enzyme should be biochemically characterized. To show the participation of the enzyme and to explore an alternative pathway in glutamate biosynthesis, tracer experiments with [1-^{14}C]acetate as well as ^{13}C-isotopomer-assisted metabolite analysis should be applied.

To study the proposed reversibility of benzoate degradation in *S. aciditrophicus* and to elucidate the structure of the energy conserving glutaconyl-CoA decarboxylase, genes encoding Gcd have to be cloned and expressed.

Materials and Methods

1. Materials

1.1 Chemicals and Reagents

All chemical compounds and reagents were purchased, if not mentioned separately in the text, from the companies, Sigma (Steinheim), Merck (Darmstadt), Roth (Karlsruhe,), Fluka (Neu-Ulm), Bio-Rad-Laboratories (München) or Serva (Heidelberg). Coenzyme A is from MP biomedicals. The materials for molecular biology were obtained from Fermentas GmbH (St. Leon-Rot). The primers were purchased from MWG-Biotech AG (Ebersberg).

1.1.1 Acetyl-CoA synthesis

To synthesize the acetyl-CoA (Simon & Shemin, 1953), 50 mg free CoASH (60.9 µmol) was added in 2 ml 1 M $NaHCO_3$ and 7 ml H_2O, which was mixed with 11 µl acetic acid anhydride in 1.5 ml acetonitrile. The reaction was kept at room temperature and was monitored by DTNB (20 mg/ml, 1 M $NaHCO_3$) dot blotting on filter paper. When no more free CoASH was detectable, the reaction was stopped by acidifying using 1 M HCl to pH 1.5 – 2, and loaded on a C18 Sep-Pak^{TM} column (Waters, USA), which was previously washed by 5 ml methanol and equilibrated by 10 ml 0.1% trifluoroacetic acid (TFA). The column was washed with 5 column volume of 0.1% TFA and the CoA-ester was eluted by 5 ml of 0.1% TFA containing 50% acetonitrile. Total CoA content was directly measured at 259 nm. After lyophilisation, the mass of the synthesized CoA-ester was confirmed by MALDI-TOF mass spectroscopy at the MPI for Terrestrial Microbiology, Marburg.

Deuterium labeled [$^2H_3$]acetyl-CoA used in kinetic isotope effect was synthesized from [$^2H_6$]acetic anhydride by Dr. Peter Friedrich (Philipps-Universität Marburg).

1.1.2 Glutaconyl-CoA synthesis

Glutaconyl-CoA was obtained by enzymatic synthesis with glutaconate CoA-transferase (GctAB) (Buckel et al, 1981). 20 µmol acetyl-CoA, 200-400 µmol glutaconate, and 5 U GctAB were mixed in a volume of 3 – 5 ml 50 mM potassium phosphate, pH 7.0 and the

mixture reacted at 37 °C for 1 h. After 1 h incubation, the mixture was acidified to pH 2.0 and filtered through a 10 kDa cut-off membrane (Amicon, Amersham Biosciences).

The CoA thioesters were purified by reverse phase chromatography through Sep-Pak C18 columns. The column was washed with methanol and equilibrated with 0.1% TFA (v/v). The reaction mixture was loaded on the column and washed with 3 volumes of 0.1% TFA. Elution was performed with 0.1% TFA containing 50% acetonitrile (v/v). The eluted CoA ester was freed from acetonitrile by drying in Speed-Vac concentrator (Bachofer, Germany). It was then refrozen and lyophilized (Alpha1-4, Christ Instruments, USA). The obtained powder was stored at − 80 °C for further use.

1.1.3 Preparation of NMR samples

The isolated ^{13}C-labeled glutamate and aspartate were dissolved in 200 µl of D_2O and filled into Wilmad 3 mm tubes obtained from Rototec Spintec. Measurements were carried out on a Bruker Avance 600 MHz spectrometer with an TXI probe installed with z-gradient. The 1D spectra ^{1}H and ^{13}C, the homonuclear 2D spectra TOCSY (Total Correlation Spectroscopy), and ^{1}H-^{13}C HSQC (Heteronuclear Single-Quantum Correlation) and HMBC (Heteronuclear Multiple-Bond Correlation) spectra were recorded at room temperature using standard pulse sequences (Berger & Braun, 2004). The TOCSY spectra were recorded with mixing time of 200 ms, while the water signal was suppressed by using excitation sculpting technique (Hwang & Shaka, 1995). The 1D spectra were acquired with 65536 data points, whereas 2D spectra were collected using 2048 points in the F_2 dimension and 512 increments in the F_1 dimension. ^{13}C spectra were recorded with 32768 transients. For 2D spectra, 32 – 64 transients were used. The relaxation delay was 2.5 s. The pH effect on the spectra was surveyed by recording ^{1}H spectra on glutamate samples of natural abundance at variable pH (1.5, 3, 4, 5, 7, 9). Chemical shifts of ^{1}H and ^{13}C were calibrated using trace of 2,2-dimethyl-2-silapentane-5-sulfonate (DSS) as internal reference. DSS is similar to tetramethylsilane but with much higher water solubility. The spectra were processed using Bruker program package Topspin 2.1.

1.1.4 Carbon isotope labeled compounds

[1-^{14}C]Acetic acid, [1-^{14}C]glutamic acid, and [5-^{14}C]glutamic acid were obtained from Perkin-Elmer (Rodgau, Germany). [^{13}C]Sodium hydrogencarbonate was purchased from Sigma Aldrich.

1.2 Instruments and columns

Beckman (München) supplied the ultra-centrifuge, Sorval (München) the cooling centrifuges. The FPLC system and Äkta were obtained from Amersham Biosciences (Freiburg). HP 8453 UV-visible diode array spectrophotometer (USA) and Ultrospec 1100 pro sepctrophotometers from Amersham Biosciences installed were used for enzyme activity assays. Quartz cuvettes were used for measuring UV-vis spectra and disposable plastic cuvettes for measurements above 320 nm. All of which had a path length of 1 cm or 0.5 cm and a volume of 0.5 ml. The column HiLoad^{TM}26/60 Superdex^{TM}200 prep grade was obtained from Amersham Biosciences (Freiburg) and Strep-Tag II column was purchased from IBA GmbH (Göttingen). Ni Sepharose 6 Fast Flow column and PD-10 Desalting colum were purchased from GE Healthcare (Sweden).

1.3 Anaerobic work

Anaerobic experiments have been done in an anaerobic glove box supplied by Coy Laboratories, Ann Arbor Ml, USA. The glove box was filled with a nitrogen atmosphere containing 5% H_2. Buffers for the assay were prepared by boiling and cooling under vacuum. Afterwards the buffers were flushed with nitrogen and transferred to the anaerobic chamber. Enzyme activity was determined inside the anaerobic chamber with an Ultrospec 1000 *pro*.

1.4 Bacteria and culture media

1.4.1 *Syntrophus aciditrophicus* SB

S. aciditrophicus SB^T (ATCC 700169^T) strain was kindly provided by the group of Prof. Michael J. McInerney (University of Oklahoma, USA). *S. aciditrophicus* was cultivated

anaerobically in 50 ml serum bottle under a nitrogen atmosphere containing 20% CO_2. The culture medium had the following composition:

Medium composition:

	Per 1L
Tanner's Minerals	10 ml
Tanner's Trace Metals	5 ml
Tanner's Vitamins	10 ml
0.1% Resazurin	1 ml
Sodium crotonate	30 mM

Tanner's Minerals	g per 1L
NaCl	80
NH_4Cl	100
KCl	10
KH_2PO_4	10
$MgSO_4 \cdot 7H_2O$	20
$CaCl_2 \cdot 2H_2O$	4

Tanner's Trace Metals	
Nitrilotriacetic acid (adjust pH to 6 w/KOH)	2.0
$MnSO_4 \cdot H_2O$	1.0
$Fe(NH_4)_2 \cdot 6H_2O$	0.8
$CoCl_2 \cdot 6H_2O$	0.2
$ZnSO_4 \cdot 7H_2O$	0.2
$CuCl_2 \cdot 2H_2O$	0.02
$Na_2MoO_4 \cdot 2H_2O$	0.02
Na_2SeO_4	0.02
$Na_2WO_4 \cdot 2H_2O$	0.02
$NiCl_2 \cdot 6H_2O$	0.02

Tanner's Vitamins	mg per 1L
Pyridoxine-HCl	10.0
Thiamine-HCl	5.0
Riboflavin	5.0
DL Calcium pantothenate	5.0
Lipoic acid (thiotic acid)	5.0
PABA (*p*-aminobenzoic acid)	5.0
Nicotinic acid	5.0
Vitamin B_{12}	5.0
MESA (mercaptoethane-sulfonic acid)	5.0
Biotin	2.0
Folic acid	2.0

Cysteine Sulfide Solution	
NaOH	1.25 g
Cysteine-HCl	5 g
$Na_2S{\cdot}9H_2O$	5 g
Distilled H_2O	200 ml

The pH of medium was adjusted to pH 7.1 – 7.3. The medium was heated to 70 °C. After taking the medium into the anaerobic chamber, 3.75 g sodium bicarbonate per L was added. After filling 50 ml medium in 120 ml anoxic serum bottles inside the anaerobic chamber, the bottles where closed with rubber stoppers and sealed with aluminum caps. Outside the chamber vacuum was applied with a needle through the rubber stopper. Then the bottles were flushed with 80% nitrogen and 20% CO_2 gas and 1 ml of 2.5% cysteine sulfide was added. The reddish blue color (resazurin) of the anaerobized medium indicated the absence of oxygen. The media were autoclaved and stored at room temperature in a dark place.

All cultures were incubated at 37 °C without shaking. For the subculturing of the organism, 10 – 20% of pre-culture was used to inoculate. The growth rate was followed by measuring optical density at 600 nm. The culture purity was checked by microscopic examination daily

and by periodic inoculation of a thioglycolate medium and sequencing the 16S rRNA gene. The grown cultures were kept at room temperature for storage and passed every four weeks.

1.4.2 *Escherichia coli*

E. coli was grown at 37 °C in LB medium (1% tryptone, 0.5% yeast extract, 1% NaCl) containing antibiotic(s) depending on the harbored plasmid. The strain DH5α [F^- endA1 glnV44 thi-1 recA1 relA1 gyrA96 deoR nupG Φ80d*lacZ*ΔM15 Δ(*lacZYA-argF*)U169, hsdR17(r_K^- m_K^+), λ–] and α-competent (Bioline GmbH) were used for gene cloning and BL21 (DE3) [$F^–$ ompT gal dcm lon $hsdS_B$(r_B^- m_B^-) λ(DE3 [lacI lacUV5-T7 gene 1 ind1 sam7 nin5])], BL21 CodonePlus(DE3)-GroEL for the gene expressions. *E. coli* as an expression-system has frequently troubles to produce proteins, e.g., inclusion body, degradation and insolubility of proteins. The BL21 CodonPlus(DE3)-GroEL contains a chaperon-plasmid, which is able to improve the gene expression. The Lemo21(DE3) [*fhuA2 [lon] ompT gal (λ DE3) [dcm]* Δ*hsdS/ pL*emo(Cam^R), *λ DE3 = λ sBamHIo* Δ*EcoRI-B int::(lacI::PlacUV5::T7 gene1) i21* Δ*nin5*, pLemo = pACYC184-*PrhaBAD-lysY*] and C43(DE3) [$F^–$ ompT gal dcm $hsdS_B$(r_B^- m_B^-)(DE3)] were used for membrane protein overproduction.

1.5 Plasmids

pASK-IBA3plus (IBA GmbH) (tet promoter/operator, C-terminal Strep-tag II, cytosolic localization of the recombinant protein, Amp^r), pASK-IBA7plus (IBA GmbH) (tet promoter/operator, N-terminal Strep-tag II, cytosolic localization of the recombinant protein, Amp^r) were used for the gene encoding *Re*-citrate synthase expression. pASK-IBA3plus, pASK-IBA7plus and pACYCDuet™-1 (Novagen) (T7 promoters, His-Tag and S-Tag, Cm^r) were used for the *gcdA* and *gcdC* expression, pASK-IBA3c (tet promoter/operator, C-terminal Strep-tag II, cytosolic localization of the recombinant protein, Cm^r) and pCDFDuet™-1 (Novagen) (T7 promoters, His-Tag and S-Tag, Sm^r) for the *gcdB* expression.

1.6 Antibiotics

The stock of antibiotics was prepared and used as described below.

Antibotic	Stock	Final concentration
Carbenicillin	50 mg/ml H_2O sterilized by filtration (0.2 μm)	50 μg/ml
Chloramphenicol	37 mg/ml 70% ethanol	37 μg/ml
Spectinomycin	50 mg/ml H_2O sterilized by filtration (0.2 μm)	50 μg/ml

2. Methods for DNA work

2.1 Genomic DNA isolation from *S. aciditrophicus* SB

For genomic DNA isolation, 2 g of *S. aciditrophicus* SB cells were suspended in 3 ml Tris-EDTA buffer (10 mM Tris/HCl, pH 7.5, 1 mM EDTA, pH 8.0). Then 30 µl of proteinase K (20 mg/ml) was added to given a final concentration of 100 µg of proteinase K in 0.5% SDS and incubated for 1 h at 37 °C. 100 µl NaCl (5 M) was added and mixed thoroughly which was by followed with addition of 80 µl of CTAB/NaCl solution (10% CTAB (hexadecyltrimethyl ammonium bromide) in 0.7 M NaCl) and mixed thoroughly and incubated for 10 minutes at 65 °C. Then the solution was tested with 700 µl chloroform/isoamyl alcohol and after centrifugation an equal volume of phenol/chloroform/isoamyl alcohol was added and centrifuged again. The nucleic acids were precipitated by 0.6 volumes of isopropanol to get a stingy white DNA pellet. The precipitated DNA was washed with ethanol and dried. The DNA was re-dissolved with Tris-EDTA buffer and stored at − 20 °C. The protocol was adapted from Current Protocols in Molecular Biology (Wilson, 2001).

2.2 Plasmid DNA isolation

Plasmid DNA isolation was done by alkaline lysis methods using GeneJET^{TM} Plasmid Miniprep Kit (Fermentas). LB medium 5 ml containing antibiotic(s) was inoculated with a

bacterial colony and incubated with gyration overnight at 37 °C. The culture was transferred into an Eppendorf tube and harvested at 13,000 × g in a microcentrifuge for 2 minutes. The bacterial pellet was taken up in 250 µl suspension buffer (50 mM glucose, 10 mM EDTA, 25 mM Tris/HCl, pH 8.0). After 2 − 3 times gentle shaking the 250 µl lysis buffer (0.2 M NaOH, 1% SDS) and 350 µl neutralization buffer (3 M potassium acetate/glacial acetic acid, pH 4.8) were added. The soluble supernatant was separated from cell debris by centrifugation for 5 minutes and transferred into a new Eppendorf tube. The plasmid DNA was washed two times and eluted in TE buffer (10 mM Tris/HCl pH 8.0, 1 mM EDTA).

2.3 DNA agarose gel electrophoresis

Agarose powder was mixed with 50 × electrophoresis TAE-buffer (2 M Tris, 1 M acetic acid, 0.1 M $Na_2EDTA{\cdot}2H_2O$ pH 8.5) to the desired concentration, and then heated in a microwave oven until it completely melted. After cooling the solution to about 60 °C, it was poured into a casting tray containing a sample comb and allowed to solidify at room temperature. After the gel had solidified, the comb was removed and the gel was inserted horizontally into the electrophoresis chamber just covered with the TAE buffer. DNA samples mixed with 6 × MassRuler^{TM} Loading Dye Solution (10 mM Tris/HCl pH 7.6, 0.03% bromophoenol blue, 60% glycerol and 60 mM EDTA) were then pipetted into the sample wells, and 100 – 120 V were applied. Bromophenol blue dye migrates through agarose gels at the front of double-stranded DNA fragments. When adequate migration had occurred, DNA fragments were stained with ethidium bromide and placed on an ultraviolet transilluminator.

2.4 Elution of DNA fragments from agarose gel

DNA bands were exposed on an UV-illuminator using a short wavelength and rapidly cut out from the agarose gel. Extraction was performed following the manual of the QIAquick Gel Extraction Kit (QIAGEN GmbH).

2.5 DNA restriction and ligation

Restriction reactions were usually performed following the enzyme insert manual. For ligations of double stranded DNA, T4-DNA ligase (Fermentas GmbH) was used following the enzyme insert manual.

2.6 Dialysis of ligation mixtures

The ligation mixture was dialyzed before electrotransformation. The ligation mixture was pipetted on Millipore-Membrane (#VSWP 02500) which was floating on the water. After 30 minutes of dialysis, the ligation mixture was carefully recovered from the membrane and used for electrotransformation.

2.7 Preparation of competent *E. coli* cells for electrotransformation

An overnight 5 ml LB medium culture with a fresh single *E. coli* colony from a plate was used to inoculate a 500 ml main culture and grown until the exponential phase (OD_{600} = 0.5 – 0.8). The cells were harvested by a pre-cooled (4 °C) high-speed centrifuge with 6000 × g for 20 minutes. The harvested cell was washed two times with 500 ml ice-cold sterile H_2O and one time with 20 ml 10% glycerol. The washed cells were suspended with 1 ml 10% glycerol and 40 µl aliquots in thin-wall 500 µl tubes were stored at − 80 °C.

2.8 Electrotransformation

The dialyzed ligation mixture was added to 40 µl electro-competent cells and transferred to a Gene-Pulser cuvette (Bio-Rad). A pulse was given to the cuvette using the following settings: 25 µF, 1.8 kV and 200 Ohm. The cuvette was washed with 300 µl LB medium and transferred to a sterile 1.5 ml Eppendorf tube. The transformation mixture was incubated for 30 minutes at 37 °C before plating on a LB agar plate containing antibiotic(s). The agar plate was incubated overnight at 37 °C to get the colonies.

2.9 Chemical transformation

The ligation mixture was added to 40 µl chemical-competent cells (Bioline) and mixed gently. After mixing the tube was immediately placed on ice for at least 10 minutes. The cells containing ligation mixture were given a heat shock for 45 seconds in a water bath at exactly 42 °C without shaking and immediately place the tube on ice for 2 minutes. 300 µl of LB medium was added to the tube and the transformation mixture was incubated for 30 minutes at 37 °C with shaking. The cells were placed on a LB agar plate containing appropriate antibiotic(s). The agar plate was incubated overnight at 37 °C.

2.10 DNA concentration and purity determination

The DNA concentration and purity were determined measuring OD_{260} and OD_{280}. DNA concentration (µg/ml) = $\Delta E_{260} \times 50 \times$ dilution

OD_{260} = 1 corresponds to 50 µg/ml of dsDNA

$OD_{260}/OD_{280} < 1.8$ indicates contamination with protein or phenol

$OD_{260}/OD_{280} > 1.8$ indicates contamination with RNA

$OD_{260}/OD_{280} \approx 1.8$ indicates pure dsDNA

2.11 PCR reactions

PCR reactions were performed using a proofreading DNA polymerase, High Fidelity DNA polymerase, Phusion polymerase and DyNAzyme (Finnzymes), and the reaction mixtures were made with following concentrations of the ingredients and cycle program:

Concentration of ingradients

	Final concentration
dNTP	200 µM
Forward primer	500 nM
Reverse primer	500 nM
Template DNA	1 to 2 ng/µl (genomic DNA)
DNA polymerase	1 U

Cycling program

1.	98 °C	3 min
2.	98 °C	10 sec
3.	68 °C (depending on primer)	20 sec
4.	72 °C	40 sec/kbp (depending on the length of target gene)
5.	72 °C	7 min

35 cycles from 2. to 4.

2.12 PCR primers

All the primers were synthesized by MWG Biotech (Ebersberg, Germany). Restriction site in the primer is underlined.

Gene	Vector		Nucleotide sequence (5' – 3')
rcs	IBA3plus, IBA7plus	F	AAG CTC TTC AAT GGC CAA ATG GAA TCC CC
		R	AAG CTC TTC TCC CCA GCC AGT GAT CTG ATT TGT ATT TCG
gcdA	pACYCDuet-1,	F	ATG GTA GAT ATC ATG AGA CAA T AC TTT GAA AAG ATG G
	MCS2	R	ATG GTA GGT ACC TGC TTC TTT TGC TGG TCT GG
	IBA3plus	F	ATG GTA GGT ACC ATG AGA CAA TAC TTT GAA AA
		R	ATG GTA CTC GAG TGC TTC TTT TGC TGG TCT GG
	IBA7plus	F	ATG GTA GGT ACC ATG AGA CAA T AC TTT GAA AA
		R	ATG GTA CTA TAG TGC TTC TTT TGC TGG TCT GG
gcdB	pCDFDuet-1, MCS*1	F	ATG GTA GGA TCC GTG ATT TTT GGA TTA ATG GA
		R	ATG GTA AAG CTT TCC CAG TAT TCC AAT GAA AA
	pCDFDuet-2, MCS2	F	ATG GTA GAT ATC GTG ATT TTT GGA TTA ATG GA
		R	ATG GTA GGT ACC TCC CAG TAT TCC AAT GAA AA
	IBA3c	F	ATG GTA TCT AGA GTG ATT TTT GGA TTA ATG GA
		R	ATG GTA CTG CAG TCC CAG TAT TCC AAT GAA AA
gcdC	pACYCDuet-1,	F	ATG GTA GAG CTC ATG GAA GTC ACT GTA CCC AT

	MCS1	R	ATG GTA AAG CTT TTC GAT GAC CAT CAA CGC AG
	IBA3plus	F	ATG GTA TCT AGA ATG GAA GTC ACT GTA CCC AT
		R	ATG GTA GAA TTC TTC GAT GAC CAT CAA CG
	IBA7plus	F	ATG GTA GGA TCC ATG GAA GTC ACT GTA CCC AT
		R	ATG GTA AAG CTT TTC GAT GAC CAT CAA CGC AG
biotin ligase	IBA3plus+*gcdAC*	F	ATG GTA ATG GTA GTC GAC GTG GTA TTC AAG GCC GCG
		R	ATG GTA ATG GTA AGA GAC CGA CCG TGA GGA GGG TCA C

*MCS: multi-cloning site

2.13 Cloning of the genes

Prior to cloning into target vector, the DNA fragments of the genes encoding *Re*-citrate synthase (1890 bp), *gcdA* (1773 bp), *gcdB* (1347 bp) and *gcdC* (210 bp), biotin ligase (1002 bp) were amplified with the designed primers, which contain restriction cut sites depending on the multicloning site of the target vector. The amplified DNA and vector were digested by restriction enzymes and purified by gel extraction. Before transformation into *E. coli* DH5α cells, the digested DNA and vector were ligated together by T4 DNA ligase and dialysed for at least 30 minutes.

2.14 Sequencing of the cloned genes

Primers listed below were synthesized and used for sequencing.

Vector	Nucleotides (5' – 3')
pASK-IBA vectors	
	F AGA GTT ATT TTA CCA CTC CCT
	R GCT CCA TCC TTC ATT ATA GC
Duet vectors	
ACYCDuetUP1	GGA TCT CGA CGC TCT CCC T
DuetDOWN1	GAT TAT GCG GCC GTG TAC AA
DuetUP2	TTG TAC ACG GCC GCA TAA TC
T7 Terminator	CCG CTG AGC AAT AAC TAG C

The standard primers were used for all sequencings and the internal primers were used to complete sequences, which were too long to be determined by the standard primers.

3. Methods for protein work

3.1 Gene expressions

3.1.1 Expression in *E. coli* of the genes encoding *Re*-citrate synthase

The plasmid harboring a gene encoding *Re*-citrate synthase was transformed into *E. coli* BL21 CodonPlus(DE3)-GroEL harboring an extra plasmid, encoding chaperone GroEL. An overnight anaerobic preculture (100 ml) inoculated with a fresh single colony from a LB agar plate was grown in the tryptone-phosphate (TP) medium (2% bactotryptone, 0.2% Na_2HPO_4, 0.1% KH_2PO_4, 0.8% NaCl, 1.5% yeast extract, 0.2% glucose) that is a valuable adjunct to limit inclusion body formation with carbenicillin and chloramphenicol was used to inoculated 2 L TP medium containing the same antibiotics at 37 °C or room temperature under aerobic conditions. When the culture reached the mid-exponential phase (A_{600} = 0.5 – 0.7) gene expression was induced with anhydrotetracycline (AHT) (200 µg/L) and the chaperone gene was induced with 0.1 mM isopropyl-β-thiogalactopyranoside (ITPG). After overnight growth, the cells were harvested and washed in 50 mM K-phosphate, pH 7.0 to remove antibiotics and inducing agents. The cells were suspended in 50 ml phosphate buffer in re-inoculated in fresh 1 L TP medium containing chloramphenicol (200 µg/L) and incubated for 2 h at room temperature. Chloramphenicol functions to inhibit new protein synthesis in *E. coli* and the 2 h additional incubation time enables the chaperone to fold the protein correctly (de Marco, 2007). After another 2 h growth, the cells were harvested and suspended in equilibration buffer (50 mM K-phosphate, pH 7.4, 75 mM NaCl).

3.1.2 Gene expression in *E. coli* of the genes encoding glutaconyl-CoA decarboxylase

For the expression of genes, plasmid constructs were transformed into *E. coli* BL21, *E. coli* C43(DE3), *E. coli* Lemo21(DE3) or *E. coli* BL21 CodonPlus(DE3). An overnight pre-culture (100 ml) inoculated with a fresh single colony from a LB agar plate was grown in the LB medium with antibiotics was used to inoculate 1 L LB medium containing the same

antibiotics at 37 °C, 30 °C, or room temperature under aerobic conditions. When the culture reached the mid-exponential phase, gene expression was induced with AHT (100 µg/L or 200 µg/L) or IPTG (50 to 500 mg/L). Cells were harvested after 2 h, 4 h, or overnight growth.

3.2 Protein purification

3.2.1 Methods of cell disruption

Ultrasonic disintegration: Cells, suspended in the appropriate buffer, were filled into a glass Rosetta cell, kept on ice and broken by ultrasonication on a Branson 250 Sonifier (Heinemann, Germany). The duty time was 5 minutes at 50% duty cycle. The process was repeated several times.

French press: The suspended cells were filled into a bottle. The cell suspension was sucked into a pre-cooled French press cell (American Instruments, Maryland, USA) and the cells were disrupted by applying a pressure of 110 MPa. The broken cells were collected into the bottle and refilled into the pressure cell for another cycle of disrupting. The cycle was repeated 3 – 4 times and the cells were observed under a microscope to verify optimal cell disruption.

3.2.2 Determination of protein concentration

Bradford method

Protein concentration was determined by the Bradford method (Bradford, 1976). The assay is based on the shift of the absorbance maximum for an acidic solution of Coomassie Brilliant Blue G-250 from 465 nm to 595 nm upon binding of protein. Standards with 0 – 1 mg of BSA were made up to 10 µl and 200 µl Coomassie Brilliant G-250 reagent. The reactions were incubated in the dark at room temperature for 30 minutes and the absorbance was measured at 595 nm by a microplate spectrophotometer.

Bicinchoninic acid (BC) assay

The BC assay (Uptima-interchim, France) is a colorimetric assay: it involves the reduction of Cu^{2+} to Cu^{+} by peptidic bounds of proteins (Smith et al, 1985). The bicinchoninic acid chelates Cu^{+} ions with very high specificity to form a water soluble purple colored complex. This assay particularly suits to analyze complex mixtures containing nucleic acids, lipids or detergents (Triton X-100, SDS extracts). Therefore, the assay was used to determine the concentration of membrane proteins.

3.2.3 Polyacrylamide gel electrophoresis (PAGE)

SDS-PAGE

The samples were mixed with SDS sample buffer (125 mM Tris/HCl pH 6.8, 10% glycerol, 10% mercaptoethanol, 4% SDS, 0.2% bromophenol blue) in the ratio of 1:1 and boiled at 95 °C for 5 minutes to denature the proteins. Boilng step was avoided in case of preparation of membrane proteins. The running buffer was 25 mM Tris pH 8.8, 190 mM glycine, 0.1% SDS. Electrophoresis was run at constant voltage of 200 mV until the bromophenolblue marker reached the end of the gel. The proteins were stained by heating the gel with 0.1% Coomassie Brilliant Blue R-250 in methanol/water/glacial acetic acid (4:5:1) shortly and leaving it at room temperature for 10 minutes. The gel was distained by heating it with ethanol/water/glacial acetic acid (4:5:1) and incubating overnight on a shaker.

SDS-PAGE gel (15% acrylamide)

Stock solution	Separating gel (µl)	Stacking gel (µl)
1M Tris/HCl, pH 8.8	2250	-
1M Tris/HCl, pH 6.8	-	353
H_2O	315	1905
10% SDS	63	30
Acrylamide/Bisacrylamide (40%/1.6%)	2780	712
5% TEMED	63	30
10% Ammonium peroxodisulfate	90	60

Native PAGE

For molecular mass determination of native enzymes, a 4 – 20% gradient gel (Mini-PROTEAN®TGX™ Precase Gels, BIO-RAD), various concentrations of acylamide gels, and a marker (SERVANative Marker Liquid Mix for BN/CN, SERVA Electrophoresis) were used. The protein samples were mixed with 2 × sample buffer for clear native electrophoresis (SERVA) in the ratio of 1:1. The running buffer was 25 mM Tris, 192 mM glycine, pH 8.3. Electrophoresis was run at voltage of 100 mV and constant current of 0.01 A until the bromophenolblue marker reached the end of the gel. Staining and destaining steps were as same as SDS-PAGE (3.2.3).

Contents for various concentrations of acrylamide gels

	10% (µl)	9% (µl)	8% (µl)	6% (µl)
1.5 M Tris/HCl, pH 8.8	1880	1880	1880	1880
H_2O	3100	3350	3600	4100
Acrylamide/Bisacrylamide (40%/1.6%)	2500	2250	2000	1500
100% TEMED	5	5	5	5
10% Ammonium peroxodisulfate	25	25	25	25

3.2.4 Preparation of soluble membrane protein

The 5 g wet packed *S. aciditrophicus* cells were suspended in 50 mM phosphate buffer pH 7.4 and the cells were broken by three passages through French press cell at 110 MPa. Cell debris was removed by centrifugation at 10,000 × *g* for 20 min at 4 °C. The crude extract was centrifuged at 120,000 × *g* for 1 h. The membrane extract was collected and washed twice with 50 mM phosphate, pH 7.4 by centrifuging at 120,000 × *g* for 30 minutes. The washed membrane extract was solubilised with 20 mM phosphate pH 7.4 containing 0.5 M NaCl, 10 mM EDTA and 2% n-dodecyl-ß-D-maltoside (DM) and homogenized well to solubilise it further. The suspension was on ice for 30 minutes. The solubilised membrane was centrifuged at 120,000 × *g* for 30 minutes and the solubilised membrane extact in the supernatant was collected (Buckel, 1986a).

3.2.5 Purification of recombinant *Re*-citrate synthase from *S. aciditrophicus*

Recombinant *Re*-citrate synthase from *S. aciditrophicus* was purified aerobically using a Strep Tactin column at 4 °C. The harvested *E. coli* cells were suspended in equilibration buffer and opened using sonication. Cell debris was removed by ultra-centrifigation at 100,000 × *g* for 1 h. The clear supernatant was filtrated and loaded on the affinity Strep Tactin column, which was equilibrated with equilibration buffer. After loading the cell free extract, the column was washed at least 10 column volumes of equilibration buffer. To release the co-purifying chaperone from the target protein, a simple one step $MgCl_2$/ATP/KCl incubation procedure was applied. Incubation of the target protein immobilized on the Strep Tactin resin with 10 mM $MgCl_2$/10 mM ATP/150 mM KCl for 2 h at 4 °C. The protein was eluted with equilibration buffer with 2.5 mM D-desthiobiotin. At last, the purified protein from Strep-Tactin column was loaded on a gel filtration column (HiLoad^{TM}26/60 Superdex^{TM}200) to achieve the pure protein.

Buffers for recombinant protein purification;

Equilibration buffer	50 mM K-phosphate, pH7.4, 75 mM NaCl
Dissociation buffer	20 mM HEPES/NaOH, pH 7.0, 10 mM $MgCl_2$, 10 mM ATP, 150 mM NaCl
Elution buffer	50 mM Tris/HCl pH, 8.0, 150 mM NaCl, 2.5 mM desthiobiotin
Gel filtration buffer	50 mM Tris/HCl pH, 8.0, 150 mM NaCl

3.2.6 Purification of glutaconyl-CoA decarboxylase from *S. aciditrophicus*

All purification procedure was carried out under aerobic conditions at 4 °C. The membrane extracts were prepared as mentioned earlier (3.2.4). The solubilised membrane was loaded onto SofLink^{TM} Soft Release Avidin (Promega, USA) column (1 × 10 cm) equilibrated with the buffer (20 mM phosphate, pH 7.0, 0.1% DM). The column was washed with 10 column volume of equilibration buffer at a rate of 0.2 ml per minute until there was no protein detected. The protein was eluted with elution buffer (20 mM phosphate, pH 7.0, 0.1% DM, 2 mM D-biotin). The enzyme containing fractions were pooled and concentrated by ultrafiltration over a Centricon (cut off size: 1 kDa) and stored at − 80 °C (Buckel, 1986a).

3.2.7 Purification of the subunits of recombinant glutaconyl-CoA decarboxylase from *S. aciditrophicus*

GcdA by Strep-tag

Wet packed cells were suspended in 100 mM Tris/HCl, pH 8.0, 150 mM NaCl and lysed by three times of French press cell at 110 Mpa. The cell free extract was prepared after centrifugation for 1 h at 100,000 × *g*. The supernatant was filtrated and loaded on the Strep Tactin column. After washing with 5 column volumes of wash buffer (100 mM Tris/HCl, pH 8.0 and 150 mM NaCl), the protein was eluted by elution buffer (100 mM Tris/HCl, pH 8.0, 150 mM NaCl, 2.5 mM desthiobiotin).

GcdB by His-tag

The membrane extracts were prepared as mentioned earlier. The solubilised membrane was load onto the Ni-Sepharose column. After washing with 5 column volumes of wash buffer (50 mM phosphate, pH 7.4, 0.5 M NaCl, 20 mM imidazole, 0.1% DM), the protein was eluted by buffer containing 50 mM phosphate, pH 7.4, 0.5 M NaCl, 500 mM imidazole containing DM.

GcdAC by affinity SofLink^{TM} Soft Release Avidin column

GcdAC was purified by SofLink^{TM} Soft Release Avidin column. Purification was performed by routine procedure mentioned above.

3.2.8 Partial purification of recombinant glutaconate CoA-transferase from *A. fermentans*

Cells of *E. coli* BL21(DE3), harboring the plasmid with glutaconate CoA-transferase from *A. fermentans*, were suspended in 15 ml of 20 mM potassium phosphate, pH 7.4 and sonicated for 15 minutes (divided in three intervals) with a Branson sonifier. Cell debris was removed by ultra-centrifugation at 100,000 × *g* for 1 h at 4 °C. Ammonium sulphate was added to the cell free extract to achieve 50% saturation. After centrifugation at 25,000 × *g* for 30 minutes, the supernatant was brought to 80% ammonium sulphate saturation and centrifuged as described above. The protein pellet was dissolved in 40 ml of 20 mM potassium phosphate

buffer, pH 7.4 and partially purified with Centricon cut-off membrane of 100 kDa. The purified protein was stored at 4 °C (Mack et al, 1994).

3.2.9 Gel filtration

To separate the *Re*-citrate synthase from co-purified chaperone, the protein solution was loaded on a HiLoad^{TM}26/60 Superdex^{TM}200 column which was prior washed by H_2O and equilibrated by 50 mM Tris/HCl, pH 8.0. The chromatography was achieved using 50 mM Tris/HCl, pH 8.0 and 150 mM NaCl with a flow rate of 2 ml/min.

3.3 N-terminal amino acid sequence analysis

The recombinant protein with co-purified chaperone, GroEL was separated by SDS-PAGE. The protein samples were transferred from an unstained SDS-PAGE gel to methanol-soaked polyvinylidene fluoride membrane (PVDF Westran STM-Membrane, Schleicher & Schuell GmbH, Dassel, Germany). The system was stacked with six layers of gel blotting filter paper which was previously equilibrated with transfer buffer (25 mM Tris-glycine, 20% methanol). By using Bio-Rad transfer-blot cell (16 × 20 cm), filled with transfer buffer. The electro transfer was performed applying a constant current of 300 mA for 1 h at 4 °C. The membrane was shortly stained with Coomassie Brilliant Blue R-250 stain and immediately destained in 80% methanol/10% glacial acetic acid. Two bands corresponding to the size of *Re*-citrate synthase and GroEL were excised from the membrane for N-terminal sequence by Edman degradation which was done by Dr. Linder at the Biochemisches Institut des Fachbereichs Humanmedizin, Justus-Liebig-Universität Gießen, Germany.

3.4 MALDI-TOF mass spectrometry

CoA derivatives

The CoA samples were purified from their synthesis or protein bands from SDS-PAGE gel were identified by MALDI-TOF mass spectrometry. The matrix was alpha-cyano-4-hydroxy cinnamic acid (CHCA, Sigma) dissolved in 70% acetonitrile/0.1% TFA (trifluoro acetic acid). 1 µl of each sample was mixed with 1 µl CHCA and spotted onto a gold plate in a dilution

series. Measurements were performed with a 355 nm laser in positive reflector mode with a delayed extraction with a positive polarity on the Proteomics Analyzer 4800 mass spectrometer (Applied Biosystems, MDS Sciex) using the 4800 Series Explorer software at the MPI for Terrestrial Microbiology, Marburg. For one main spectrum at least 80 subspectra with 30 spots per subspectra were averaged.

Peptide analysis of protein samples after SDS-PAGE separation and tryptic digestion

Protein samples were suspended in SDS-PAGE sample buffer and boiled for 5 minutes. Proteins were separated on 15% SDS-PAGE gels and stained with Coomassie Brilliant Blue R-250. The gel bands were cut out and destained with 30% isopropanol (v/v) containing 20 mM NH_4HCO_3. The gel pieces were dehydrated with 100% isopropanol and dried. Than the pieces were rehydrated in 5 mM NH_4HCO_3 in 10% acetonitrile (v/v) containing 0.013 g/L sequencing-grade modified trypsin (Promega) and incubated for 12 h at room temperature. The tryptic digested peptides were analyzed by Nano-LC/MS using the Proteomics Analyzer 4800 mass spectrometer mentioned above and see below.

3.5 Chemical labeling studies

Labeling of the *Re*-citrate synthase with the cysteine-modifying agent, iodoacetamide was performed with the following mixtures in potassium phosphate buffer, pH 8.0 with and without 5 mM DTT incubated under aerobic conditions for 15 minutes.

a) 10 µl *Re*-citrate synthase + 5 mM iodoacetamide

b) 10 µl *Re*-citrate synthase + 2 mM oxaloacetic acid

c) 10 µl *Re*-citrate synthase + 5 mM iodoacetamide + 2 mM oxaloacetic acid

After the incubation period, the protein samples were digested with trypsin in Tris/HCl pH 7.8 for 3 h at 37 °C and separated and analyzed at the MPI for Terrestrial Microbiology, Marburg with the Nano-LC/MS system Ultimate 300 (Dionex, Idstein, Germany). The column was PepMap100, C18, 3 µm, 100 A, ID 75 µm, length 15 cm. The buffers were 0.05% trifluoroacetic acid in water and 0.04% trifluoroacetic acid in 80% acetonitrile in water. The flow rate was 0.3 µl/min. A protein sample without idoacetamide subjected to the same digestion procedure was used as reference. Using the Mascot Search system (Matrix Xcience

Ltd., UK), the sequences were matched to the known sequences of the proteins available in the NCBI (National Center for Biotechnology Information) database and modified residues were identified.

3.6 Metal ion analysis

Inductively Coupled Plasma-Optical Emission Spectrometer (ICP-OES) was used for analyzing metal ion of recombinant *Re*-citrate synthase. The recombinant enzyme was inactivated by adding 10 µM EDTA, pH 8.0 and incubated at room temperature for 10 minutes. To remove EDTA, the sample was applied to PD-10 Desalting column. The presence of protein in the elution fractions was followed by the Bradford assay and fractions without EDTA were sorted by enzyme activity assay. Enzyme only fractions were collected and concentrated. Buffer (50 mM Tris/HCl, pH 8.0, 150 mM NaCl), enzyme with and without EDTA treatment were sent to The Chemical Analysis Laboratory - center for applied isotope studies (University of Georgia, Athens, USA) for ICP-OES analysis.

3.7 Enzyme activity assays

3.7.1 Citrate synthase

Citrate synthase activity was measured at room temperature aerobically. The assay mixture contained 100 mM Tris/HCl, pH 8.0; 0.2 mM 5,5'-dithiobis(2-nitrobenzoic acid) (DTNB); 0.2 mM oxaloaceate; and 0.1 mM acetyl-CoA. The activity with and without 0.2 mM metal ion was also measured. The reaction was started by addition of enzyme and monitored spectrophotometically by the formation of the anion of thionitrobenzoate from DTNB and CoA at 412 nm ($\Delta\varepsilon_{412}$ = 14.2 $mM^{-1}cm^{-1}$) (Riddles et al, 1983)

$$\text{Acetyl-CoA} + \text{Oxaloacetate} + H_2O \rightarrow \text{Citrate} + \text{CoA-SH}$$

$$\text{CoA-SH} + \text{NBS-SBN (DTNB)} \rightarrow \text{CoA-S-S-BN} + \text{NB-S}^- + H^+$$

The reaction could also be measured by the absorbance change of the thioester bond of acetyl-CoA at 232 nm ($\Delta\varepsilon_{232}$ = 5.4 $mM^{-1}cm^{-1}$) (Buckel & Eggerer, 1965; Srere & Kosicki, 1961).

3.7.2 Carboxyltransferase of glutaconyl-CoA decarboxylase

The carboxyltransferase (GcdA) of glutaconyl-CoA decarboxylase activity was determined using the same assay for native glutaconyl-CoA decarboxylase but in the presence of 5 mM D-biotin. The auxiliary enzymes (glutaconate CoA-transferase, enoyl-CoA hydratase, (3*S*)-3-hydroxybutyryl-CoA dehydrogenase, acetyl-CoA acetyltransferase, phosphate acetyltransferase) and Gcd from *A. fermentans* were purified by Iris Schall (Philipps Universität Marburg). The assay was started by addition of the recombinant GcdA, and followed by the increase of the absorbance of NADH at 340 nm ($\Delta\varepsilon_{340}$ = 6.3 $mM^{-1}cm^{-1}$). Contents in total volume of the assay (500 µl) were as shown below (Buckel, 1986a).

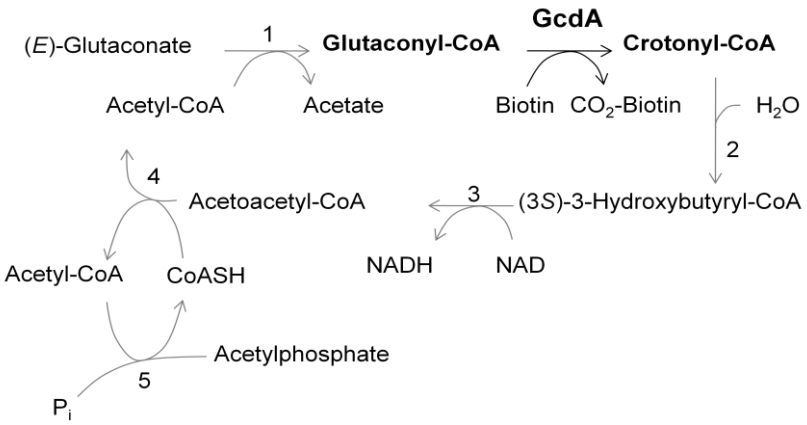

Sum: $Glutaconate^{2-} + H_2O + NAD^+ + HPO_4^{2-} \rightarrow Acetate^- + CO_2 + NADH + acetyl\text{-}phosphate^{2-}$

Scheme 3. Assay of glutaconyl-CoA decarboxylase (Gcd). 1, Glutaconate CoA-transferase (EC 2.8.3.12); 2, eonyl-CoA hydratase (crotonatse) (EC 4.2.1.17); 3, (3*S*)-3-hydroxybutyryl-CoA dehydrogenase (EC 1.1.1.35); 4, acetyl-CoA acetyltransferase (thiolase) (EC 2.3.1.9); and 5, phosphate acetyltransferase (EC 2.3.1.8).

Reagents in 1 ml test,

H_2O	up to 1 ml
0.5 M phosphate, pH 7, 0.1% DM	100 µl
1 M NaCl	20 µl
0.1 M DTE/0.1 M EDTA	20 µl
0.1 M NAD	10 µl
2 mg/ml Acetylphosphate	10 µl
10 mg/ml CoASH	10 µl

10 mg/ml Auxiliary enzymes	20 µl
0.1 M Glutaconic acid	10 µl
5 mM D-Biotin	
Enzyme	x µl

3.7.3 Glutaconate CoA-transferase from *A. fermentans*

Glutaconate CoA-transferase activity was assayed aerobically at room temperature. The increase of absorbance was followed at 412 nm ($\Delta\varepsilon_{412}$ = 14.2 $mM^{-1}cm^{-1}$). Reagents used in assay are 0.1 M potassium phosphate, pH 7.0, 0.2 M sodium acetate, 1 mM oxaloacetate, 1 mM DTNB, 20 µg citrate synthase, 0.1 mM glutaryl-CoA, total volume in 0.5 ml (Buckel et al, 1981; Jacob et al, 1997). The assay is based on reaction of free thiol of CoA with DTNB.

3.7.4 Glutamate determination

The concentration of glutamate was measured at room temperature. The assay contained 100 mM potassium phosphate, pH 7.4, 1 mM oxaloacetate, 0.2 mM NADH, 4 U (*R*)-2-hydroxyglutarate dehydrogenase and up to 0.1 mM (*S*)-glutamate. The reaction was started with 2 U aspartate aminotransferase. The commercial enzyme was obtained as suspension in 2 M ammonium sulfate and 2 mM 2-oxoglutarate. Prior to the assay, the enzyme suspension was centrifuged and the pellet was dissolved in the assay mixture. The oxidation of NADH was followed at 340 nm. In the rage of 0 – 100 µM glutamate, the change of absorbance was linear (Bennett et al, 2009).

3.8 Determination of the stereospecificity of citrate synthase

3.8.1 Enzymatic [^{14}C]citrate synthesis

The synthesis was performed under aerobic conditions. The 1 ml reaction mixture contained 50 mM Tris/HCl, pH 8.0, 1 mM ATP, 0.1 mM CoASH, 2 mM malate, 1 mM NAD^+, 20 mM $MgCl_2$, 100 mM KCl, and 0.2 mM $MnCl_2$. [1-^{14}C]Acetyl-CoA was generated from [1-^{14}C]acetate by acetyl-CoA synthetase using ATP and CoASH. Malate dehydrogenase

catalyzed the oxidation of malate to oxaloacetate by NADH consumption. The reaction was followed by monitoring NADH spectrophotometrically at 340 nm. After overnight incubation at room temperature, the reaction was stopped by heating the mixture to 95 °C for 10 minutes. Proteins were removed by centrifugation, and the supernatant was applied to an ion-exchange column (Dowex 1×8 formate, 200 − 400 mesh). After loading the sample, the column was washed with 10 volumes of 1 M formic acid to elute unreacted [^{14}C]acetic acid. Citric acid was eluted with 4 M formic acid. The fractions were combined and concentrated by evaporation and the citric acid was dissolved in 500 µl 50 mM Tris/HCl, pH 8.0. A 50 µl sample of each fraction was added to 5 ml Quicksave A scintillation fluid (Zinsser Analytic, Frankfurt) and ^{14}C-radioactivity was measured by scintillation counting machine (Li et al, 2007).

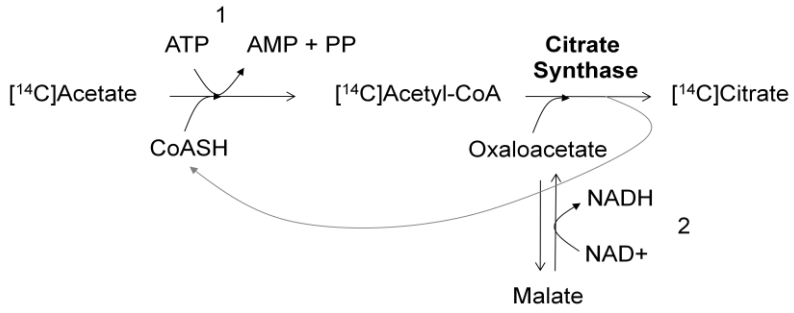

Scheme 4. Enzymatic [^{14}C]citrate synthesis. 1, Acetyl-CoA synthetase; 2, malate dehydrogenase.

3.8.2 Enzymatic [^{14}C]citrate cleavage

The reaction mixture, total volume 1.0 ml, contained 50 mM Tris/HCl, pH 8.0, 0.3 mM NADH, 0.2 mM $MgCl_2$, malate dehydrogenase, *Si*-specific citrate lyase, and [^{14}C]citrate synthesized and purified as described above. *Si*-Face specific citrate lyase cleaves citrate in such a way that the *Si*-'arm' of citrate yields acetate and the remaining part oxaloacetate. Malate dehydrogenase converted oxaloacetate to malate by using NADH. The reaction was observed by monitoring NADH at 340 nm spectrophotometrically. After 30 minutes incubation at room temperature, the sample was heated. The supernatant was applied to a column (Dowex 1×8 formate, 200 − 400 mesh). Acetate was eluted with 0.2 M formic acid and malate was eluted with 1 M formic acid (Li et al, 2007).

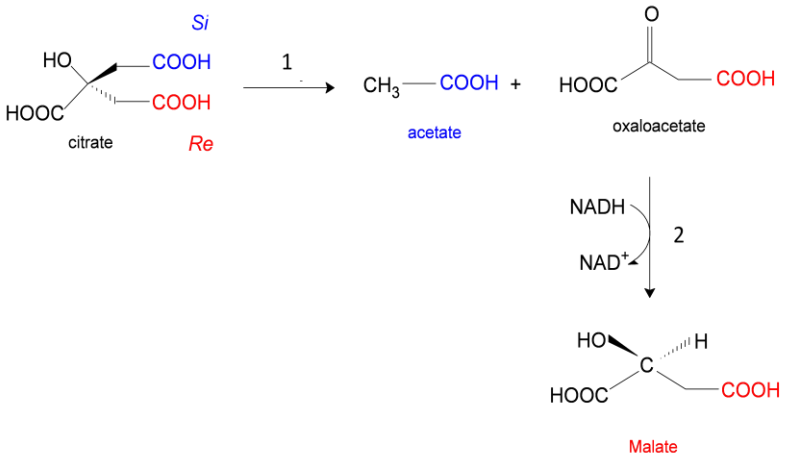

Scheme 5. Enzymatic [^{14}C]citrate cleavage. 1, *Si*-specific citrate lyase; 2, malate dehydrogenase.

3.9 Growing cells with [1-^{14}C]acetate or NaH^{13}CO$_3$

Growing with [1-^{14}C]acetate

The *S. aciditrophicus* pure culture in 500 ml defined medium containing 20 mM crotonate, 1 mM acetate and 100 µCi [1-^{14}C]acetate was incubated at 37 °C without shaking until the growth rate reached the beginning of the stationary phase. Samples of 1 ml were taken daily to measure growth and radioactivity. The purity of the preculture was checked by sequencing the 16S rRNA gene.

Growing with NaH^{13}CO$_3$

A basal medium with 20 mM crotonate containing 1 g of sodium hydrogen [^{13}C]carbonate in 250 ml was prepared according to the anaerobic techniques described earlier. Cultures were incubated at 37 °C without shaking. The cells were incubated until the growth rate reached to stationary phase.

3.10 Separation of labeled glutamate from the culture

In case of the ^{14}C-labeled culture, each step was monitored by adding a certain amount of medium to 5 ml Quicksave A scintillation fluid, and the ^{14}C radioactivity (counts per minute, cpm) was determined by liquid scintillation counting.

Separation of amino acids from the medium

The cells were harvested and washed with buffer (Tris/HCl, pH 8.0). The cell pellet was acidified by adding in 1.5 ml of 6 M HCl and hydrolyzed at 99 °C over a weekend. The hydrolyzed cell lysate was divided into supernatant and pellet by centrifugation.

The supernatant was applied to an ion exchange column (Dowex 50W × 8) at room temperature. After the column was washed with 5 volumes of water, the amino acids were eluted followed by 5 – 6 volumes of 1 N NH_3. The fractions obtained were combined and concentrated by flash evaporation, and the concentrated sample was dissolved in 1 ml H_2O.

Isolation of labeled glutamate

To isolate labeled glutamate from the amino acid mixture, the sample mentioned above was loaded on an ion exchange column (Dowex formate, 200 − 400 mesh) at room temperature. Neutral amino acids were eluted with H_2O and glutamate and aspartate with 1 M HCOOH. Fractions were collected and concentrated by evaporation.

The labeled glutamate was separated from aspartate by thin-layer chromatography (TLC). The solvent system used for descending chromatography on TLC Silica gel 60 F_{254} aluminum sheet (Merck) were isobutanol-formic acid-water (30:5:7.5, by volume). Radioactive spots were located by means of a Storm 860 Molecular Imager (Molecular Dynamics, Sunnyvale, USA). A region relevant to the labeled glutamate was cut and the glutamate was extracted from the silica gel by H_2O.

3.11 Determination of labeled carbon in the carboxyl group of glutamate

A Warburg vessel contained 0.8 ml of 0.5 M acetate buffer, pH 4.0, 1.5 ml of 10% (w/v) chloramine-T, and 0.1 ml of 20% (w/v) formaldehyde in the main compartment; 0.1 ml of labeled glutamate in the side arm; and 0.1 ml of 1 M hyamine hydroxide in methanol in filter paper in the center well. The vessel was shaken for 1 h at 30 °C after the amino acid was added to the chloramines-T solution. Radioactivity of carbon dioxide trapped by hyamine was determined in the scintillation counter (Gottschalk & Barker, 1966).

3.12 Crystallization

The recombinant *Re*-citrate synthase was purified by Strep-Tactin and gel filtration columns. The purity of the protein was tested by SDS-PAGE. The crystallization screening kits were kindly provided from a group of Dr. S. Shima, MPI Marburg. Initial crystallization trials were performed with the sitting drop vapor diffusion method using Wizard I/II/III random sparse matrix crystallization screen from Emerlad BioSystems (USA) and Basic crystallography and Extension kits for proteins (#82009 and #70437, respectively) from Sigma. At a 96 well protein crystallization plate, 100 µl of screening reagent was put in a reservoir well. 1 µl of protein was placed on a drop well and mixed with 1 µl of the screening reagent. After loading and mixing the protein and screening reagents, the plate was covered tightly by a sealing tape and kept at 4 °C. Regularly, the precipitants in the wells were checked under a microscope.

3.13 Antibody production

For the successful production of polyclonal antibodies, antigen purity and quantity are the most important factors. To exclude any contaminant protein from the antigen, purified *Re*-citrate synthase was loaded on SDS-PAGE. The advantage of antibody production with gel fragments is that the antigen diffuses just slowly out of the gel and ensures antigen presentation for a long time. The standard Coomassie staining procedure was used because the dye did not interfere with the antibody evolution. The gel was washed thoroughly in water to remove acetic acid and methanol residues and the bands of interest were cut out. The gel was cut into pieces and stored in separate tubes for each injection (100 µg per injection) containing 100 µl of H_2O to avoid drying of the gel fragments. The tubes were sent to Eurogentec, Belgium. Two rabbits were selected as hosts and the classic program was applied for 3 months. With SDS-PAGE gel fragments the speedy protocol that requires only one month is not compatible and for ethical reasons mouse, rat or Guinea pig cannot be selected as hosts. Blood samples were collected before and after immunization (at 38, 66 and 87 days). The obtained antisera were checked for antibody titer level and screened against pure *Re*-citrate synthase by western blot.

3.14 Western blot

The protocol was kindly provided from Sarah Schladebeck (group of Prof. Hans-U. Mösch, Philipps-Universität Marburg). A purified protein aliquot was transferred from a SDS-PAGE gel to a Protran nitrocellulose transfer membrane (Whatman, GE Healthcare) by either wet transfer at 100 V for 1 − 2 h or semi-dry at 10 V for 1 h. The membrane was equilibrated in 1 × TBS and proteins on membrane were stained unspecifically by Ponceau S solution for 5 – 10 minutes to check blotting efficiency. Afterwards, the membrane was neutralized by 1 × TBS for 5 minutes, 3 times and blocked by 1 × TBS containing 2 − 4% milk powder and 0.1% Tween for 45 minutes. Detecting antibody was performed by following chemicals and procedures:

1. incubate the membrane in 10 ml 1 × TBS + 2 – 4% milk powder + 0.1% Tween + antiserum for 1 – 3 h or overnight at 4 °C.
2. rinse the membrane 1 × 10 minutes by 1 × TBS + 2 – 4% milk powder + 0.1% Tween
3. remove the non-bound antibody by 1 × TBS + 0.1% Tween for 2 × 10 minutes
4. incubate the membrane in 10 ml of 1 × TBS + 2 – 4% milk powder + 0.1% Tween + secondary antibody (goat anti rabbit IgG peroxidise-label (SantaCruz, CA) for 1 − 2 h at room temperature
5. discard buffer and add and mix ECL solution A and B to the membrane and incubate it for 1 minute with gentle shaking
6. discard the solution and wrap the membrane in polythene foil
7. expose the membrane under the Chemo Star Imager (INTAS Science Imaging Instruments, Göttingen, Germany)

Singals were quantified using a scanner and the ImageQuant TL software (GE Healthcare, Freiburg, Germany).

Solutions for western blot:

10 × Transfer buffer	0.25 M Tris, 2 M glycine, 0.2% SDS, freshly add 20% methanol to 1 × diluted buffer
10 × TBS	200 mM Tris, 1.37 M NaCl, adjust pH with HCl to 7.6
Ponceau S solution	0.2% Ponceau S, 3% TCA
ECL solution A	2.5 mM Luminol in DMSO, 400 µM paracumaric acid in DMSO, 100 mM Tris/HCl pH 8.5
ECL solution B	5.4 mM H_2O_2, 100 mM Tris/HCl pH 8.5

Results

I. Biosynthesis of glutamate in *S. aciditrophicus*

1. Putative genes for the biosynthesis of glutamate in *S. aciditrophicus*

Glutamate is usually synthesized from acetyl-CoA via parts of the TCA cycle; citrate, isocitrate and 2-oxoglutate. The genome of *S. aciditrophicus* reveals that the there is an incomplete TCA cycle in this organism (Fig. 11). A gene cluster for TCA cycle is not present. No genes for *Si*-citrate synthase and malate dehydrogenase have been detected. There is a gene encoding NAD-dependent malic enzyme (SYN_00517), which catalyzes the oxidative decarboxylation of malate to pyruvate. The protein deduced from the gene SYN_00517 shares 60% amino acid sequence identity with malate dehydrogenase, oxaloacetate-decarboxylating from *Thermoanaerobacter* sp. and 22% with the malate dehydrogenase from *C. acetobutylicum* ATCC824.

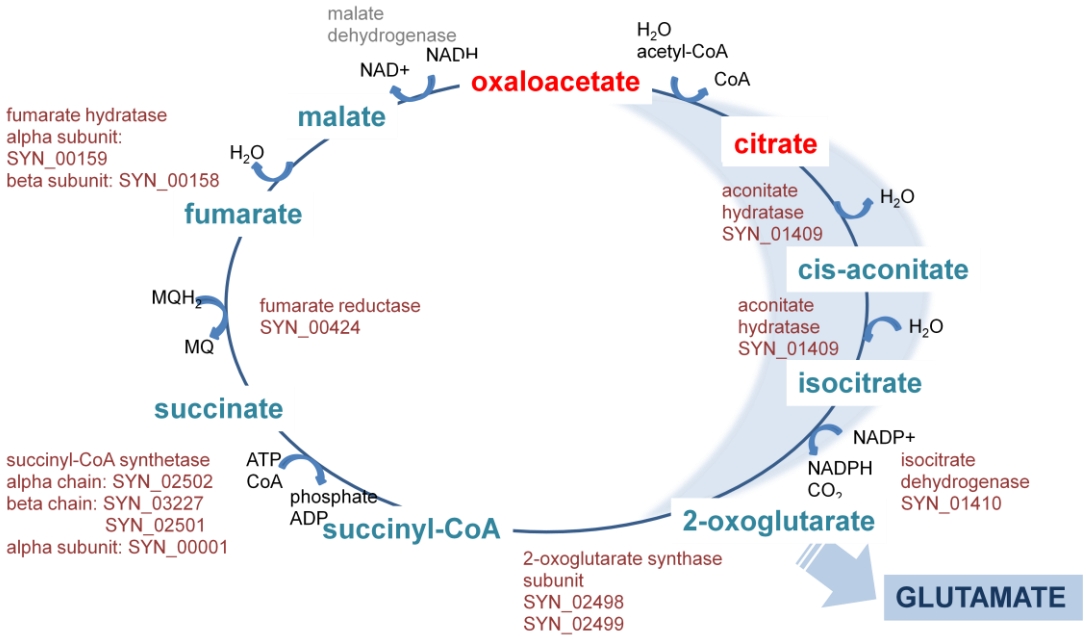

Fig. 11. The TCA cycle and the genes annotated as the enzymes catalyzing the reactions in *S. aciditrophicus*. The genes were found by the BIOCYC database collection (http://biocyc.org) and Kyoto Encyclopedia of Genes and Genomes (KEGG, http://www.genome.jp/kegg). The substrate and product of the entry step of the TCA cycle catalyzed by citrate synthase were coded as red color.

It has been proposed that glutaconyl-CoA cold be the precursor of 2-oxoglutarate obtained by benzoyl-CoA degradation or carboxylation of crotonyl-CoA pathway depending on the carbon source of the organism either benzoate or crotonate. Glutaconyl-CoA can be hydrated to 2-hydroxyglutaryl-CoA. CoA-transfer and oxidation would lead to 2-oxoglutarate, the direct precursor of glutamate. Some of the genes involving this hypothesis were detected, for example, SYN_01576 and SYN_00371 encoding activators of 2-hydroxyglutaryl-CoA dehydratase; SYN_00370, SYN_00369, and SYN_00368 are annotated as benzoyl-CoA reductase/2-hydroxyglutaryl-CoA dehydratase subunits.

2. The recombinant *Re*-citrate synthase in *E. coli*

2.1 Sequence analysis of the putative gene for *Re*-citrate synthase

The genome of *S. aciditrophicus* contains no gene for *Si*-citrate synthase but a gene for isopropylmalate/homocitrate/citramalate synthase (SYN_02536, *rcs*) similar to the gene coding for *Re*-citrate synthase from *Clostrsium kluyveri* (Li et al, 2007). The gene is composed of 1,905 base pairs (GC content: 50.76%) and codes for 634 amino acids with a calculated molecular mass of 72.4 kDa and an isoelectric point of 4.38. The direction of the transcription was forward. A Shine Dalgarno sequence was found after the first leucine which was predicted as start codon but this mis-prediction led to include a non-protein coding sequence of the N-terminus. Therefore, the first 15 nucleotides were omitted for heterologous gene expression (Fig. 12). The gene starts with the second methionine, consists of 1,890 base pairs and is predicted to encode a 629 amino acid polypeptide with a calculated mass of 71.8 kDa. The deduced amino acid sequence showed 49% identity to *Re*-citrate synthase from *C. kluyveri* but ca. 20% identity to *Re*-specific citrate synthase and isopropylmalate synthase from *Syntrophomonas wolfei*, *Dehalococcoides sp*. VS, and *Mycobacterium tuberculosis*, respectively (Fig. 13). Substrate and metal binding site are relatively conserved (Li et al, 2007). Comparison of the amino acid sequence with sequences in the databank revealed additional levels of identity to several pyruvate carboxyltransferases from *Deltaproteobacteria* and Gram positive anaerobic bacteria.

attttctgtaactgctatagaaaatagtctctttagcgaaaactatttgcgttggagtttgagatcATGgccaaa
tggaatccccagaaaagagtgttgaatcatgagcatacccgattctggcgctttgaattgcgggatgtggatgaa
ccgaatcttcagaaagaagtattcccctatgacgaagtcagccggatcgactttgatcaccggattattcccatc
cagcccgctgaagaaatttttattaccgatacgacatttcgggatgggcagcaggccagacctccttacacgact
cagcagatcgtcgacctttaccagatgatgagccgccttggcggatacaatggaattatccggcagacggagttt
tttctttacagcaatcgggataaggaagccgtcagaatgtgccaggaccttggcctgcaatatcctgaaattacg
ggttggatccgggctgcccgggaagacatccccctggtgaaagaagccggtctgaaggaaacagggattctgacc
tccgtgtccgactatcacatcttccttaaattgaacatgacccgaagtcaggcccttgaagaatatctgggaatc
gtcaaggcgatcctggatgccggcatcgttccccgctgccacttcgaagatatcacccgtgcggacatttatgga
ttctgcatccccttcgccatcgagctgatgaagcttcgggaggaaagcggtgtggatatcaagatcaggctctgc
gataccatgggatacggtgtgacctatccgggcgcttcgctgccgcgtggtgtcgacaaactggtgcgggcgttc
attgatgacgccgatgtgcccggccgacttctggaatggcatggccacaacgattttcataaagccctgatcaac
gcgactaccgcatggctttacggctgcagcgccgccaattccactctgctcgggctgggcgagcggacgggcaat
ccccctattgaggggcttattattgaatatatcgggctcatgggaaagacaaacgggatcgacacgacggtgatt
actgatatcgcaaattactttaaaaatgaaatcgaatacaaaatcccgtccaattacccctttgtcggcgcggat
ttcaatgttacccgggctggtgttcacgctgacggcctgatcaagagtgaagagatctacaacatcttcaacacg
acgaagattctgaagcgtcccatcgtacccatgatcaccgacaagtccggaaaagctggcatcgcttactggatc
aactcgcatttcggactgtccggcgacagtaccgtggataagcgacaccccggcatttcgaagatcaacaaatgg
atcgcggatgagtatgaattggggcgagtcaccaccatttccacggaagaactcgaggcgaaggttcgcaagtat
atgccggaactcttcatgtctgatctggaaaggatcaaattcaaagcggcggaagcagccatcgccgtactgcgc
aagatcatcgatgatccggccatgaaaacgatgcaacctgaactccaggaaccggtaatgcagcggtttatcgag
gaataccccctcgatccagtttgcatacgtggtggacatgaacggcaagaagaccacgagaaacatcacgaatatc
gttgatcgcgccaaatatgaaaactacggcgtgggaacggatcagtccgatcgggaatggttcatcaagccgctg
cagacgggcaaacttcatgtgactgatttttacatttccaaaatgacgggcgccctctgctttaccgtttcagaa
ccgattacagatgacaatgacgatatggtcggaatttttggagtggatattcgcgttgaagatctggttaaagag
cctgaatatatcgccgaagcaacgcagatcgccctgaaagcggaatatgacgcgaaatacaaatcagatcactgg
ctgTAAacagataaatacaggaactcaccactgctcttcgacaac

Fig. 12. The reverse complement nucleotide sequence of isopropylmalate/homocitrate /citramalate synthase (SYN_02536, *rcs*) of *S. aciditrophicus* SB. A predicted start codon of the database is underlined. The Shine-Darlgano sequence is depicted in bold letters and in a grey box. Start and stop codons are depicted as bold capital letters and underlined.

```
SWol          ----------------------------------------MTRSSMNKDWFLEEGARV- 18
Dehalo        ------------------------------------------------------MGKI- 4
SAcidi        MAKWNPQKRVLNHEHTRFWRFELRDVDEPNLQKEVFPYDEVSRIDFDHRIIPIQPAEEI- 59
CKluy         MKKCS-------------YDYKLNNVNDPNFYKDIFPYEEVPKIVFNNIQLPMDLPDNI- 46
MTuber        ----------------------------MPVNRYRPFAEEVEPIRLRNRTWPDRVIDRAP 32

SWol          NIVDTTLRDGEQTAGVVFTNNEKIQIARYLDMIGVDQIEAGIP----VMGGFEKDCIKEI 74
Dehalo        FIIDVTNRDGVQTARLGLSKLEKTLINMYLDEMGIFQSEFGFPTTKHERGYVEANLELAK 64
SAcidi        FITDTTFRDG-QQARPPYTTQQIVDLYQMMSRLGGYNGIIRQTEFFLYSNRDKEAVRMCQ 118
CKluy         YITDTTFRDG-QQSMPPYTSREIVRIFDYLHELDNNSGIIKQTEFFLYTKKDRKAAEVCM 105
MTuber        LWCAVDLRDGNQALIDPMSPARKRRMFDLLVRMGYKEIEVGFPSAS-QTDFDFVREIIEQ 91

SWol          VALGLKSSIMAWNRAVIADIKESLDCG--VDAVAISISTSDIHIEHKLQTTR--QDVLNR 130
Dehalo        MGVIKNLRLEGWIRAIVADVDLAFRRAPGLKHLNLSISTSEQMINGKFQGRKVFTDIIDD 124
SAcidi        DLGLQYPEITGWIRAARED IPLVKEAGLKETGILTSVSDYHIFLKLNMTRSQALEEYLGI 178
CKluy         ERGYEFPEVTSWIRADKEDLKLVKDMGIKETGMLMSCSDYHIFKKLKMTRKETMDMYLDL 165
MTuber        GAIPDDVTIQVLTQCRPELIERTFQACSGAPRAIVHFYNSTSILQRRVVFRANRAEVQAI 151

SWol          MADAVKFAKDKGLYIS-VNAEDASRSDIDFLTEFALLAKRS-GADRLRFCDT-----VGT 183
Dehalo        MTVAVNAAYAKGAETVGVNAEDASRTSIVNLIEFGKAAKAA-GAARLRYCDT-----LGY 178
SAcidi        VKAILDAGIVPRCHFEDITRADIYGFCIPFAIELMKLREESGVDIKIRLCDT-----MGY 233
CKluy         AREALNNGIRPRCHLEDITRADFYGFVVPFVNELMKMSKEANIPIKIRACDT-----LGL 220
MTuber        ATDGARKCVEQAAKYPGTQWRFEYSPESYTGTELEYAKQVCDAVGEVIAPTPERPIIFNL 211

SWol          LTPLS-------AFRYIKTLIDAVGIN---IEMHTHNDFGMATANALAGVYAGAN----- 228
Dehalo        DNPFT-------IYETARTLSEKVEMP---IEIHCHGDLGMAIGNSLAGAKGVVDGGQDV 228
SAcidi        GVTYPGASLPRGVDKLVRAFIDDADVPGRLLEWHGHNDFHKALINATTAWLYGCS----- 288
CKluy         GVPYNGVEIPRSVQGIIHGLRNICEVPSESIEWHGHNDFYGVVTNSSTAWLYGAS----- 275
MTuber        PATVEMTTPNVYADSIEWMSRNLANRESVILSLHPHNDRGTAVAAAELGFAAGAD----- 266
```

```
SWol            YVGVTINGLGERAGNACLQETIMGLKYLMNVNLTYNT------TLFREVAEYVAQASGRA 282
Dehalo          YVNTTINGIGERAGNADLVAFLLAVLKSKGFGEKYQLGHEVDLSKAWKIARFASYAFDVE 288
SAcidi          AANSTLLGLGERTGNPPIEGLIIEYIGLMGKTNGIDT------TVITDIANYFKNEIEYK 342
CKluy           SINTSFLGIGERTGNCPLEAMIFEYAQIKGNTKNMKL------HVITELAQYFEKEIKYS 329
MTuber          RIEGCLFGNGERTGNVCLVTLGLNLFS-RGVDPQIDF------SNIDEIRRTVEYCNQLP 319

SWol            LSVSKPIVGSGIFAHESGIHGDGVLK-------NPLTYEVFSPEEVG--------LERQI 327
Dehalo          IPINQPGVGRNCFAHASGIHADGVIK-------DSQNYELYGYEELGRGEALMVETGREI 341
SAcidi          IPSNYPFVGADFNVTRAGVHADGLIK-------SEEIYNIFNTTKILKRPIVPMITDKSG 395
CKluy           VPVRTPFVGTDFNVTRAGIHADGILK-------DEEIYNIFDTDKILGRPVVVAVSQYSG 382
MTuber          VHERHPYGGDLVYTAFSGSHQDAINKGLDAMKLDADAADCDVDDMLWQVPYLPIDPRDVG 379

SWol            VIGKHSGTAAVRSKFT-REYNIELND---------TEAAQILARVREMSIELKRSLFDKE 377
Dehalo          CAGQYSGISGFRHVMGNMSVELPEDK---------DEANKILELVRYANVEAHKPLVEDE 392
SAcidi          KAGIAYWINSHFGLSG--DSTVDKRH---------PGISKINKWIADEYELGRVTTISTE 444
CKluy           RAGIAAWVNTYYRLKD--EDKVNKND---------SRIDQIKMWVDEQYRAGRTSVIGNN 431
MTuber          RTYEAVIRVNSQSGKGGVAYIMKTDHGLSLPRRLQIEFSQVIQKIAEGTAGEGGEVSPKE 439

SWol            LMYIYEELYGK--AR---------------------------------------------- 390
Dehalo          LIFIAKYPEIS--RRLLTLTPLMND---------------------------------- 415
SAcidi          ELEAKVRKYMP--ELFMSDLERIKFKAAEAAIAVLRKIIDDPAMKTMQPELQEPVMQRFI 502
CKluy           ELELLVSKVMP--EVIEKTEERAS------------------------------------ 453
MTuber          MWDAFAEEYLAPVRPLERIRQHVDAADDDGGTTSITATVKINGVETEISGSGNGPLAAFV 499

SWol            ------------------------------------------------------------
Dehalo          ------------------------------------------------------------
SAcidi          EEYPSIQFAYVVDMNGKKTTRNITNIVDRAKYENYGVGTDQSDREWFIKPLQTGKLHVTD 562
CKluy           ------------------------------------------------------------
MTuber          HALADVGFDVAVLDYYEHAMSAG---------DDAQAAAYVEASVTIASPAQPGEAGRHA 550

SWol            ------------------------------------------------------------
Dehalo          ------------------------------------------------------------
SAcidi          FYISKMTGALCFTVSEPITDDNDDMVGIFGVDIRVEDLVKEPEYIAEATQIALKAEYDAK 622
CKluy           ------------------------------------------------------------
MTuber          SDPVTIASPAQPGEAGRHASDPVTSKTVWGVGIAPSITTASLRAVVSAVNRAAR------ 604

SWol            -------
Dehalo          -------
SAcidi          YKSDHWL 629
CKluy           -------
MTuber          -------
```

Fig. 13. Homology analysis of *Re*-citrate synthase from *S. aciditrophicus*. The abbreviated sequence names indicate following genes: Swol, *Re*-citrate synthase from *Syntrophomonas wolfei*; Dehalo, 2-isopropylmalate/homocitrate/*Re*-citrate synthase from *Dehalococcoides sp*. VS; SAcidi, SYN_02536 from *S. aciditrophicus*; Ckluy, *Re*-citrate synthase from *Clostridium kluyveri*; MTuber, *Re*-specific isopropylmalate synthase from *Mycobacterium tuberculosis*. Conserved amino acids are highlighted in red (metal binding), blue (substrate binding), and black (cysteine).

2.2 Cloning and expression of *rcs* and protein purification

PCR primers were designed as described in Materials and Methods. The restriction enzyme *LguI* site was introduced in the primers for in-frame cloning into the vector pE plasmid. The amplified DNA fragment was cut with *LguI* and ligated into the entry vector. Then it was subcloned into the pASK-IBA3plus and pASK-IBA7plus vectors which support and C-/N-terminal fused *Strep-tag* II peptide protein for one-step purification. Three clones were sequenced to exclude possible errors of the DNA polymerase. The cloned gene is composed of 1,890 nucleotide base pairs as compared to the sequence from the nucleotide database of

the National Center for Biotechnology Information (NCBI) and the deduced 629 amino acids are 100% identical to the known sequence.

The constructed plasmid was transformed into *E. coli* Rosetta (DE3) pLysS strain to get more efficient protein production. The cells were grown aerobically in LB medium at 37 °C to an OD at 600 nm of 0.5 to 0.8. Expression of the cloned gene was induced by ATH (100 µg/L). After 3 h of growth, cells were harvested and cell free extract was obtained as described in Materials and Methods. N- and C-terminal Strep-tagged proteins were tried for purification using Strep-Tactin affinity chromatography, which was followed by SDS-PAGE. The protein of interest was always found in inclusion bodies, in spite of efforts to test various different induction conditions.

Therefore, coexpression with a molecular chaperone in *E. coli* was used to improve solubility of the target protein. The recombinant plasmid was transformed into *E. coli* strain BL21 GroEL, which contains the GroEL chaperone plasmid. The cells were grown in tryptone-phosphate (TP) medium that is a valuable adjunct to limit inclusion body formation (Moore et al, 1993). Two-step expression (de Marco, 2007) and purification were performed as mentioned at Materials and Methods (3.1.1). Co-expression with the molecular chaperone and the two-step culture were effective which resulted in over 50% soluble protein. But there was a contaminant protein band near target protein on SDS-PAGE (Fig. 14). The extra band was identified as co-purified chaperone by N-terminal Edman sequencing (Dr. Linder, Justus-Liebig-Universität, Gießen) and MALDI-TOF analysis (Jörg Kahnt, MPI Marburg) (Table 1).

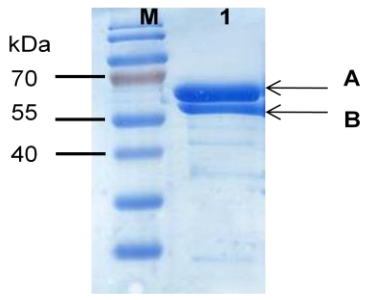

Fig. 14. SDS-PAGE of purified recombinant *Re*-citrate synthase and the contaminant protein. M, molecular mass marker; 1, purified fraction obtained by elution with D-desthiobiotin.

Table 1. N-terminal Edman sequencing of SDS-PAGE bands of Fig. 14.

	Deduced sequence	Sequence alignmnet	Sequence identity (%)
A	AKWNPQK-VLNHE-T(M)-FW(W)-	SYN_02536	77
B	AAKDVKFGNDA-VKML-GVN	Chaperonin GroEL	90

The coverage of the residues, i.e. the fraction of residues identified from the tryptic digest analyzed by MALDI-TOF was 72% for the deduced amino acid sequence of *rcs* and 69% for the chaperone. The sequences of peptides were identified by the database in EXPASY. Results of N-terminal Edman sequencing and MALDI-TOF mass spectrometry were consistent with the co-purification of the chaperone GroEL as contaminant protein band near the target protein on SDS-PAGE.

To remove the co-purifying chaperone impurity, a simple one step $MgCl_2$/ATP/KCl incubation procedure was applied (Joseph & Andreotti, 2008). Since the chaperone is likely to be bound to the protein of interest, mechanistic aspects of chaperone function have to be considered. Potassium ions when combined with $MgCl_2$/ATP promote disassembly of certain classes of chaperones into their component subunits. Potassium ions stimulate the ATPase activity of some chaperones and their disassembly into subunits, especially chaperonin 60 (GroEL), whereby the substrate is released. Incubation of the target protein immobilized on the Strep-Tactin resin with $MgCl_2$/10 mM ATP/KCl for 2 h at 4°C released the co-purified chaperone yielding around 95% pure protein. 20 mM ATP did not improve the purity of the protein and trace amounts of ATP during the elution seemed to inhibit the enzyme activity. Finally, remaining chaperone and chaperone-protein complex were removed by gel filtration (Fig. 15).

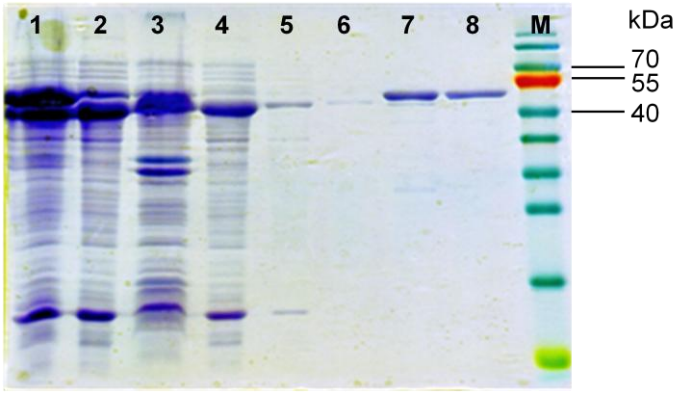

Fig. 15. SDS-PAGE of purified recombinant *Re*-citrate synthase. 1, cell lysate; 2, cell free extract after induction with AHT (200 µg/L); 3, pellet; 4, flow through of the Strep Tactin column; 5, washing; 6, 2nd washing after dissociation; 7, elution; 8, gel filtration; M, molecular mass marker.

2.3 Physical characterization of the recombinant protein

The purified protein (Rcs) showed a molecular mass of approximately 65 kDa on SDS-PAGE, which did not agreed well with the calculated mass of the deduced amino acids (71.8 kDa + 1 kDa Strep-tag II peptide). The molecular mass of the protein was measured by Electrospray-time of flight (ESI-TOF) mass spectrometry (Milko Velarde, MPI Martinsried). The predicted molecular mass in absence of the N-terminal methionine was 72891.16 Da and the measured mass was 72891.78 Da. The data of mass spectrometry reveal that Co^{2+} ion is not irreversibly incorporated into the enzyme. The metal content analysis by inductively coupled plasma optical emission spectrometer showed no metal tightly bound to the recombinant enzyme.

The quaternary structure of holoenzyme was determined by native PAGE (Fig. 16). Horse ferritin (450/720 kDa), jack bean urease (272/545 kDa), porcine lactate dehydrogenase (146 kDa), bovine serum albumin (67 kDa), egg albumin (45 kDa), and soybean trypsin inhibitor (21 kDa) from SERVA were used as molecular mass markers. The apparent molecular mass of the recombinant protein amounts to 146 kDa. On a gradient gels, as proteins migrate through the increasing acrylamide concentration, into regions of ever smaller pore sizes, their mobility decreases. In the end, each protein reaches its pore-limit, at which point it slows to minimum migrate rate, which is constant for all proteins at their pore limit. Once proteins reach their pore limit, their relative positions are a direct reflection of their molecular weight. In a linear gradient, log MW is proportional to log Rf over a wide range, although the curve is actually sigmoid in shape. This type of analysis is more subject to artefacts than the Ferguson

Plot (Ferguson, 1964). Thus, different concentrations of acrylamide gels for Native-PAGE were prepared and the recombinant Rcs was run along with bovine serum albumin (BSA) and the native molecular mass marker. Since the protein aggregation was observed by freezing and thawing, the recombinant protein was loaded on the Native gel directly after the gel filtration. On a Native gel, BSA forms monomer (64 kDa), dimer (128 kDa), trimer (192 kDa), and tetramer (256 kDa). Therefore, it was used as standard for calibrating Ferguson plot. Unfortunately, the BSA standard bands were smeared and undistinguishable so that it made calibration be difficult. Taken together, according to the native molecular mass marker loaded on the same gel, the holoenzyme seemed like a homodimer.

The purified protein was frozen at − 80°C. Thawing caused loss of 20% activity and protein aggregation as observed by native PAGE (data not shown), regardless how long the enzyme was kept at − 80 °C.

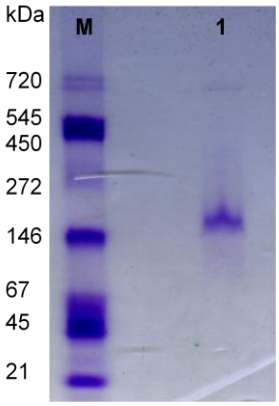

Fig. 16. Native PAGE of purified Rcs. The gel was stained with Coomassie Brilliant Blue R-250. M, SERVA Native Marker liquid mix; lane 1, 3.6 µg of purified recombinant Rcs.

2.4 Substrate specificity and catalytic properties

The gene was annotated as isopropylmalate/homocitrate/citramalate synthase. There sequence-related enzymes are *Re*-face stereospecific with respect to their substrates, 2-oxo-3-methylbutanoate, 2-oxoglutarate, and pyruvate. Thereby these substrates and oxaloacetate, in case of citrate synthase, were examined. The enzyme activity was measured at 412 nm by the formation of thionitrobenzoate from DTNB and CoA ($\Delta\varepsilon_{412}$ = 14.2 $mM^{-1}cm^{-1}$) at room temperature aerobically (Riddles et al, 1983).

Table 2. Determination of substrate specificity of the putative *Re*-citrate synthase

Substrate	Corresponding enzyme	$MnCl_2$	Specific activity (U/mg)
Pyruvate	Citramalate synthase	+/-	0
2-Oxoglutarate	Homocitrate synthase	+/-	0
2-Oxo-3-methylbutanoate	Isopropylmalate synthase	+/-	0
Oxaloacetic acid	*Re*-Citrate synthase	+	0.72
Oxaloacetic acid	*Re*-Citrate synthase	-	1.18

Table 2 shows that the purified gene product only catalyzes the synthesis of citrate from oxaloacetate (K_m = 85 µM) and acetyl-CoA (K_m = 130 µM). The activity with and without 0.2 mM $MnCl_2$ was also measured. The highest specific activity obtained was 1.6 U/mg in presence of with 0.2 mM $CoCl_2$. A sigmoidal curve ($\Delta A/min = f$ [oxaloacetate]) was detected when 0.2 mM $MnCl_2$ was absent in the assay mixture (Fig. 18). Preincubation of the enzyme with 0.2 mM metal ion at least 10 minutes helped to eliminate the sigmoidal curve. The activity of citrate synthase has been also measured by the absorbance change of the thioester bond of acetyl-CoA at 232 nm ($\Delta\varepsilon_{232}$ = 5.4 $mM^{-1}cm^{-1}$). Relative specific activity measured at 232 nm was 30% higher than the activity measured by DTNB assay at 412 nm (Fig. 19). The citrate synthase reaction was inhibited by iodoacetamide or carboxymethyl-CoA. The enzyme was inactivated by *p*-hydroxymercuribenzoate and EDTA. The EDTA-inactivated enzyme regained activity by addition of Mn^{2+}, Zn^{2+}, or Co^{2+} ions at a final concentration of 0.2 mM. However, 0.2 mM Zn^{2+} was not sufficient to convert the sigmoidal curve into a saturating curve. Co^{2+} was the most effective in restoring activity but Mg^{2+} had not effect. The enzyme was stable with Mn^{2+} or Co^{2+} at 4°C. After 14 days, the enzyme kept at 4°C with metal ions, showed 50% activity. The catalytic properties were similar to those reported from *Re*-citrate synthase partially purified from *C. acidiurici* and *C. kluyveri* except the enzyme from *S. aciditrophicus* is not oxygen-sensitive.

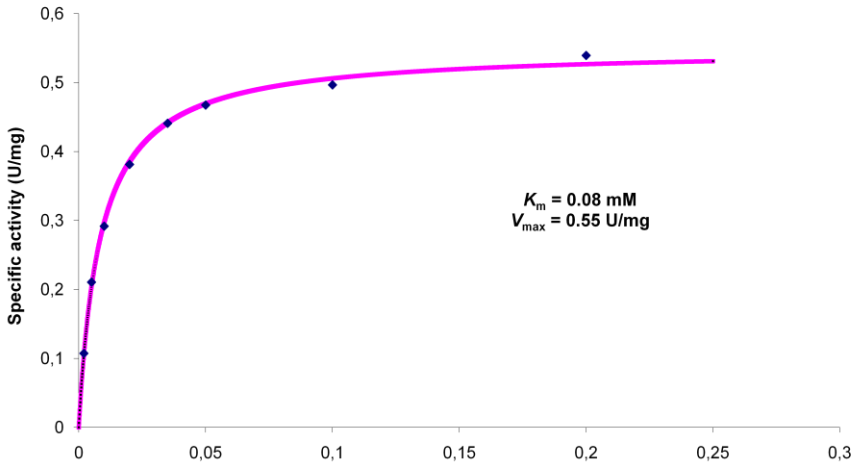

Fig. 17. Michaelis-Menten kinetics of the Rcs activity with oxaloacetate. The solid line represents the simulated curve and the concentration of acetyl-CoA was 0.2 mM.

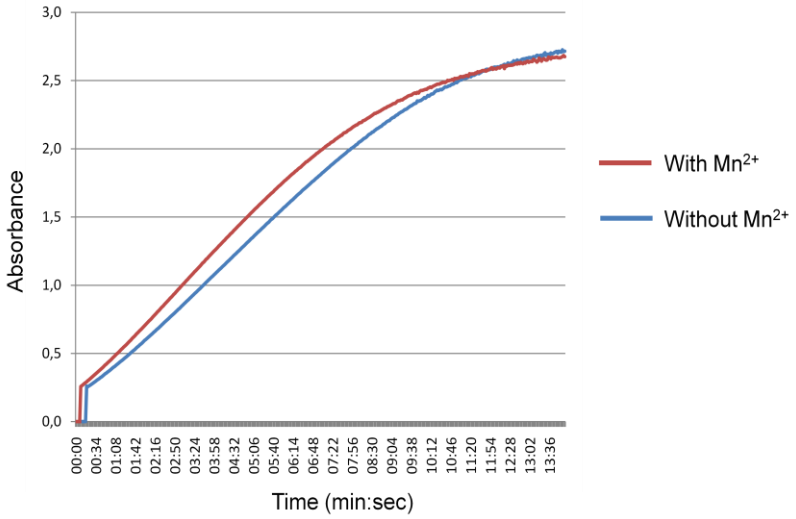

Fig. 18. Comparison of kinetics with and without Mn^{2+} in the assay mixture.

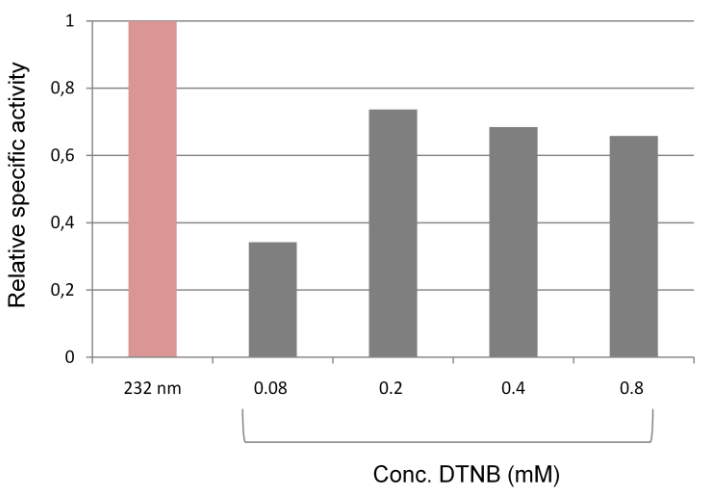

Fig. 19. Comparison of relative specific activity measured at 232 nm and at 412 nm with various concentrations of DTNB in the assay mixture.

2.5 Deuterium kinetic isotope effect

The kinetic isotope effect (KIE) on the Rcs was obtained with deuterium labeled acetyl-CoA by measuring the V_{max}/K_m values. Labeled [2-$^2H_3$]acetyl-CoA was synthesized and the activity was measured as described in Materials and Methods.

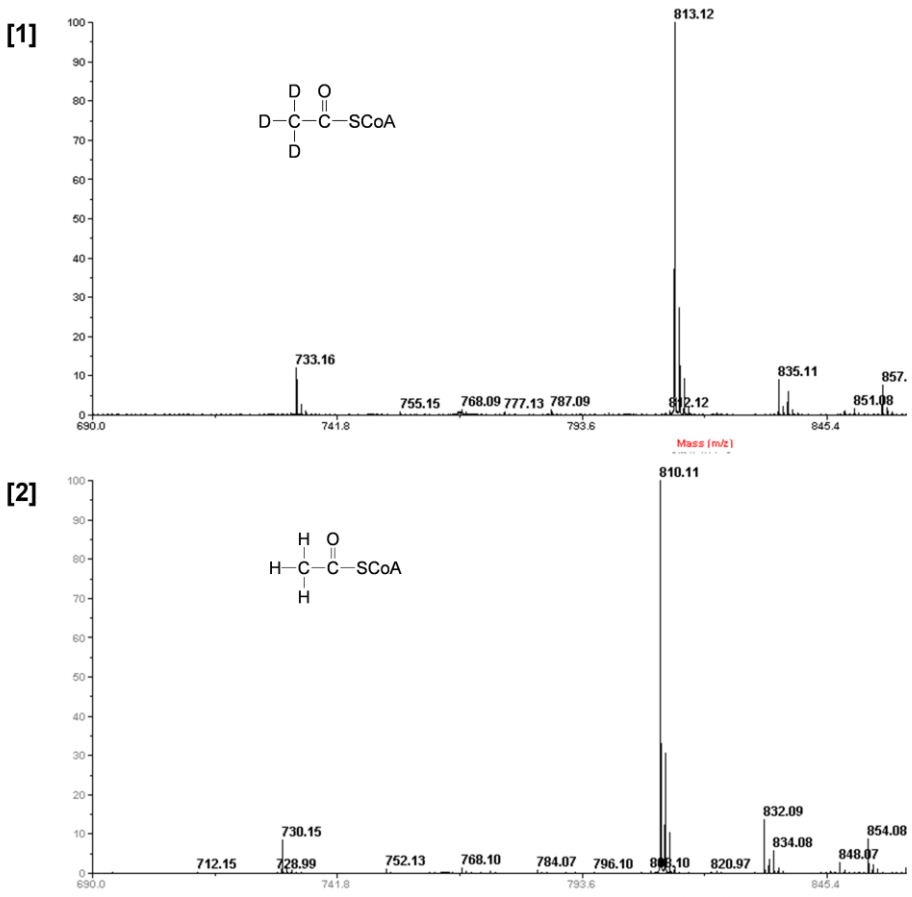

Fig. 20. MALDI-TOF mass spectra showing the peak [1] at 813.12 Da corresponding to [$^{2}H_3$]acetyl-CoA and [2] at 810.11 Da to [$^{1}H_3$]acetyl-CoA. X-Axis is mass (m/Z) and Y-axis is % intensity.

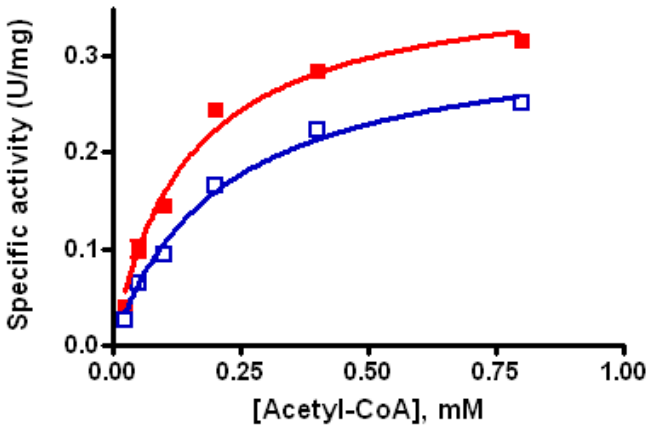

Fig. 21. Michaelis-Menten plot of the reaction rate as a function of acetyl-CoA concentration. ■ [$^{1}H_3$] unlabeled acetyl-CoA; □ [$^{2}H_3$] acetyl-CoA.

Table 3. K_m and V_{max} for kinetic isotope effect study.

	K_m (μM)	V_{max} (U/mg)
[$^1H_3$]Acetyl-CoA	147 ± 18	0.39 ± 0.02
[$^2H_3$]Acetyl-CoA	214 ± 21	0.33 ± 0.01

The kinetic isotope effect (k_H/k_D) on the Rcs was obtained with deuterium labeled acetyl-CoA by measuring the V_{max}/K_m values (Fig. 21 and Table 3). Labeled substrate was synthesized and the activity was measured as described in Materials and Methods. KIE calculated was 1.72 by Michaelis-Menten plot using the equation ($V_{max}[^1H]/K_m[^1H]$)/($V_{max}[^2H_3]/K_m[^2H_3]$).

2.6 Structural aspects

2.6.1 Chemical labeling

Iodoacetamide preferentially reacts with the SH group of cysteine which displaces the iodine resulting carboxyamidomethylated protein. If a cysteine sits in the active site, the substrate may protect it from modification. The reaction was performed with 5 mM iodoacetamide in 100 mM Tris/HCl pH 8.0 containing 5 mM DTT with and without 2 mM oxaloacetate. The reaction was incubated under aerobic conditions for 15 minutes. The samples and a control without iodoacetamide subjected to tryptic digestion, Nano-LC and MALDI-TOF mass spectrometry. The sequences were matched by using the Mascot Search system and modified residues were identified. The gene encoding Rcs contains six cysteines. The residues showing in boldface with underline at Fig. 22 modified as oxidation. The cysteine in this residue (C117) is not conserved; it could have no function in catalysis. In addition, DTNB also reacting with SH group inhibits the activity (30% inhibition, Fig. 19). Probably it reacts with cysteine, but not at the active site because it is too big to reach there.

```
S.aciditrophicus      -----MEFEIMAKWNPQKRVLNHEHTRFWRFELRDVDEPNLQKEVFP--YDEVSRIDFDH 53
C.kluyveri            ----------MKKCS-------------YDYKLNNVNDPNFYKDIFP--YEEVPKIVFNN 35
M.tuberculosis        MTTSESPDAYTESFGAHTIVKPAGPPRVGQPSWNPQRASSMPVNRYRPFAEEVEPIRLRN 60
                                . .                 . .    ..:  : :    :**  * : :

S.aciditrophicus      RIIPIQPAE-EIFITDTTFRDGQQARP-PYTTQQIVDLYQMMSRLGGYNGIIRQTEFFLY 111
C.kluyveri            IQLPMDLPD-NIYITDTTFRDGQQSMP-PYTSREIVRIFDYLHELDNNSGIIKQTEFFLY 93
M.tuberculosis        RTWPDRVIDRAPLWCAVDLRDGNQALIDPMSPARKRRMFDLLVRMG---YKEIEVGFPSA 117
                         *    :       . :***:*:   * :. .   ::: : .:.       :. *

S.aciditrophicus      SNRDKEAVRMCQDLGLQYPEITGWIRAAR--EDIPLVKEAGLKETGILTSVSDYHIFLKL 169
C.kluyveri            TKKDRKAAEVCMERGYEFPEVTSWIRADK--EDLKLVKDMGIKETGMLMSCSDYHIFKKL 151
M.tuberculosis        SQTDFDFVREIIEQGAIPDDVTIQVLTQCRPELIERTFQACSGAPRAIVHFYNSTSILQR 177
                      :: * . ..   : *    ::*  : :    * :  . :     .  :    :   : :
```

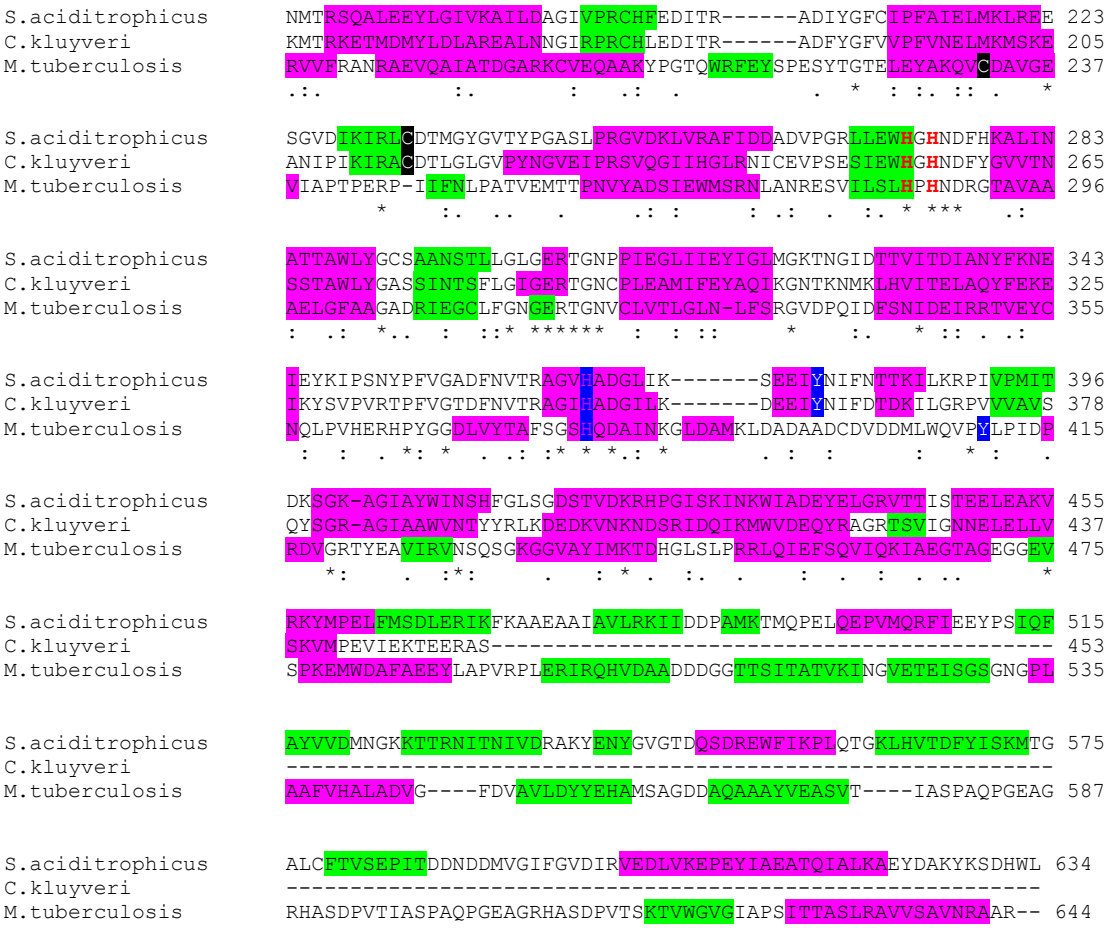

Fig. 22. Amino acid sequence of Rcs from *S. aciditrophicus* and from *C. kluyveri* aligned with the amino acid sequence of isopropylmalate synthase (LeuA) from *M. tuberculosis*. Conserved amino acids are highlighted in red (metal binding), blue (substrate binding), white in a black box (cysteine), pink (α-helix) and green (β-sheet). The underlined sequence shown bold was modified by iodoacetamide.

2.6.2 Structure prediction

The crystal structure of *Re*-citrate synthase has not been determined. The amino acid sequence alignment by ClusterW and secondary structure prediction by PSIPRED were performed based on the crystal structure of isopropylmalate synthase (LeuA) from *M. tuberculosis*. The amino acid sequence identity between Rcs from *S. aciditrophicus* and *Re*-citrate synthase from *C. kluyveri* is 49%. The identity between Rcs of *S. aciditrophicus* or *C. kluyveri* and LeuA of *M. tuberculosis* is 23% and 27%, repectively. Rcs from *S. aciditrophicus* has extended N-terminal β-sheets (Fig. 22). The metal binding site is conserved even though no metal is tightly bound to the recombinant Rcs from *S. aciditrophicus* by metal analysis.

Although the overall amino acid sequence identity between pig heart and *E. coli* citrate synthase is only 27%, there is a high conservation of sequence within the active site regions. But only one conserved substrate binding site (H367) was found in an α-helix of Rcs from *S. aciditrophicus*.

2.6.3 Crystallization

The purified recombinant Rcs in 100 mM Tris pH 8.0 and 100 mM NaCl was sent for crystallization to a group of Prof. A. Messerschmidt, MPI Martinsried. Various conditions were tested, but before getting crystals the collaboration ended due to the retirement of Prof. Messerschmidt. Therefore, the crystallization was tried by screening kits kindly provided from the group of S. Shima, MPI Marburg. Five different screening kits described in Materials and Methods were used and the plate containing protein and screening reagent mixtures were kept at 8 °C. No crystal was formed up to now. A problem was that the protein concentration (2 mg/ml) was lower than that used for most crystallization trails.

2.7 Stereospecificity of the *Re*-citrate synthase

Both *Re*- and *Si*-citrate synthase yield the identical product, citrate from oxaloacetate and acetyl-CoA. The carbonyl carbon of oxaloacetate has two sides, designated *Re*-face (rectus, clockwise) and *Si*-face (sinister, antoclockwise). The substituents of this carbon are ordered by their molecular masses. O > COO > CH_2. On the *Re*-face they are arranged clockwise and vice versa. In *Re*-citrate synthase the methyl group of acetyl-CoA attacks this carbonyl group from the *Re*-face and in *Si*-citrate synthase from the *Si*-face. If isotopically labeled acetyl-CoA is used, the result can be distinguished by the different labeling patterns. Starting with [1-^{14}C]acetyl-CoA, *Si*-citrate synthase yields [5-^{14}C]citrate, whereas *Re*-citrate synthase gives [1-^{14}C]citrate (Fig. 23).

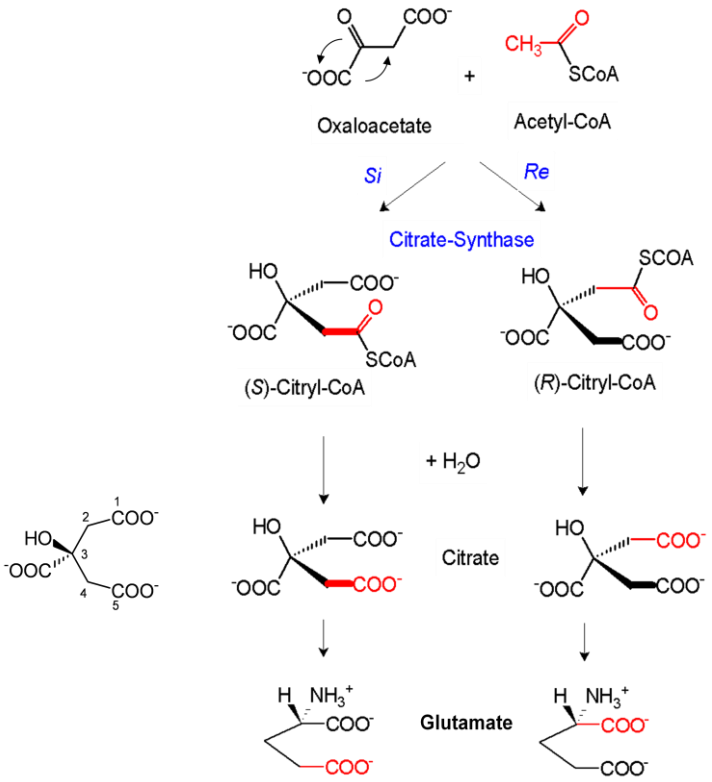

Fig. 23. Stereospecific pathway of glutamate biosynthesis via *Si*-/*Re*-citrate synthase. *Si*- and *Re*-citrate synthase catalyze the formation of the identical product, citrate from oxaloacetate and acetyl-CoA. The red color reveals the residue from the isotopically labeled acetyl-CoA during the glutamate synthesis pathway.

2.7.1 [^{14}C]Citrate synthesis

To distinguish the different stereospecificity of the enzyme, citrate was synthesized from [1-^{14}C]acetate by one-pot method using acetyl-CoA synthetase, ATP, $MgCl_2$, CoA, (*S*)-malate, NAD^+, malate dehydrogenase and either the recombinant Rcs or *Si*-citrate synthase from porcine heart. The reaction was followed spectrophotometrically by the formation of NADH at 340 nm (Buckel & Eggerer, 1965). The enzymatically synthesized citrate was isolated by Dowex 1 (formate) ion-exchange chromatography (Fig. 24). After loading the sample, the column was washed with10 column volumes of 1 M formic acid to elute unreacted [^{14}C]acetic acid. Citrate was eluted with 4 M formic acid.

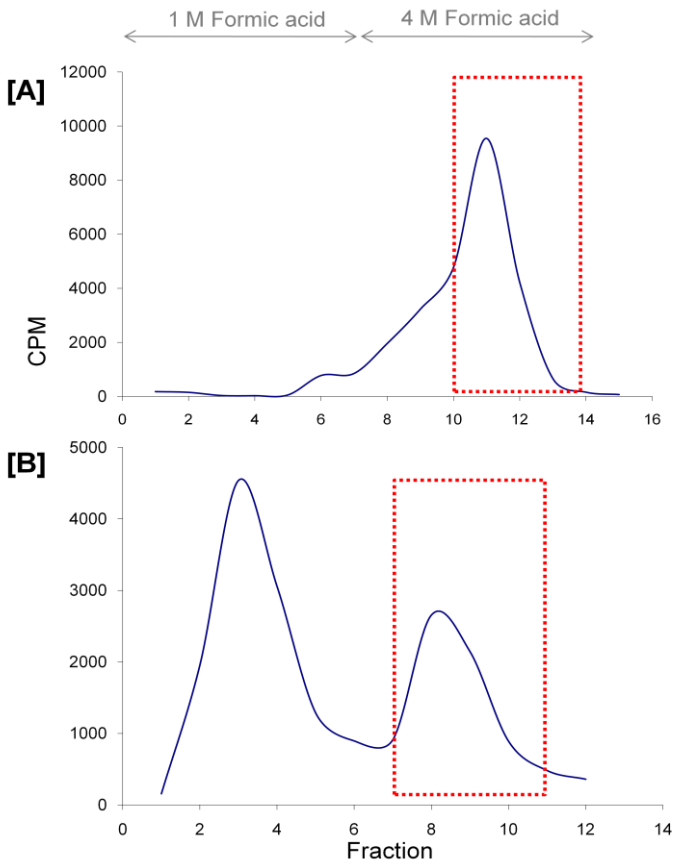

Fig. 24. Isolation of [^{14}C]citrate by Dowex 1 (formate) column. The unreacted [^{14}C]acetate was eluted by 1 M formic acid and citrate by 4 M formic acid. Fractions marked as red dotted line were pooled and concentrated for further [^{14}C]citrate cleavage.

2.7.2 [^{14}C]Citrate cleavage

The radioactively labeled citrate obtained with Rcs was subsequently cleaved to oxaloacetate and acetate by the catalytic action of *Si*-citrate lyase. After enzymatic conversion of oxaloacetate to malate and separation from acetate via ion-exchange chromatography, the entire radioactivity was found in malate (Fig. 25) (Gottschalk & Barker, 1967). As practically no labeled acetate was found, it indicated that the enzyme was highly *Re*-face stereospecific with respect to the C-2 of oxaloacetate. In the control with *Si*-citrate synthase the whole radioactivity was obtained in the acetate as expected. The result clearly indicates that the gene annotated as isopropylmalate/homocitrate/citramalate synthase actually encodes a *Re*-citrate synthase.

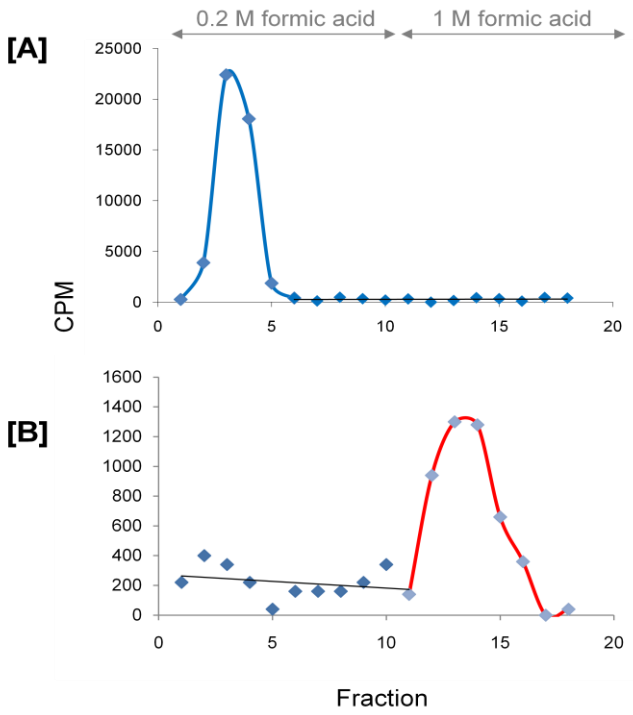

Fig. 25. Determination of the stereospecificity of citrate synthase by analysis of the [^{14}C]citrate synthesized by [A] *Si*-citrate synthase from pig heart and [B] the putative *Re*-citrate synthase from S. *aciditrophicus*. After citrate separation (Fig. 24), the [^{14}C]citrate was converted to acetate and malate in the presence of *Si*-citrate lyase, NADH, and malate dehydrogenase. Acetate was eluted by 0.2 M formic acid whereas malate by 1 M formic acid.

3. Role of *Re*-citrate synthase in *S. aciditrophicus*: atypical glutamate biosynthesis in vivo

3.1 Antibodies against *Re*-citrate synthase

To define the active expression of the gene encoding *Re*-citrate synthase in *S. aciditrophicus* cells, antibodies against *Re*-citrate synthase were tried to produce. SDS-PAGE gel fragments with pure recombinant *Re*-citrate synthase were used as antigen for antibody production in rabbits as hosts. To check whether the sera produced by Eurogentec (Belgium) contained antibodies, the proteins were transferred to a Protran nitrocellulose membrane, together with cell free extracts of *E. coli* as a negative control. The production of antibodies in the antisera was checked by Western blot and chemiluminescence analysis. The existence of antibodies is indicated when a peroxidase conjugated secondary antibody (goat anti rabbit IgG-peroxidase) binds to the primary antibody–*Re*-citrate synthase complex. In an alkaline mixture the peroxidase catalyzes the oxidation of luminol with hydrogen peroxide. The product of the

reaction emits light while it decomposes to a lower electronic ground state (Fig. 26) (Herrmann, 2008). This chemiluminescence can be detected under a photo-scanner.

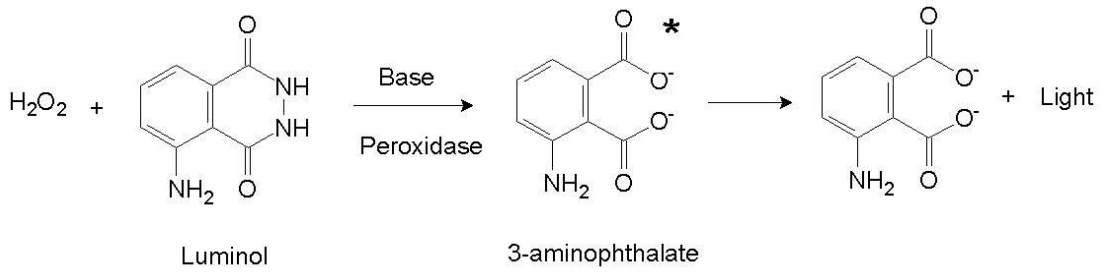

Fig. 26. Chemiluminescence reaction for antibody detection.

Before immunization, the serums from two rabbits were tested by Western blot to prove the lack of positive signal at the corresponding mass of *Re*-citrate synthase. At the initial phase of immunization, nonspecific signals were detected. The severe problem arose because the antisera collected at 66 and 87 days after immunization did not react specifically against *Re*-citrate synthase. This result suggested that no immunization was happened. To confirm it, the indirect enzyme-linked immunosorbent assay (ELISA) was carried out by Eurogentec. A constant amount of antigen (100 ng/well) were coated into the wells of the ELISA plate and tested with different dilutions of the serum in question. The development was done colorimetrically using a secondary horseradish peroxidase conjugated antibody and o-phenylenediamine as chromogenic substrate. The optical density of the chromogenic substrate was measured at 492 nm. No positive signal was obtained by ELISA assay. The Western blot and ELISA assay confirmed that the antibody was not produced in the host, which suggested that the antigen was not immunogen.

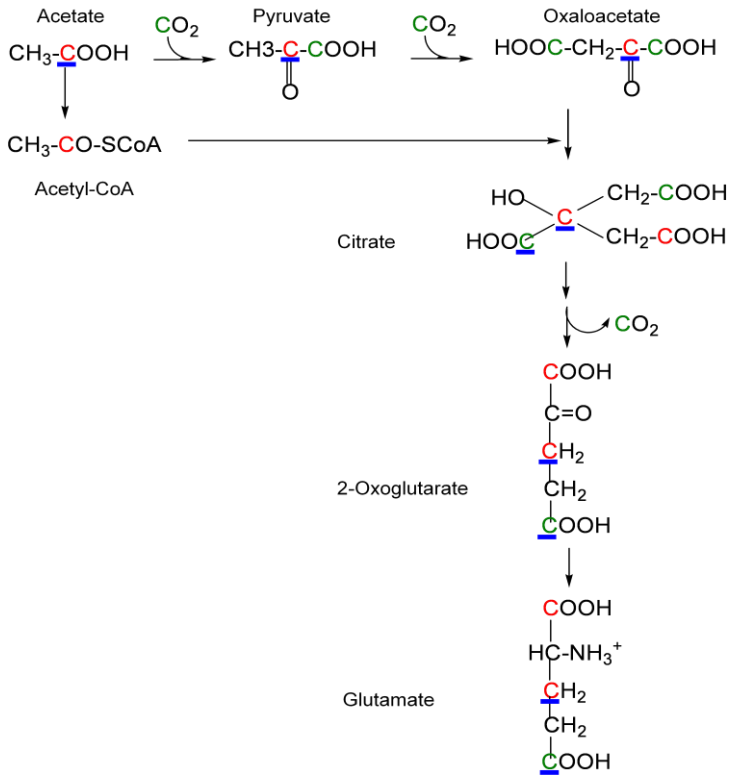

Scheme 6. Biosynthetic pathway of glutamatate via *Re*-citrate synthase in the oxidative branch of the TCA cycle. The red and green color point out the carbon flow during glutamate biosynthesis via *Re*-citrate synthase in the cells on grown with [1-^{14}C]acetate and NaH$^{13}CO_3$, respectively. By contrast, the blue underlined carbons trace the flow in glutamate biosynthesis via *Si*-citrate synthase in cells grown with [1-^{14}C]acetate.

3.2 ^{14}C-tracer experiments

3.2.1 Growing *S. aciditrophicus* with [1-^{14}C]acetate

To show that *Re*-citrate synthase is involved in glutamate biosynthesis in *S. aciditrophicus*, ^{14}C-tracer experiments were applied (Scheme 6). The *S. aciditrophicus* was grown axenically on a defined medium containing 20 mM crotonate, 1 mM acetate, 100 µCi [1-^{14}C]acetate until growth reached the beginning of stationary phase. A negligible decrease of the radioactivity of the medium was observed during growth. The difference of radioactivity between before and after growth was 2.8 ± 2.3%. The total activity of the medium was 161,365,000 cpm and the total activity of the cells was 10,553,580 cpm. Hence, 6.5% of [1-^{14}C]acetate was incorporated into the cells.

3.2.2 Isolation of [^{14}C]glutamate from whole cells

The *S. aciditrophicus* cells were harvested and hydrolyzed by 6 M HCl. The supernatant of hydrolyzed cells was loaded onto the Dowex 50 (H^+) and the ^{14}C-labeled amino acids were eluted by 1 N ammonia (Fig. 27-[A]). The concentrated amino acids pools were loaded to the Dowex 1 (formate). Neutral amino acids were eluted by water and glutamate and aspartate were eluted by 1 M formic acid (Fig. 27-[B]). The glutamate and aspartate were separated by TLC using the solvent system, isobutanol-formic acid-water (30:5:7.5 by volume). The detected radioactive glutamate and aspartate spots (Fig. 27-[C]) were extracted with H_2O.

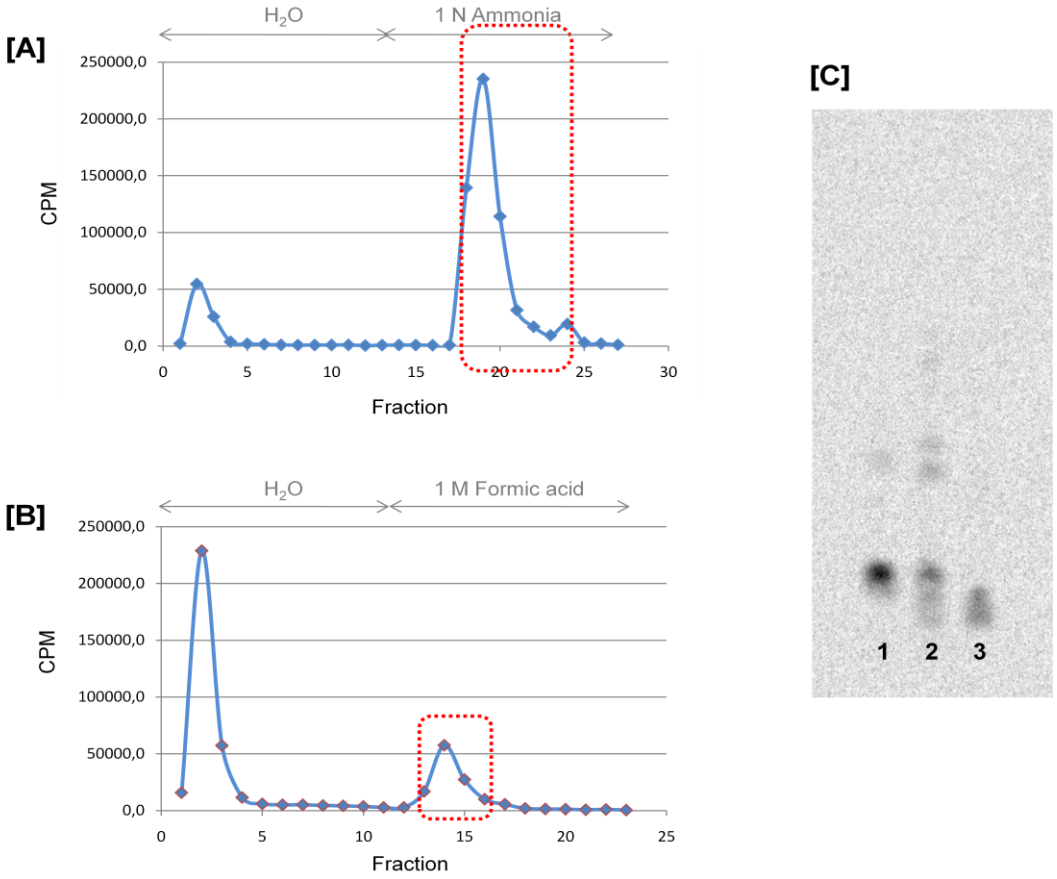

Fig. 27. Isolation of [^{14}C]glutamate from *S. aciditrophicus* whole cells. Purification was followed by measuring radioactivity of each fraction by a scintillation counter. The fractions in the red dotted line were collected and concentrated by flash evaporation. [A], Purification of ^{14}C-labeled amino acids from whole cells by Dowex 50 (H^+). [B], Purification of glutamate and aspartate from the amino acid mixture by Dowex 1 (formate). [C], Separation of glutamate and aspartate on a TLC plate. The standards and sample were dissolved in 1 M formic acid. The solvent system used was isobutanol-formic acid-H_2O (30:5:7.5). The radioactive spots on the TLC plate were detected by Storm 860 Molecular Imager. Lane 1, [1-^{14}C]glutamate; 2, ^{14}C-labeled glutamate and aspartate from *S. aciditrophicus*; 3, [1-^{14}C]aspartate.

3.2.3 Determination of labeled carbon in the carboxyl groups of glutamate

To explore the labeling pattern of glutamate, the decarboxylation of the 1-carboxyl groups of glutamate and aspartate was performed by the treatment with chloramine-T solution (Fig. 28) in a Warburg vessel as previously described in Materials and Methods. The Warburg vessel consisted of three parts; main compartment with chloramine T, center wall with a filter paper soaked in 1 M hyamine hydroxide in methanol, and side arm with the labeled glutamate. The vessel was closed and the glutamate from the side arm was mixed with the content of main compartment. $^{14}CO_2$ derived from α-carboxyl group was trapped on the filter paper and counted in a vial with scintillation fluid. The radioactivity derived from rest of carbon skeleton remained in the main compartment of the vessel. The distribution of radioactivity in the glutamate and aspartate isolated from whole cells is shown in Table 4.

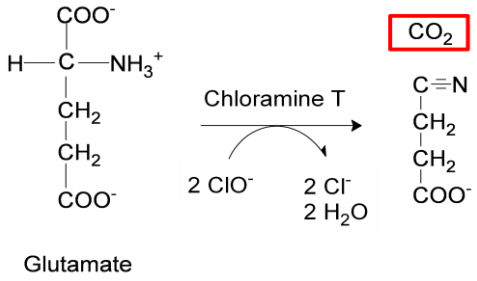

Fig. 28. Reaction of glutamate with chloramine-T

Table 4. Distribution of radioactivity in the carbon skeleton of differently labeled glutamates.

	Total	C1 carbon		C2-C5 carbon	
	(cpm)	(cpm)	(%)	(cpm)	(%)
[1-^{14}C]Glutamate	326255.5	318202	97.5	20196	6.2
[5-^{14}C]Glutamate	12935	491.5	3.8	11364	87.9
SB Glutamate[1]	9794.25	2007.75	20.5	7548	77.1

[1] ^{14}C-labeled glutamate isolated from *S. aciditrophicus* whole cells grown on [1-^{14}C]acetate.

Fifty % of the radioactivity was supposed to be detected at the α-carboxyl group (C1) of glutamate. But the proportion of radioactivity found in C1 of glutamate was 20%, whereas 80% of the label was retained in C2-C5. The distribution of radioactivity in C2-C5 could not be studied yet.

3.2.4 Radioactivity of aspartate

The distribution of radioactivity in aspartate isolated from whole cells is shown in Table 5. 82.6% of radioactivity was measured after treatment with chloramines T. 15.5% of the total radioactivity in aspartate was recovered as $^{14}CO_2$, showing that 67.1% of the label was in remaining carbons (C2-C4).

Table 5. Distribution of radioactivity in carbon skeleton of the aspartate formed from *S. aciditrophicus* cells grown with [1-^{14}C]acetate.

	Total	C1 carbon		C2-C4 carbons	
	(cpm)	(cpm)	(%)	(cpm)	(%)
SB Aspartate	7866	1218	15.5	5280	67.1

3.3 ^{13}C-labeled metabolites analysis by NMR

3.3.1 Incorporation of ^{13}C to metabolites

A basal medium was prepared with 20 mM crotonate containing 1 g of $NaH^{13}CO_3$ to get a final concentration of 44 mM in 250 ml on which *S. aciditrophicus* was grown. The stationary phase cells were harvested. To test the incorporation of ^{13}C into metabolites, the whole-cell was analyzed by NMR (Fig. 29). The broad signal that appeared at around 174 ppm is supposed to be due to ^{13}C-labeled carbonyl carbons of the amino acids, while the three strong groups of peaks between 69 and 79 ppm are supposed to be due to lipids of cell walls. As a negative control, whole cells grown at the same growth medium containing unlabeled $NaHCO_3$ were analyzed by NMR spectroscopy. Transition metal hydroxides and sulfides from the medium of the negative control, which interfered with the NMR measurement, were removed by mild centrifugation (500 rpm, 1 min), but this modified method caused a different sample condition. The peaks in the region from 69 to 79 ppm were still similar to the signals from ^{13}C-labeled whole cells but showed much weaker intensities (spectrum not shown).

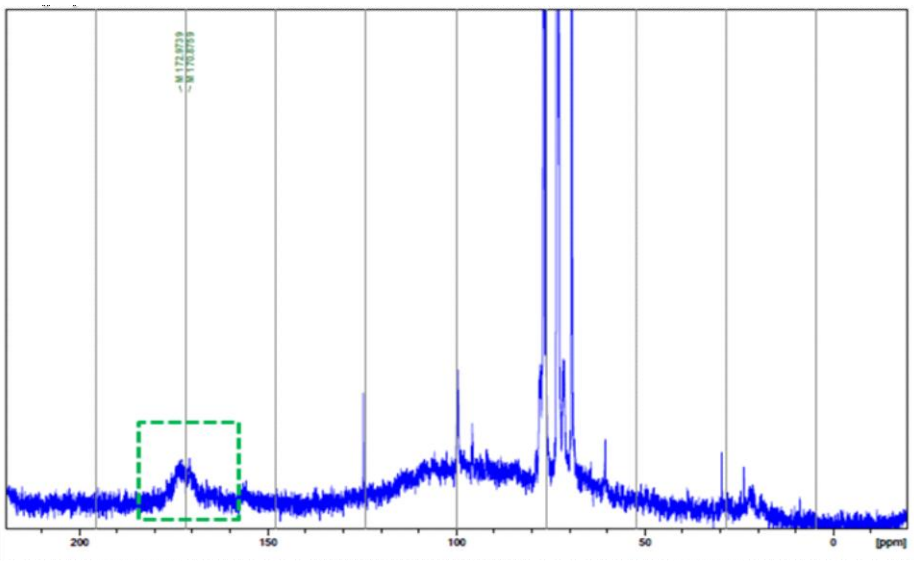

Fig. 29. ^{13}C-NMR spectrum of whole *S. aciditrophicus* cells grown on 20 mM crotonate and 44 mM NaH^{13}CO$_3$. The peaks in the green dotted square indicate ^{13}C-labeled carbonyl groups.

3.3.2 Isolation of ^{13}C-labeled glutamate and aspartate from whole cells

The first isolated sample was a mixture of glutamate and aspartate, whereby the amino acids were isolated from the hydrolyzed metabolites by the Dowex 50 (H^+) as described in Materials and Methods. Glutamate and aspartate were separated from neutral amino acids by a Dowex 1 (formate) column and analyzed by NMR spectroscopy. The major peaks in the region from 69 to 79 ppm (Fig. 29) were eliminated by purification using Dowex columns. The isolated samples were pure enough for further analysis.

3.3.3 Determination of labeled carbon in the carboxyl groups of aspartate and glutamate

To recognize the individual labeling of glutamate and aspartate, the two dimensional techniques TOCSY and HMBC (see Materials and Methods 1.1.3) were applied and the spectra were interpreted by Dr. X. Xie (Fachbereich Chemie, Philipps-Universität Marburg). The TOCSY experiment correlates all protons of a spin system. Therefore, signals which originate from the interaction of all protons of a spin system that are not directly connected via three chemical bonds are visible. Thus, characteristic patterns of signals result and can often be used to identify different amino acids. The HMBC experiment, through the so called

long-range or multiple-bond correlations, provides us proton-carbon connectivities through couplings over two or three bonds. Signals of such long-range proton-carbon linkages can also be used to identify various amino acids.

The chemical shifts of amino acids vary at different pH values. The known chemical shifts of most amino acids are usually given at neutral pH (Wüthrich, 1986). The pH of the sample dissolved in D_2O was assumed approximately 4 due to the residual effect from the elution solution (1 M formic acid) of the Dowex column. In order to verify our assignment, the pH dependence of ^{1}H chemical shifts of glutamate was studied. Therefore, 20 mM glutamate at various pHs were simulated with NaOH and spectra of the samples for NMR were adjusted with NaOD. The ^{1}H spectra of glutamate at different pH are shown in Fig. 30. The spectra of ^{13}C glutamate at pH 4 and 7 were also measured. The comparison of the spectra showed resemblance among the spectra of the ^{13}C-labeled glutamate at pH 4 and unlabeled glutamate at pH 3 and 5. This thus verified our assignment. Therefore, the ^{13}C-labeled sample at pH 4 was chosen for further anlaysis.

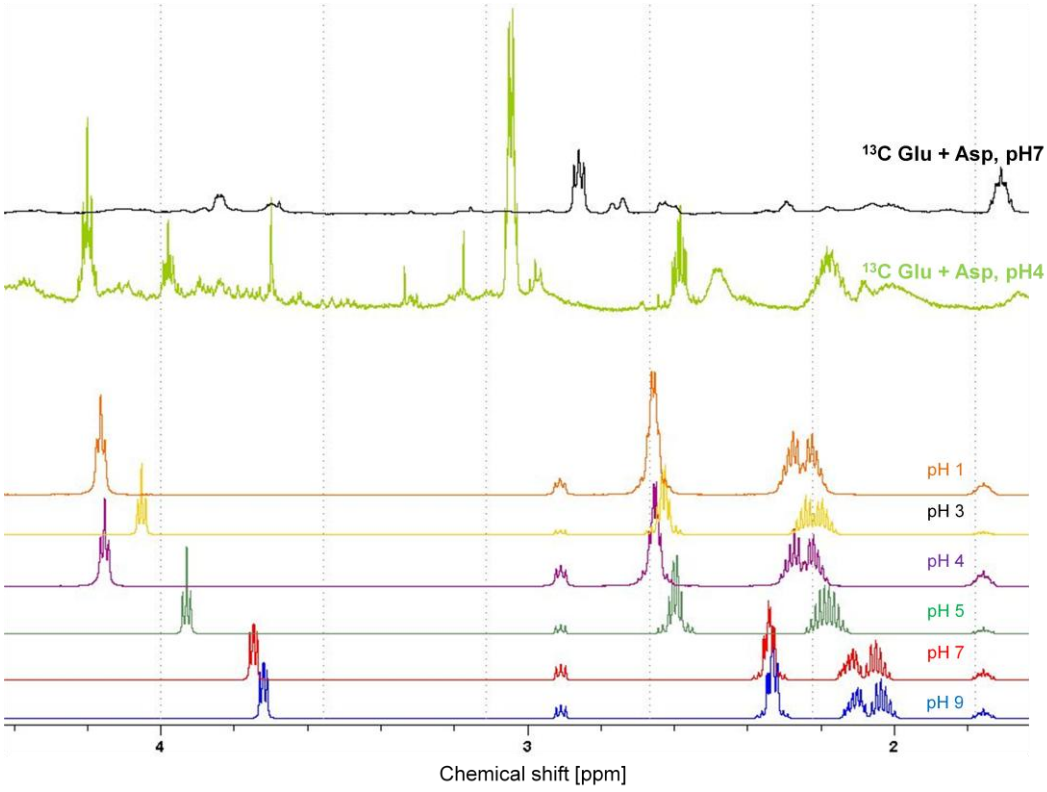

Fig. 30. The ^{1}H spectra of ^{13}C-labeled and unlabeled glutamates and the isolated ^{13}C-labeled glutamate and aspartate at different pHs.

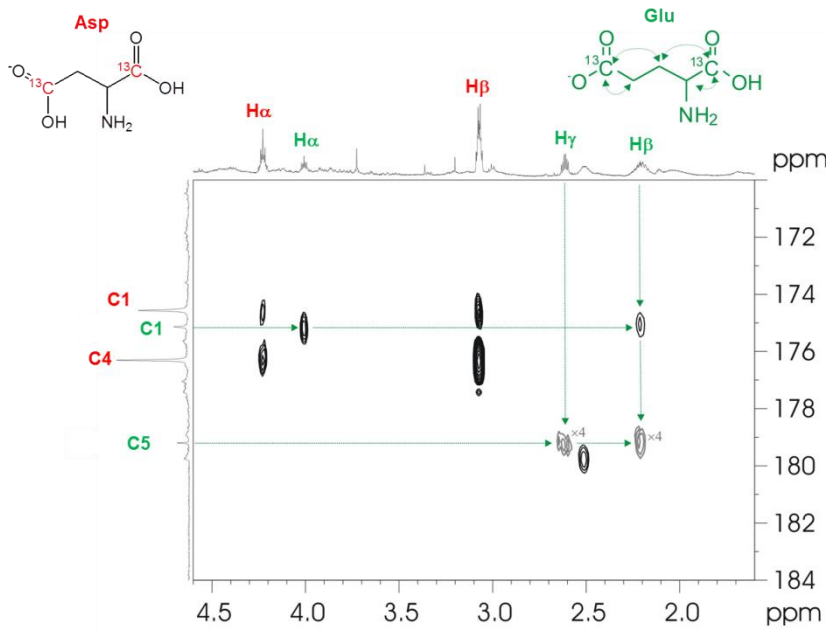

Fig. 31. HMBC spectrum of the fingerprint regions of glutamate and aspartate in D_2O. Section of long-range ^{1}H, ^{13}C correlation spectrum of isolated aspartate and glutamate. The red lables are corresponding to the aspartate and the green arrows indicates isolated glutamate at 300 K. Aspartate, ^{1}H NMR δ ppm : 4.2 (m, 1H), 3.0 (m, 2H);^{13}C NMR δ ppm: 171.9 (C1), 173.6 (C4): Glutamate, ^{1}H NMR δ ppm: 3.9 (m, 1H), 2.6 (td, 2H), 2.18 (m, 2H); ^{13}C NMR δ ppm: 172.5 (C1), 176.5 (C5).

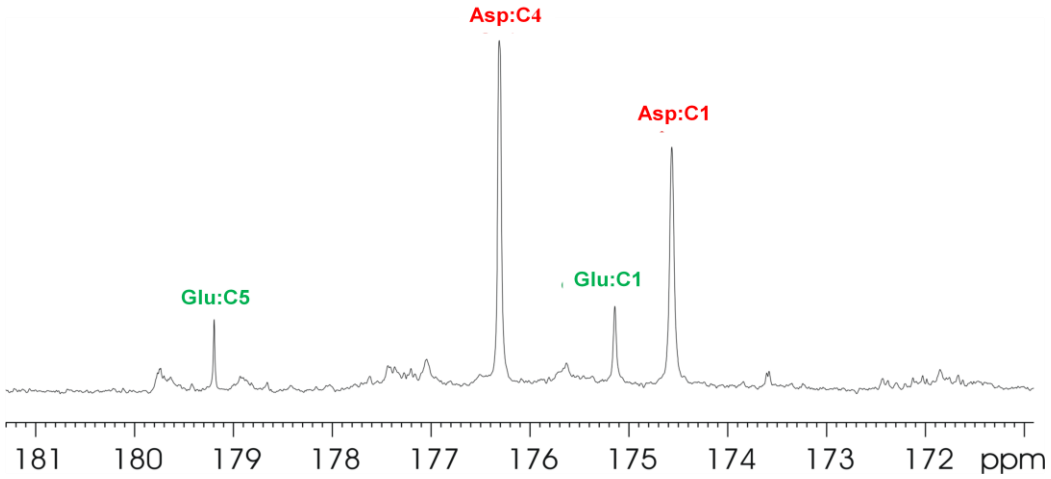

Fig. 32. Extended ^{13}C spectrum of isolated products in D_2O at 300 K. The chemical shift was referenced to 2,2-dimethyl-2-silapentane-5-sulfonate (DSS).

The purified aspartate and glutamate mixture was measured by ^{13}C NMR and showed ^{13}C-labeled signals around 176 ppm. To assign these signals, two dimensional ^{1}H, ^{13}C correlation spectrum was applied (Fig. 31). A splitting pattern of doublet in ^{13}C signals of

carbons with natural abundance at C2 and C3 positions of aspartate and C4-position of glutamate was observed. The pattern came from the ^{13}C-^{13}C *J* coupling separated by one chemical bond. The coupling constant is about 30 Hz, which is in agreement with literature values (Kalinowski et al, 1984) According to the splitting and the intensities of the Asp:C4 and Asp:C1 signals (Fig. 32), the mixture contains [1,4-$^{13}C_2$]Asp-and Asp-4-^{13}C, with a ratio of approximately 2:1.

The datas given in Fig. 31 and Fig. 32 confirm that the ^{13}C labeling to glutamate produced by *S. aciditrophicus* was successful. By the comparison of the spectra of the ^{13}C-labeled glutamate and unlabeled glutamate at pHs 3 and 5, the stubby spectra (Fig. 32, at 177.3 ppm and 179.5 ppm) could be excluded from possible labeling position. However, after raising the threshold of the HMBC spectrum, we found long-range correlation peaks H2 – C1, H3 – C1, H3 – C5, and H4 – C5 of ^{13}C-labeled Glutamate (Fig. 31). Therefore, the observed HMBC cross peaks verified our assignment to C1 and C5 of the ^{13}C-labeled Glutamate. Nevertheless, it is still unclear whether the positions are simultaneously or separately labeled. This can be determined if the coupling patterns of the ^{13}C signal with C2 and C5 are observable, or distinguishable by a mass spectrum. For more accurate observations, separation of aspartate and glutamate on a TLC plate was attempted. The ^{13}C-labeled sample adjusted to pH 7 was used. The presence of additional Na^+-phosphate buffer crystals hindered the solubility during evaporation. Consequantely, it affected the development of TLC and disrupted the separation. To achieve strong signals for clarifying the labeling pattern, higher concentration of the ^{13}C-labeled glutamate will be prepared in future.

II. Biosynthesis of benzoate in *S. aciditrophicus*

1. Glutaconyl-CoA decarboxylase

Energy-limited microorganisms contain glutaconyl-CoA decarboxylase (Gcd), which is a Na^+-dependent and biotin-containing integral membrane enzyme composed of 4 − 5 different subunits (Buckel, 2001a). The genome of *S. aciditrophicus* contains three genes for Gcd, carboxytransferase, α-subunit (*gcdA*, SYN_00481), hydrophobic transmembrane β-subunit (*gcdB*, SYN_01431), and biotin carrier γ-subunit (*gcdC*, SYN_00479). Between *gcdA* and *gcdC*, there is a gene encoding acyl-CoA dehydrogenase (SYN_00480). In addition, the genes (SYN_02637 and SYN_02636) encoding electron transferring flavoprotein (Etf), which could

be responsible for the subsequent reduction of glutaconyl-CoA to glutaryl-CoA (Fig. 33). A gene encoding a small δ-subunit (GcdD) was not detected.

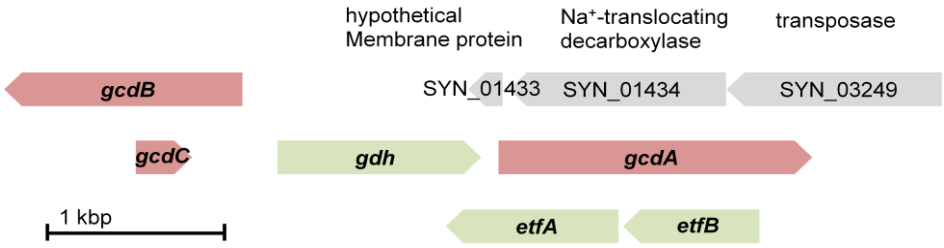

Fig. 33. Arrangement of the genes encoding glutaconyl-CoA decarboxylase (*gcd*) and genes involved in the subsequent benzoate biosynthesis. The red colored genes encode *gcdABC*. The green colored genes (*gdh*, acyl-CoA dehydrogenase; *etfA*, electron transferring flavoprotein alpha subunit; *etfB*, etf beta subunit) are supposed to be involved in the subsequent reduction of glutaconyl-CoA to glutaryl-CoA for benzoate biosynthesis. There are two genes encoding membrane proteins on the upstream of the *gcdB*.

There are genes encoding a hypothetical membrane protein (SYN_01433) and Na^+-translocating decarboxylase beta subunit (SYN_01434) upstream of *gcdB* (Fig. 33). It was suspected that SYN_01433 could be expressed as the small subunit, GcdD, and SYN_01434 as GcdB. To identify the gene encoding the functional subunit GcdB, homologies of deduced amino acid sequences were searched by ClusterW2 (Fig. 34). The deduced amino acid sequence of the hydrophobic subunit GcdB matches well with those from *A. fermentans*, *Fusobacterium sp.*, and *C. symbiosum* as the range of ca. 50% but comparing with SYN_01434 reveals a relatively low (27%) amino acid sequence identity. Other β-subunits of Na^+-dependent and biotin-containing decarboxylases, for example, methylmalonyl-CoA decarboxylase, oxaloacetate decarboxylase, or other sodium ion-translocating decarboxylases from various microorganisms showed ca. 50% sequence identity with GcdB. Moreover, there was no significant similarity found between SYN_01433 and the GcdDs from *A. fermentans* and *C. symbiosum* (Fig. 35). Therefore, the possibility of SYN_01433 as the *gcdD* was turned down and *gcdB*, not SYN_01434, was chosen for the overproduction of hydrophobic Na^+-translocating subunit of Gcd.

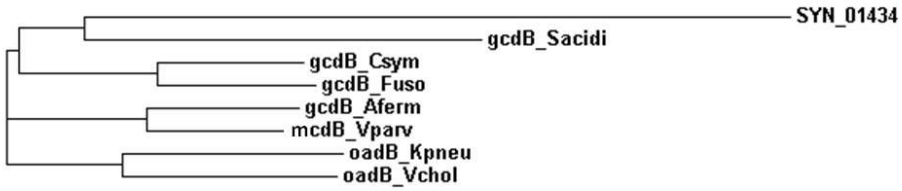

Fig. 34. Guide tree based on multiple alignments by ClusterW2. The Guide tree shows most closely or more distantly related sequences but does not mean evolutionary relationships. mcdB_Vparv is the gene encoding methylmalonyl-CoA decarboxylase beta subunit from *Veillonella parvula*, oadB_Kneu as oxalocetate decarboxylase beta subunit from *Klebsiella pneumonia* and oadB_Vchol from *Vibrio cholera*.

```
gcdD_Aferm      -MTDN--PW----LIMMINMTIVFGVLIVLGILMVLIHAVDPTKKVQGKKKPVVAKPAPS 53
gcdD_Csym       MWTEATMPFGQSVIVSLLGISVVFITLVTLALAIVLISKILRSIIKDGAQKP---APAAA 57
SYN_01433       MFKQKR-QW-----WWVIGTCIALS-------GVALVRLLAP-------EYP----PGAL 36

gcdD_Aferm      AAASKRQEEEKVAAMAAVLALVQDEDDMIAAALSAAIAEHKRKMEPMNLPHHSF 107
gcdD_Csym       PVVSDEADKETLAVLMATIGMDLELP-----------ADQFKIVNVKEL----- 95
SYN_01433       RLAIKIG-----GYTLVIIGL-FSLP--------------LAMRKDDE------ 64
```

Fig. 35. Comparison of the amino acid sequences of GcdD from *A. fermentans, C. symbiosum,* and SYN_01433 from *S. aciditrophicus*. Conserved residues are marked in gray.

2. Carboxytransferase, GcdA

2.1 Sequence analysis of *gcdA*

The gene encoding GcdA (SYN_00481) is composed of 1,773 base pairs (GC content: 53.13%) and coding for 590 amino acids with a calculated molecular mass of 65.37 kDa and estimated isoelectric point of 7.02. The direction of the transcription is forward. Comparing the deduced amino acid sequence of *gcdA* in the data bank revealed a high level of identity (ca. 55%) to glutaconyl-CoA decarboxylase subunit alpha from *Desulfobacterium autotrophicum*, *Geobacter* sp., *Fusobacterium.* sp., *Acidaminococcus* sp., *A. fermentans* and *C. symbiosum*. Prediction of transmembrane regions and orientation by the TMpred program (http://www.ch.embnet.org/software/TMPRED_form.html) showed that there are 2 strong transmembrane helices among 4 possible transmembrane helices. But the prediction of signal sequence with SignalP 3.0 (http://www.cbs.dtu.dk/services/SignalP) based on the Gram-

negative bacteria networks revealed that there is no signal peptide and it is a non-secretory protein.

2.2 Cloning and expression of *gcdA* and protein purification

The *gcdA* gene encoding carboxytransferase of Gcd was amplified by PCR using the desired primers containing restriction sites. The PCR product and the pACYCDuet-1, pASK-IBA3plus, and pASK-IBA7plus plasmids were digested by restriction enzymes and ligated with one another. The products were then transformed into an *E. coli* DH5α. The DNA sequences of three clones were analyzed by restriction enzymes to detect the expected size of amplified insert and vector. Before transformation of the recombinant plasmid in *E. coli* Rosetta (DE3) pLysS or BL21 (DE3), the gene was sequenced. The *gcdA* in pACYCDuet-1 was expressed in TP medium with chloramphenicol and the cloned gene was induced by adding different concentrations of IPTG aerobically. The expression of *gcdA* in pACYCDuet-1 vector was negligible and trying various expression conditions did not improve the expression. The *gcdA* was designed to be cloned in pACYCDuet-1 vector at second multi-cloning site (MCS) which contains S-tag for the coexpression of *gcdA* and *gcdC*. To avoid harsh condition of S-tag purification, a DEAE Sepharose column was applied but the high background activity of the fractions interfered distinguishing the GcdA fraction. Therefore, *gcdA* was cloned into pASK-IBA3plus and pASK-IBA7plus vectors which are high-copy number plasmids and have C- or N-terminal Strep-tag II. For overproduction, the plasmid was introduced into in *E. coli* Rosetta (DE3) pLysS or BL21 (DE3) cells. The cells were grown aerobically in TP medium at 37 °C to an absorbance difference at 600 nm of 0.6 to 0.8. Expression of the *gcdA* was induced by adding AHT (200 µg/L). The cells were harvested after 3 h or overnight incubation. Purification of GcdA was carried out aerobically according to the manufacturer's specifications using Strep-Tactin column and purification was followed by SDS-PAGE. The low yield of recombinant GcdA was probably due to the loss of most of the overproduced GcdA during cell disruption. An extra band above the GcdA band on SDS-PAGE was identified as the chaperone of *E. coli* by MALDI-TOF analysis. The preparation of cell lysates in presence of a commonly used protease inhibitor, phenylmethanesulfonylfluoride (PMSF) or cell disruption by osmotic shock by adding 0.5 M sucrose showed no significant improvement for protein yield.

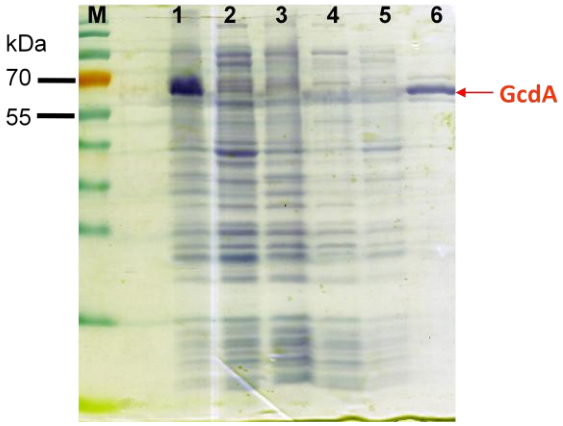

Fig. 36. SDS-PAGE of purified recombinant GcdA. M, Molecular mass marker; 1, cell lysate; 2, cell free extract after induction with AHT (200 µg/L); 3, pellet; 4, flow through of the Strep Tactin column; 5, washing; 6, elution. The red arrow points out the purified recombinant GcdA.

2.3 Determination of the enzyme activity of GcdA

GcdA catalyzes the transfer of CO_2 from glutaconyl-CoA to biotin. The carboxytransferase activity of GcdA was determined using the assay for native glutaconyl-CoA decarboxylase in the presence of 5 mM D-biotin. The assay is based on the hydration of the product crotonyl-CoA and oxidation of the formed 3-hydroxybutyryl-CoA by NAD^+. After adding recombinant GcdA, the increasing concentration of NADH was measured at 340 nm (ε = 6.3 $mM^{-1}cm^{-1}$). The specific activity of GcdA was 2 mU/mg in presence of D-biotin and 0.6 mU/mg without D-biotin.

3. Hydrophobic Na^+-translocating subunit, GcdB

3.1 Sequence analysis of *gcdB*

The gene encoding GcdB is composed of 1,347 base pairs (GC content: 53.1%) and codes for 448 amino acids with a calculated molecular mass of 47.5 kDa and estimated isoelectric point of 4.75. The direction of the transcription is reverse. Prediction of transmembrane regions and orientation by the TMpred and TMHMM 2.0 (http://www.cbs.dtu.dk/services/TMHMM) showed that there could be 9 − 10 transmembrane helices. The prediction of signal sequence with SignalP 3.0 based on the Gram-negative bacteria networks revealed a signal sequence (Fig. 37, 38).

MIFGLMETGF PLFYWGNALM IAIALVLIYL AIAKEMEPLL LVPIGFGMIL VNLPLGGMMD
YEMMLKAPQA GTVVEVSTQE GKGFDKGGVI CKLDSGEVVA PVFGRVDKLN VEQGQHVEKG
QVIASILTME QTDQAVLPSR PVGLLSRIFQ FGVMWQILPP LMFLCLGALT DFGPMLANPK
TLLLGAAAQF GVYLAFFMAL FVGFSLPEAA SIGIIGGAEG PTTIYVSSVL APHIIGATAV
ACYSYMALVP IIIPPVIRLL TTKKERGIFM KPSMRKVSKL EKILFPLITA IIVILIVPTS
AALMGCFMIG NLFKECGVTE RLNKTAQTTF VDLITIFLTL AIGASMPAQN FLQSKTLLVL
VLGVVSFAAA AGAGVLLAKF MNLFLKEKIN PMIGGAGVSA VPMSARVVQV MGQKENPKNF
LLMHAMGPNV AGAIGAAIAG GVFIGILG

Fig. 37. The deduced amino acid sequence of GcdB. The gray box indicates the most likely cleavage site (AIA-KE) predicted by SignalP 3.0.

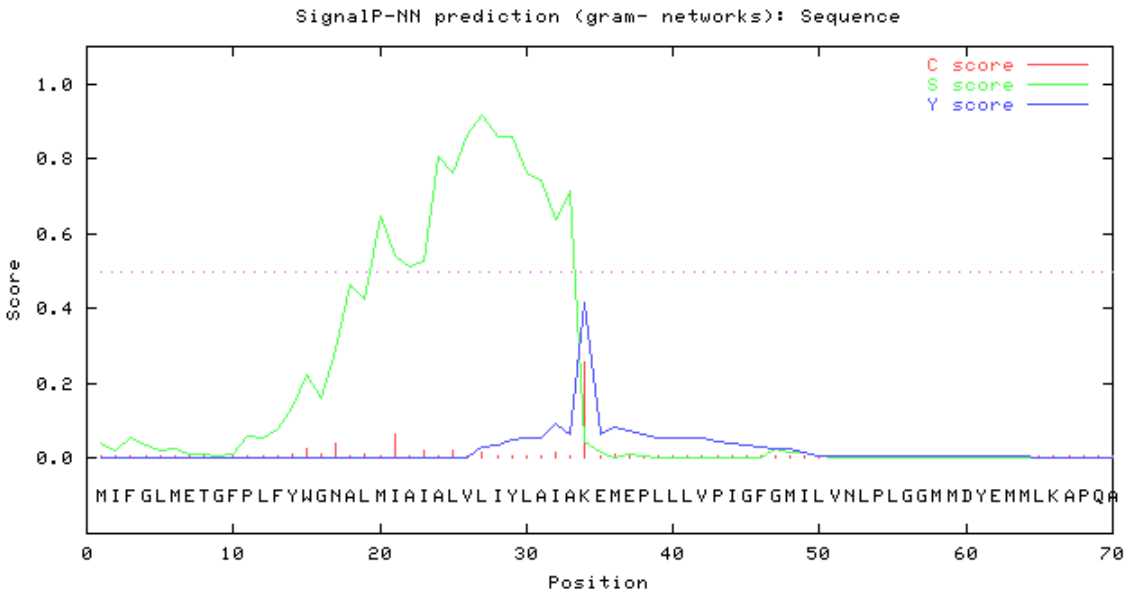

Fig. 38. Predicted signal peptide of GcdB by SignalP 3.0 (http://www.cbs.dtu.dk/services/SignalP). The green colored S score is reported for every single amino acid position in the submitted sequence, with high scores indicating that the corresponding amino acid is part of a signal peptide, and low scores indicating that the amino acid is part of a mature protein: The red colored C score is the cleavage site score. Multiple high-peaking C-scores can be found in one sequence, where only one is the true cleavage site. The cleavage site is assigned from the Y-score where the slope of the S-score is steep and a significant C-score is found.

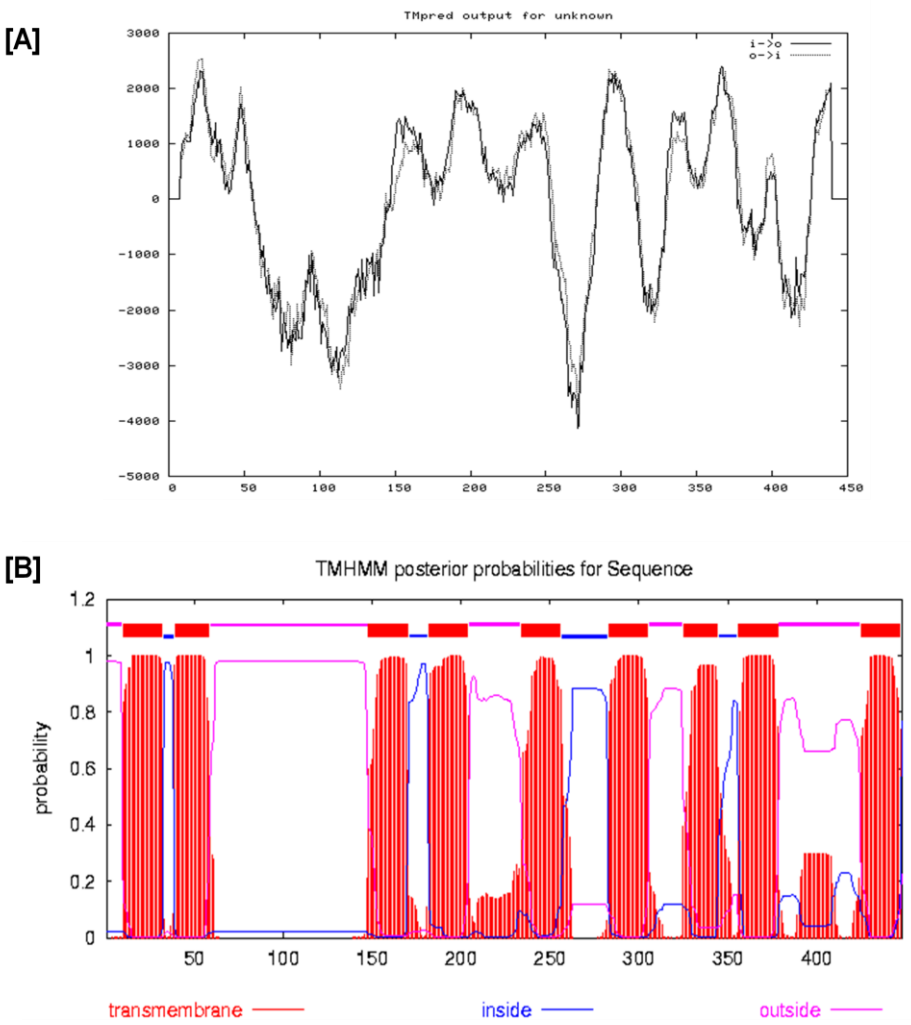

Fig. 39. Predicted probable transmembrane helices of GcdB by (A) TMpred (http://www.ch.embnet.org/software/TMPRED_form.html) and (B) TMHMM 2.0 (http://www.cbs.dtu.dk/services/TMHMM).

3.2 Cloning and expression of *gcdB*

The gene for GcdB was cloned into the expression vector pCDFDuet-1 and pASK-IBA3 plasmids. The plasmid construct was transformed into *E. coli* Rosetta (DE3) pLysS or BL21 (DE3) to get more efficient protein production. Cultures were grown under aerobic conditions at room temperature, 30 °C, or 37 °C with 5% inoculation and induced with various concentration of IPTG for pCDFDuet-1 vector or ATH in the early exponential phase (OD_{600} = 0.4). After 3 – 4 h of growth, cells were harvested. The preparation of soluble membrane extract and purification were performed as mentioned in Materials and Methods. To Purification was monitored by SDS-PAGE. No overproduction of GcdB was detected.

To find out the optimal condition of overexpression of *gcdB*, different *E. coli* competent cells which are usually applied for membrane protein production, Lemo21(DE3) and C43(DE3), were tested.

3.2.1 Overexpression in *E. coli* Lemo21(DE3)

Lemo21(DE3) offers the host features of BL21(DE3) while also allowing for tunable expression of difficult clones. Tunable expression is achieved by varying the level of lysozyme (*lysY*), the natural inhibitor of T7 RNA polymerase. The level of lysozyme is modulated by adding L-rhamnose to the expression culture at levels from 0 to 2 mM. When Lemo21(DE3) is grown without rhamnose, the strain performs the same as a pLysS containing strain. However, optional addition of rhamnose tunes the expression of the protein of interest. This tuning the expression level may also result in more soluble, properly folded protein. The Lemo21(DE3) strain was kindly given by Dr. Chris van der Does (MPI Marburg). The plasmid harboring *gcdB* was transformed into Lemo21(DE3) strain. The preculture was inoculated to 1 L LB medium supplemented with 500 µM of rhamnose and incubated at 30 °C. At the exponential phase (OD_{600} = 0.5 – 0.7), the expression was induced by adding 500 µM IPTG and incubate the culture for 2 h. Optical density before and 2 h after induction were measured to anticipate the level of overexpression. In general, there is no significantly different optical density observed between before and after induction while overexpression actually occurs, because most of energy in a cell is used not for growth but for recombinant protein synthesis. The average difference of optical density was 0.4 during 2 h incubation after induction. Due to the observed growth there was most likely no expression of *gcdB* in Lemo21(DE3). The cells were harvested and opened by a French press to avoid heating of the membrane enzymes. The inner membrane fraction was prepared as described in Materials and Methods. Western analysis of his-tagged GcdB showed no meaningful expression in Lemo21(DE3). Diverse concentrations of rhamnose at various growth conditions are required in future.

3.2.2 Overexpression in *E. coli* C43(DE3)

The strain C41(DE3) was derived from BL21(DE3) (Miroux & Walker, 1996). This strain has at least one uncharacterized mutation, which prevents cell death associated with the expression of toxic recombinant proteins. The strain C43(DE3) was further derived from C41(DE3) transformed with the F-ATPase subunit gene and cured, therefore it contains no plasmid. The strain carries the lambda DE3 lysogen which expresses T7 RNA polymerase gene from the lacUV5 promoter by IPTG induction. This strain is reported as the tuned *E. coli* for membrane protein overexpression (Wagner et al, 2008). The pCDFDuet vector containing *gcdB* was transformed in *E. coli* C43(DE3). The preculture was inoculated to 1L LB medium containing antibiotic and the gene was induced by adding 0.5 mM IPTG. After 3h incubation, the cells were harvested and membrane fractions were prepared by the same method mentioned above. The level of expression was detected by SDS-PAGE, but it seemed that the *gcdB* was not expressed in *E. coli* C43(DE3).

Several technical points should be considered carefully to improve the overproduction of GcdB in *E. coli*. Especially, modifying the position of the tag is required. The *gcdB* is located at the first multicloning site of pCDFDuet-1 and the his-tag is ahead of the signal peptide of GcdB. This tag position could disturb and result in failing the correct insertion of membrane protein (Wagner et al, 2006). Furthermore, if the signal peptide is cut off, the His-tag cannot be used for purification. Trying other types of tags is also demanded. Recently developed methodologies to rapidly monitor yields of membrane protein overproduction enable different conditions and hosts to be screened. Fusing GFP to the C terminus of membrane proteins enables overproduced proteins to be monitored in intact cells. The GFP moiety folds properly and becomes fluorescent only if a membrane protein is stably inserted into the membrane. In addition, the GFP moiety facilitates purification and quality assessment of the membrane-protein-GFP fusion directly coupled to fluorescence detection (Drew et al, 2005; Drew et al, 2001).

4. Biotin carboxyl carrier protein, GcdC

4.1 Sequence analysis of *gcdC*

The gene encoding biotin carrier protein, GcdC, is composed of 210 base pairs (GC content: 53.13%) and coding for 69 amino acids with a calculated molecular mass of 7.37 kDa. The direction of the transcription is forward. The two GcdC subunits ($GcdC_1$ and $GcdC_2$) are encoded by slightly different genes in *C. symbiosum* (Kress et al, 2009). The GcdC from *S. aciditrophicus* shares 46% and 42% amino acid sequence identity with $GcdC_1$ and $GcdC_2$ from *C. symbiosum*, and 36% of it from *A. fermentans*, respectively. Interestingly, the alanine-proline (AP)-rich domain, which is typically observed in the GcdCs from *C. symbiosum* and *A. fermentans*, is not present in GcdC of *S. aciditrophicus* (Fig. 40). This AP-rich linker domain is highly flexible stretch and it seems to interfere with crystallization of Gcd by. This feature may increase the chance to solve the complete structure of Gcd of *S. aciditrophicus*.

```
Csym_gcdC1      -MKYIATINGKRYEVEVERVEGYKSLDRNGVAAPKAPALASTAPVQRPAAPAPA-APAPA 58
Csym_gcdC2      -MKYTATLNGKQYDVELERIGEYEPIPRYGEAAP-APAAPITAP---AAAPAPV-AAAPA 54
Afer_gcdC       MRKFNVNVNGTVYTVEVEEVGGAVTAAPAAPAAPAAAPAAAPVAAAPAAAPAPAPAAAPA 60
SB_gcdC         ------------------------------------------------------------

Csym_gcdC1      AAPAPAAAPAPVAAPAPAAAGATTVEAPMPGKVLDVKVTAGQVVKYGDVVAIMEAMKMET 118
Csym_gcdC2      PAPAPAAP-----APAPAAGG-TTVEAPMPGKVLDVKVAAGQAVKFGQVVITMEAMKMET 108
Afer_gcdC       AAPAPAAK-----PAAAAPAGSVTVSAPMPGKILSVNVKPGDKVEAGDVLLILEAMKMQN 115
SB_gcdC         ----------------------MEVTVPMEGKVVAIKVNVGDKVEEDDEIAVMEAMKMEM 38

Csym_gcdC1      EIVAPADGTVSQILVKAGDPVDTGAAMVVLN 149
Csym_gcdC2      EIVAPADGTVAQILVKAGDAVETGTAMVVLN 139
Afer_gcdC       EIMAPEDGTVSEVRVNAGDTVATGDVMVIL- 145
SB_gcdC         PVPSPVSGVVKQIMVKVGDKVAAEAALMVIE 69
```

Fig. 40. Comparison of the deduced amino acid sequences of GcdCs from *C. symbiosum*, *A. fermentans*, and *S. aciditrophicus*. Conserved residues are marked in gray. Bold amino acids indicate the AP-rich linker domain and underline reveals the biotin-binding site. The highly conserved motif is highlighted in yellow while the lysine to which biotin is attached is shown in red.

4.2 Cloning and expression of *gcdC*

The ORF, *gcdC* was cloned into pACYCDuet-1 at multi-cloning site 1, pASK-IBA3plus, and pASK-IBA7plus. To overexpress *gcdA* and *gcdC* together, *gcdC* was cloned into pACYCDuet-1 and pASK-IBA3plus which already harbors *gcdA*. The recombinant plasmid was transformed into *E. coli* Rosetta (DE3) pLysS or BL21 (DE3) to increase the yield of the

protein. The culture was incubated in the medium supplemented with 50 μM D-biotin. The overproduction and purification was performed as described in Materials and Methods. GcdC could be purified by two different affinity chromatographies depending on the binding strength between (1) monomeric avidin column (SofLink^{TM}) and biotin, (2) His-tag (pACYCDuet-1 vector) and NiNTA column. On SDS-PAGE, the *gcdC* cloned in pASK-IBA3plus and pASK-IBA7plus showed overexpression, in contrast, *gcdC* in pACYCDuet-1 was not expressed.

5. Coexpression of *gcdAC, gcdABC* in *E. coli*

Coexpression involves the transformation of *E. coli* with several plasmids that have compatible origins of replication and independent antibiotic selection for maintenance. The vector, pACYCDuet-1 contains a chloramphenicol resistant gene and pCDFDuet-1 has a streptomycin/spectinomycin resistance gene. These vectors can be used in combination in an appropriate host strain for the coexpression according to the Novagen's manual. To achieve the complete recombinant Gcd complex in *E. coli*, simultaneous expression was designed. First, the recombinant plasmid harboring *gcdA* and *gcdC* was constructed into pACYCDuet-1 and pASK-IBA3plus vectors and transformed in *E. coli* DH5α. Second, the *gcdB* introduced in pCDFDuet-1 vector was transformed into the *E. coli* cells containing the *gcdAC* in pACYCDuet-1 vector. At last the *E. coli* cells resistant to both antibiotics were selected for coexpression of *gcdABC*. Up to now, only coexpression of *gcdAC* in pASK-IBA3plus vector was successful. None of the gene introduced in Duet vector system led to any tangible expression.

6. Sequence analysis and cloning of biotin ligase

To enhance the yield of incorporation of biotin into Gcd, the gene encoding biotin ligase could be used. The gene, SYN_00211 is annotated as biotin-(acetyl-CoA carboxylase) ligase in the genome database of *S. aciditrophicus*. The gene consists of 1,002 base pairs (GC content: 56.86%) and codes for 333 amino acids with a calculated molecular mass of 36.95 kDa.

For coexpression with *gcdAC*, the restriction enzyme *SalI* and *BsaI* (= *Eco31*) was introduced in the primers for cloning into the expression vector pASK-IBA3plus which contains *gcdAC*. The gene was amplified by PCR. The PCR product and the vector were digested by restriction enzymes and ligated with each other. Analysis of the recombinant plasmid by restriction enzymes showed that ligation did not occur properly, presumably, either due to the short space between the *SalI* and *BsaI* restriction sites on the vector or due to an inactive T4 DNA ligase.

7. Enzyme assays of Gcd from *S. aciditrophicus*

To determine the presence of Gcd in vivo and its ability to convert glutaconyl-CoA to crotonyl-CoA, a coupled assay was performed mentioned before. There was no activity present for the Gcd in the membranes of *S. aciditrophicus* grown on crotonate. This could be for many reasons including: the subunits of the enzyme were separated during preparation or the membrane enzymes were too diluted to detect the activity. The activity of Gcd was also measured by J. Sieber (University of Oklahoma, USA) by using another coupled assay in which glutaconyl-CoA was produced by the transferring of a CoA group acetyl-CoA to glutaconate. The next step is the decarboxylation of glutaconyl-CoA to crotonyl-CoA by the solubilised membrane proteins of *S. aciditrphicus*. To determine this reaction, the crotonyl-CoA and CO_2 are reduced and isomerized to ethylmalonyl-CoA by a crotonyl-CoA reductase/isomerase which utilizes NADPH (Erb et al, 2009). The enzyme reaction can be followed by the oxidation of NADPH at 340 nm. No activity was observed from the membrane proteins. The assay was then attempted on the cell free extracts of *S. aciditrophicus*, which contains soluble and membrane proteins. The cell free extracts of *S. aciditrophicus* could oxidize the NADPH without any of the other components of the assay. The NADPH oxidation occurred at the same rate whether or not glutaconate or acetyl-CoA was present.

8. Purification of Gcd from *S. aciditrophicus*

Frozen *S. aciditrophicus* cells grown on crotonate anaerobically (20 g) were obtained from the group of Prof. M. Boll, Universität Leipzig. For each purification 7 – 8 g cells were used.

Preparation of membrane extracts and purification were performed at 4 °C aerobically. The activity from the whole cells was exceedingly negligible. The solubilized membrane was loaded onto the monomeric avidin column and Gcd was eluted in 20 mM phosphate buffer pH 7.0 containing 0.1% dodecylmaltoside and 2 mM D-biotin. The protein containing fractions were concentrated. The estimated molecular mass of GcdA is 65.37 kDa and of GcdB is 47.5 kDa. The three bands close by the sizes of GcdA and GcdB from solubilized membrane and the elution fraction on SDS-PAGE were cut and extracted for analysis of MALDI-TOF. The fragmented peptides (Fig. 41. a, b, and c) by tryptic digestion were compared with the deduced amino acid sequences of GcdA and GcdB from *S. aciditrophicus*. Contrary to the expectation, none of the bands specifically matched the sequence of GcdA or GcdB. Identification of the fragmented peptide sequences by comparison with the database of *S. aciditrophicus* could not be done because uploading the database to the in-house system was not completed. The concentrated elution fraction did not show glutaconyl-CoA decarboxylase activity.

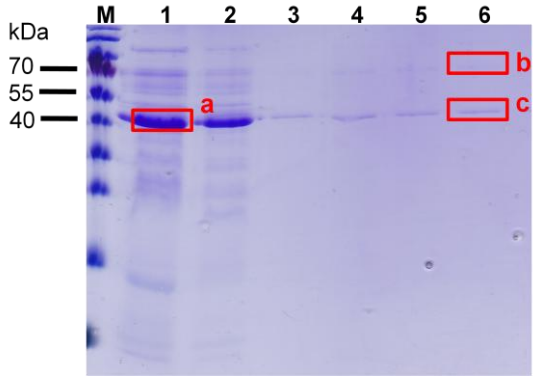

Fig. 41. SDS-PAGE of solubilized membrane from *S. aciditrophicus* and fractions of purification by the avidin column. M, Molecular mass marker; 1, solubilized membrane; 2, flow through of the Avidin column; 3, washing; 4-6, elution fractions. The bands (a, b, and c) in red boxes on SDS-PAGE gel were cut out and analyzed by MALDI-TOF.

Discussion

1. *Re*-Citrate synthase

The genome of *S. aciditrophicus* provides general schemes of carbon flow, electron transfer and energy-transducing systems needed to survive as a syntroph at the thermodynamic limit. However, the genomic analysis does not reveal the complete metabolic pathways. Therefore, integrated biochemical analysis is indeed required to bridge and comprehend the nonconventional mode of syntrophic life. For example, glutamate is usually synthesized from acetyl-CoA via citrate, isocitrate and 2-oxoglutarate in TCA cycle. The first step of the pathway involves a citrate synthase. But no gene for *Si*-citrate synthase has been detected in the genome of *S. aciditrophicus*.

The presence of a different stereospecific citrate synthase from anaerobic bacteria has been reported (Feng et al, 2009; Gottschalk, 1969; Li et al, 2007; Tang et al, 2007) and the gene encoding *Re*-citrate synthase has been detected in *C. kluyveri* (Li et al, 2007). The genome of *S. aciditrophicus* contains a gene for isopropylmalate/homocitrate/citramalate synthase (SYN_02536) which has 49% deduced amino acid sequence identity with *Re*-citrate synthase from *C. kluyveri* but not with *Si*-citrate synthase from *E. coli*. The presence of isopropylmalate/homocitrate/citramalate synthase was detected in crotonate grown cells by proteomic analysis (personal communication, Dr. H. Mouttaki, University of Oklahoma, USA). To elucidate whether the gene functions as *Re*-citrate synthase and contributes to most likely glutamate biosynthesis in *S. aciditrophicus*, the recombinant protein was produced for biochemical studies.

The *Si*-citrate synthases from Gram-positive bacteria and archaea are generally homodimers, whereas the major conformation of those from Gram-negative bacteria is a homohexamer (Gerike et al, 1998; Wiegand & Remington, 1986). Interestingly, *Si*-citrate synthase from the Gram-negative *Geobacter sulfurreducens* is dimer and similar to that of eukaryotes (Bond et al, 2005). The quaternary structure of the clostridial *Re*-citrate synthases has not been analysed. The monomer of recombinant *Re*-citrate synthase from *S. aciditrophicus* fused with 1 kDa Strep-tag revealed by mass spectrometry the calculated value of 72.8 kDa. The quaternary structure of the holoenzyme was attempted to determine by native PAGE using a 4 − 20% gradient gel and by gel filtration. Although the results could be inferred that the

enzyme consists of homodimer, a trimer or tetramer cannot be excluded. The quaternary structure of *Re*-citrate synthase should be analysed further in future.

To characterize the *Re*-citrate synthase, purification of the native protein from *S. aciditrophicus* cells was performed by using an ion-exchange column. But it was not successful because other enzymes and components in the purification fractions interfered in distinguishing the actual activity of *Re*-citrate synthase. For instance, there are 2 copies of acetyl-CoA acetyltransferase gene in the genome of *S. aciditrophicus*. The enzymes coded by those genes react with the acetyl-CoA in assay mixture and yield free CoASH that is detected by DTNB.

The specific activity of *Re*-citrate synthase was around 1 U/mg using oxaloacetate and acetyl-CoA as substrates. The highest specific activity (1.6 U/mg) was achieved in the presence of 0.2 mM Co^{2+} in an assay mixture. Approximately 1 U/mg is also observed in *C. kluyveri*, *Re*-citrate synthase from *C. acidiurici* showed 5.5 U/mg (Goschalk & Dittbrenner, 1970). On the other hand, *Si*-citrate synthases from other microbes show much higher specific activities and the one from pig heart is around 100 U/mg (Zhi et al, 1991). The *Si*-citrate synthase from *G. sulfurreducens*, an anaerobic metal-reducing bacterium, showed ca. 20 U/mg (Bond et al, 2005). Up to now, *Re*-citrate synthase has been reported only from anaerobic microorganisms, while *Si*-citrate synthase exist from bacteria to mammals. Owing to the low activity found in anaerobic bacteria, we can speculate that *Re*-citrate synthase has evolved very early during the emergence of life with a biosynthetic anabolic function. Citrate is a symmetrical molecule, but aconitase is known to be stereospecific for the prochiral structure of citrate, providing the stereochemical bias of the reaction. This means that either *Si*- or *Re*-citrate synthase could provide a proper stereospecific substrate for the subsequent reaction catalyzed by aconitase whereas only the *Re*-type of homocitrate or isopropylmalate synthase can do it. Therefore, it is hypothesized that the ancient *Re*-citrate synthase was replaced by the higher active and divalent metal ion-independent *Si*-citrate synthase during the evolutional history of life and the *Re*-citrate synthase only remained in few anaerobic bacteria. On the other hand, the homocitrate or isopropylmalate synthases could not be replaced by the advanced *Si*-type.

The partially purified ‘oxygen sensitive’ *Re*-citrate synthase (Gottschalk, 1969) might have contained iron that may have generated highly reactive hydroxyl radicals (˙OH, Fenton’s reaction). Moreover, the *Re*-citrate synthase does not contain any other cofactors, for example,

iron-sulfur cluster or flavin which cause oxygen sensitivity. Therefore, it is logical that the recombinant *Re*-citrate synthase from *S. aciditrophicus* is not oxygen-sensitive.

p-Hydroxymercuribenzoate, iodoacetamide and DTNB are known as sulfhydryl reagents that react with thiol groups (R-SH) particularly in proteins. The recombinant *Re*-citrate synthase was inactivated by *p*-hydroxymercuribenzoate almost instantly and also lost 30% activity by incubation with 0.2 mM iodoacetamide. A sigmoidal curve and slightly decreased relative activity (70%) was observed by the DTNB assay compared to the direct assay detecting absorbance change of the thioester bond of acetyl-CoA at 232 nm. Probably it reacts with one of the six cysteines in the deduced amino acid sequence of *Re*-citrate synthase. Nano LC of tryptic peptides and MALDI-TOF mass spectrometry of the enzyme treated with iodoacetamide in presence of oxaloacetate and DTT revealed C117 as the target of the reagent. Regarding the crystal structure of *Re*-isopropylmalate synthase (LeuA) from *M. tuberculosis* (Koon et al, 2004), it seems that C117 does not place around the active center. To sum it up, these sulfhydryl reagents partially inactivate the enzyme, but a cysteine residue in the catalytic activity seems not to be involved.

EDTA (0.2 mM) almost immediately inactivated the enzyme. EDTA is widely used as a hexadentate ligand and chelating agent, in other word, its ability to bind to metal ions and form strong complexes. Once metal ions are extensively enveloped by EDTA, their catalytic properties are suppressed (Auld, 1995). The activity of the EDTA-inactivated enzyme was restored by addition of 0.2 mM Mn^{2+} or Co^{2+} and to a smaller extent by Zn^{2+} but not by Mg^{2+}. In the absence of these metal ions the enzyme showed activity but the time course of the reaction was sigmoidal. Preincubation of the enzyme with 0.2 mM Mn^{2+} or Co^{2+} converted the sigmoidal curve into a saturating curve. It is speculated that trace amounts of contaminating metal ions in the assay buffer could activate the metal-free enzyme and the additional metal ions such as Mn^{2+} or Co^{2+} supplement to overcome the sigmoidal curve.

Metal ions also helped to stabilize the enzyme at 4 °C whereby Co^{2+} was the most effective one. The metal binding amino acid residues Asp81, His285 and His287 in the Zn^{2+}-containing LeuA from *M. tuberculosis* (Koon et al, 2004) are conserved in the amino acid sequences of *Re*-citrate synthase from *C. kluyveri*. In LeuA, Zn^{2+} plays roles in substrate binding and polarizing the carbonyl bond of the substrate whereas histidine residues do in *Si*-citrate synthase. But no metal ion was detected in the recombinant protein of *S. aciditrophicus*.

Moreover, mass spectrometry of the recombinant enzyme supplemented with and without Co^{2+} yielded identical values.

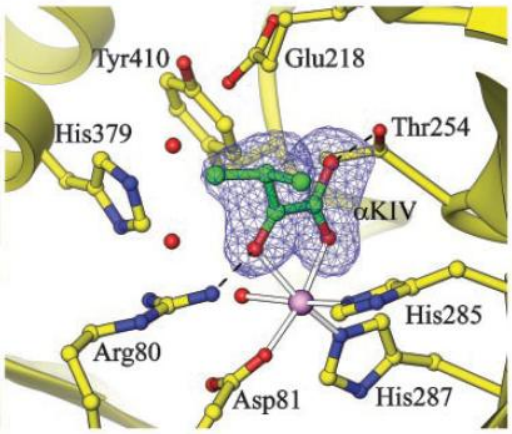

Fig. 42. Active site of α-isopropylmalate synthase from *M. tuberculosis* (Koon et al, 2004). The bound substrate α-ketoisovalerate is depicted with its electron density. The Zn^{2+} ion is a magenta sphere. Red spheres in red are two water molecules in the adjacent acetyl-CoA cavity. Hydrogen bond is shown as a broken line.

Even though both *Si*- and *Re*-citrate synthase catalyze the formation of citrate, the enzymes should have different active sites due to the different stereospecificity. In Fig. 43, the different mechanisms of the *Si*- and *Re*-specific enzymes have been shown by the comparison of crystal structure of LeuA from *M. tuberculosis* (Koon et al, 2004) and *Si*-malate synthase from *E. coli* (Anstrom et al, 2003). The primary sequence identity analysis displays that the main substrate- and metal-binding residues, as well as a number of other residues, whose roles have not yet been identified in LeuA, are conserved in *Re*-citrate synthase from *C. kluyveri* and S. *aciditrophicus*. As both LeuA and *Re*-citrate synthase are *Re*-specific enzymes catalyzing the same Claisen-type condensation with similar substrates requiring divalent metal ions, we can assume that the catalytic centers should be comparable to each other. Up to now, no crystal structure of a *Re*-citrate synthase is known. To explore the catalytic mechanism of the enzyme, further attempts for crystallization are planned in near future.

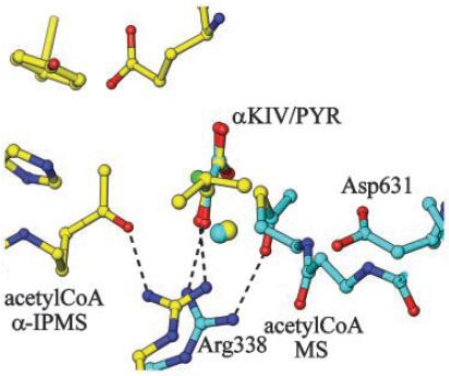

Fig. 43. Comparison of the active sites of *Re*-specific α-isopropylmalate synthase (yellow) and *Si*-specific malate synthase (cyan). Acetyl-CoA modeled for LeuA (α-IMPS) and located experimentally for malate synthase (MS) approaches from opposite sides to the carbonyl group of the substrate (α-ketoisovalerate or pyruvate; αKIV/PYR)

Si-Citrate synthase performs two half-reactions: (1) the mechanistically intriguing condensation of acetyl-CoA with oxaloacetate to form citryl-CoA and (2) the subsequent hydrolysis of citryl-CoA. The condensation reaction requires the abstraction of a proton from the methyl carbon of acetyl-CoA to generate a reactive enolate intermediate. However, the exact mechanism of *Re*-citrate synthase is still unknown.

To elucidate the reaction mechanism and to defined the rate-limiting step, the primary kinetic isotope effect (KIE) was determined by using [$^1H_3$] and [$^2H_3$]acetyl-CoA. If the proton is replaced by the heavier isotope, a slower rate of reaction should be observed because the C-D bond has lower zero-point energy than the C-H bond and therefore requires a higher activation energy for bond cleavage. A small kinetic isotope effect (KIE 1.7, calculated via V_{max}/K_m) was observed at a fixed saturating concentration of oxaloacetate and variable concentrations of [$^1H_3$] and [$^2H_3$]acetyl-CoA. Both V_{max} from *Re*-citrate synthase were nearly the same (0.39 U/mg from [$^1H_3$]Acetyl-CoA vs. 0.33 from [$^2H_3$]acetyl-CoA) but the K_m values differed more (147 µM vs. 214 µM). In case of malate synthase (Cornforth et al, 1969) and *Si*-citrate (Kosicki & Srere, 1961) similar low intermolecular deuterium isotope effects (1.4) were measured by comparing V_{max}. Other data could not be found in the literature.

2. Glutamate biosynthesis pathway

Glutamate, one of the cellular building blocks, is generally synthesized by the reductive amination of 2-oxoglutarate, an intermediate of the TCA cycle. The reductive amination of 2-oxoglutarate is catalyzed by glutamate dehydrogenase, glutamate synthase or an amino transferase.

2.1 Genomic evidences and proposed labeling patterns

Among many possibilities, we could deduce biosynthetic pathways for glutamate based on the genomic analysis. The following proposed labeling patterns are estimated in *S. aciditrophicus* grown on crotonate with [1-^{14}C]acetate (red) or $^{13}CO_2$ (blue).

2.1.1 Glutamate biosynthesis via the 2-hydroxyglutarate pathway

Glutaconyl-CoA is the key intermediate for bidirectional metabolic flow in *S. aciditrophicus* depending on the carbon sources. If the 2-hydroxyglutarate pathway is active in vivo, 2-oxoglutarate, the precursor of glutamate, could be synthesized from glutaconyl-CoA by hydration to (*R*)-2-hydroxyglutaryl-CoA, CoA transfer and oxidation of (*R*)-2-hydroxyglutarate.

The (*R*)-2-hydroxyglutarate dehydrogenase catalyzes the reduction of 2-oxoglutarate to (*R*)-2-hydroxyglutarate in *A. fermentans* (Martins et al, 2005), which ferments glutamate via 2-hydroxyglutarate pathway. In *S. aciditrophicus*, two candidate genes were detected by BLAST search: SYN_00123 annotated as D-3-phosphoglycerate dehydrogenase, SYN_01083. The catalytically important amino acid residues (Arg 52, Arg235, Glu264 and His297 of the dehydratase from *A. fermentans*) are conserved in both two genes.

The reversible dehydration of (*R*)-2-hydroxyglutaryl-CoA to (*E*)-glutaconyl-CoA is catalyzed by 2-hydroxyglutaryl-CoA dehydratase consisting of two protein components (A, the homodimeric activator, and D, the heterodimeric dehydratase) (Bendrat et al, 1993; Müller & Buckel, 1995; Schweiger et al, 1987). Three possible genes for 2-hydroxyglutaryl-CoA dehydratase and two genes encoding the activator were found in genome of *S. aciditrophicus* by the homology study and conserved cysteine residues from the deduced amino acid sequences. The results indicate that two of three genes for the dehydratase seem to resemble

the α-subunit of component D containing three conserved cysteines for iron-sulfur cluster but no conserved glutamate at the active site. The deduced amino acid sequence of gene for the activator reveals that the two cysteines required for an [4Fe-4S] between two identical subunits are conserved. Thus, the presence of 2-hydroxyglutaryl-CoA dehydratase and its activator in *S. aciditrophicus* is controversial so far.

The gene for glutaconate CoA-transferase does not exist in *S. aciditrophicus*. It is logical that glutaconate CoA-trasnferase is not necessary for benzoate synthesis and degradation, because glutaconyl-CoA is not obtained from glutaconate but from crotonyl-CoA by carboxylation most likely catalyzed by glutaconyl-CoA decarboxylase in *S. aciditrophicus*. In glutamate synthesis also a 2-hydroxyglutaryl-CoA hydrolase could be involved.

The labeling pattern of glutamate synthesized via 2-hydroxyglutarate is shown in Scheme 7. Starting from unlabeled crotonate and CO_2 glutamate would be unlabeled. However, by rapid equilibration between crotonyl-CoA and labeled acetyl-CoA as observed earlier (Mouttaki 2007) glutamate would exhibit the same labeling pattern as derived via *Re*-citrate synthase (see below). This rapid equilibration could be possible, because the carboxylation to glutaconyl-CoA that requires $\Delta\mu Na^+$ may be rate limiting.

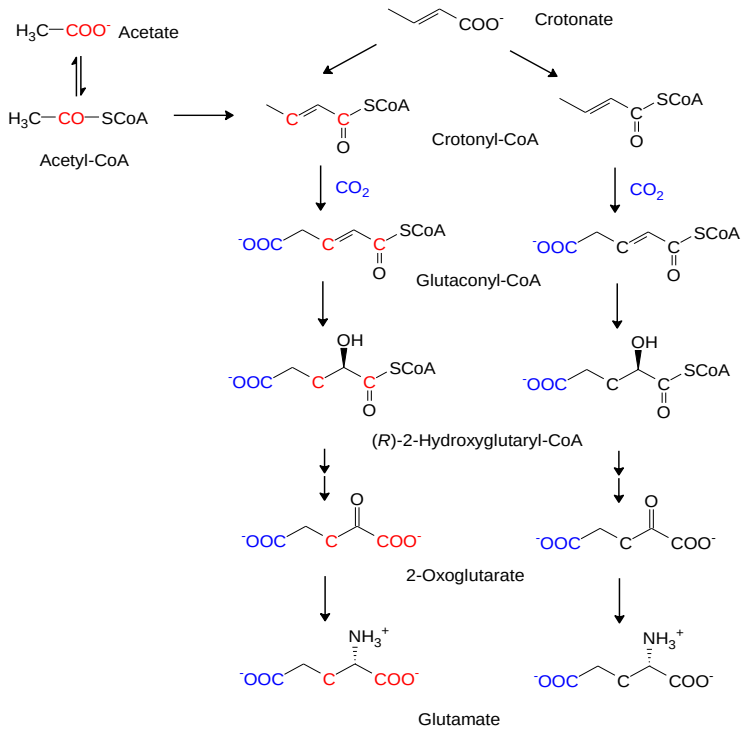

Scheme 7. Predicted labeling patterns for biosynthesis of glutamate via 2-hydroxyglutarate pathway.

2.1.2 Glutamate biosynthesis via the ethylmalonyl-CoA pathway

Recently, the ethylmalonyl-CoA pathway for synthesis of C_5-dicarboxylic acids from C_2-units has been newly found in isocitrate lyase-negative *Rhodobacter sphaeroides* (Erb et al, 2007) and *Methylobacterium extorquens* (Peyraud et al, 2009). In this pathway, in general, 3 acetyl-CoA and 2 CO_2 are converted to malate and succinate (Fig. 44). Crotonyl-CoA carboxylase/reductase catalyzes the carboxylation of crotonyl-CoA together with CO_2 and NADPH to ethylmalonyl-CoA and $NADP^+$. The enzyme can be the marker for the existence of the pathway. Interestingly, two coenzyme B_{12}-dependent enzymes, ethylmalonyl-CoA mutase (ethylmalonyl-CoA → methylsuccinyl-CoA) and methylmalonyl-CoA mutase (methylmalonyl-CoA → succinyl-CoA) are involved in the intermediate steps. The BLAST search reveals that no genes similar to crotonyl-CoA carboxylase/reductase and to these two B_{12}-dependent mutases are detected in *S. aciditrophicus*. Furthermore, it seems that genes encoding β-methylmalyl-CoA/L-malyl-CoA lyase (β-methylmalyl-CoA → glyoxylate + propionyl-CoA) and malate synthase also do not exist. Therefore, the ethylmalonyl-CoA pathway of acetate and CO_2 assimilation can be excluded in glutamate biosynthesis.

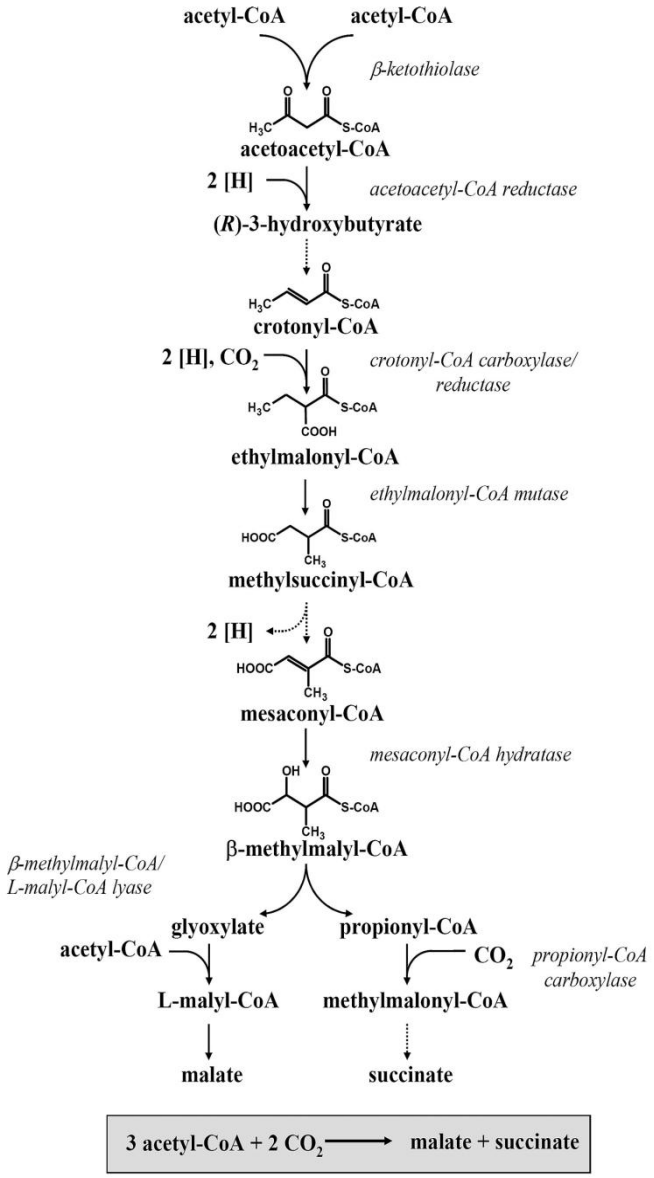

Fig. 44. Ethylmalonyl-CoA pathways in isocitrate lyase-negative *R. sphaeroides* (Erb et al, 2007). The reactions have not been elucidated are depicted as dotted lines.

2.1.3 Syntheses of pyruvate and oxaloacetate

Pyruvate is the most common α-ketoacid and a key molecule in several metabolic pathways (Lengeler et al, 1999). In *S. aciditrophicus* pyruvate is formed from acetyl-CoA by carboxylation mediated by a pyruvate:ferredoxin 2-oxidoreductase (SYN_00691 – 00694) or a pyruvate synthase (SYN_00154 – 00157).

Oxaloacetate is most likely obtained from pyruvate according to the genome analysis. Firstly, oxaloacetate could be formed by the initial step of gluconeogenesis, the carboxylation of pyruvate catalyzed by the biotin-containing pyruvate carboxylase (SYN_01040, SYN_01041). The conserved biotin binding motif (EAM**K**M) was found in the deduced amino acid sequence of the gene for the carboxyltransferase subunit (SYN_01040) of the complex. Secondly, the genes encoding phosphoenolpyruvate carboxykinase (SYN_02086) which catalyzes the subsequent carboxylation from phosphoenolpyruvate to yield oxaloacetate and ATP is present. Phosphoenolpyruvate could be derived from pyruvate by phosphoenolpyruvate synthase (SYN_01243, SYN_02383, and SYN_02966). Interestingly, downstream of SYN_01243, the gene encoding glutamate dehydrogenase (SYN_01242) is placed.

2.1.4 Glutamate biosynthesis via the TCA cycle

The TCA cycle comprises a series of enzyme-catalyzed chemical reactions, which are of central importance for generation of reducing equivalents to be fed into the respiratory chain and in all living cells for the formation of building blocks. Genome analysis shows that only few microorganisms such as *E. coli*, *Bacillus subtilis*, *M. tuberculosis* and *Saccharomyces cerevisiae*, and the small genome of *Rickettsia prowazekii* contain the complete set of genes for TCA cycle (Huynen et al, 1999).

S. aciditrophicus has an incomplete TCA cycle as revealed by genome analysis. Besides *Re*-citrate synthase (see above), McInerney et al. reported (McInerney et al, 2007) that genes for malate dehydrogenase, isocitrate dehydrogenase, 2-oxoglutarate synthase, aconitase, and fumarase were identified. In addition, the recent genome database of *S. aciditrophicus* (http://biocyc.org, http://www.genome.jp/kegg) shows that the gene for fumarate reductase (SYN_00424) and genes encoding subunits of succinyl-CoA synthetase catalyzing formation of succinate and CoA from succinyl-CoA exist. But the genes for malate dehydrogenase and the *Si*-type of citrate synthase could not be detected in the data base.

The reductive branch of the TCA cycle

Interestingly, there is a gene annotated as NAD-dependent malic enzyme (SYN_00517) catalyzing the oxidative decarboxylation of malate to pyruvate. The deduced gene shows 60% amino acid sequence identity with the gene for malate dehydrogenase from *Thermoanaerobacter* sp., in which evidence for the presence of *Re*-citrate synthase by isotopomer-assisted metabolic pathway analysis was obtained (Feng et al, 2009). As shown with *Re*-citrate synthase, gene annotation often does not reveal the real function of the gene. In the same context, the gene annotated as NAD-dependent malic enzyme (SYN_00517) could function as malate dehydrogenase in vivo. If glutamate is synthesized via the reductive branch of the TCA cycle using [1-^{14}C]acetate and unlabeled CO_2 as carbon sources, it should be equally labeled at C3 or C4. (Scheme 8, magenta color).

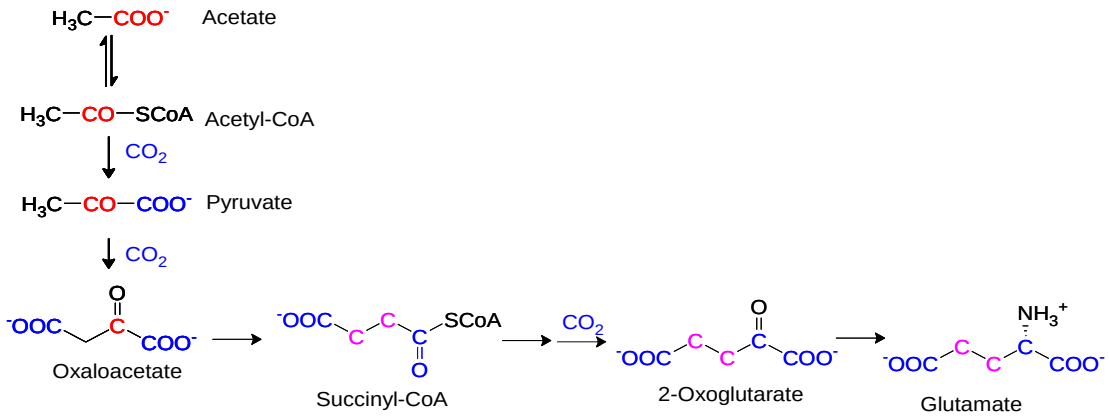

Scheme 8. Predicted labeling patterns for biosynthesis of glutamate via the reductive branch of the TCA cycle.

The oxidative branch of the TCA cycle

In this study, the presence of the *Re*-type of citrate synthase and the catalytic properties of the enzyme have been shown. Thus in *S. aciditrophicus*, the oxidative branch of the TCA cycle from oxaloacetate via citrate could yield 2-oxoglutarate. In addition, the genes for glutamate dehydrogenase and glutamate synthase are found in the genome. Therefore, we hypothesized that glutamate could be synthesized via the oxidative branch of the TCA cycle.

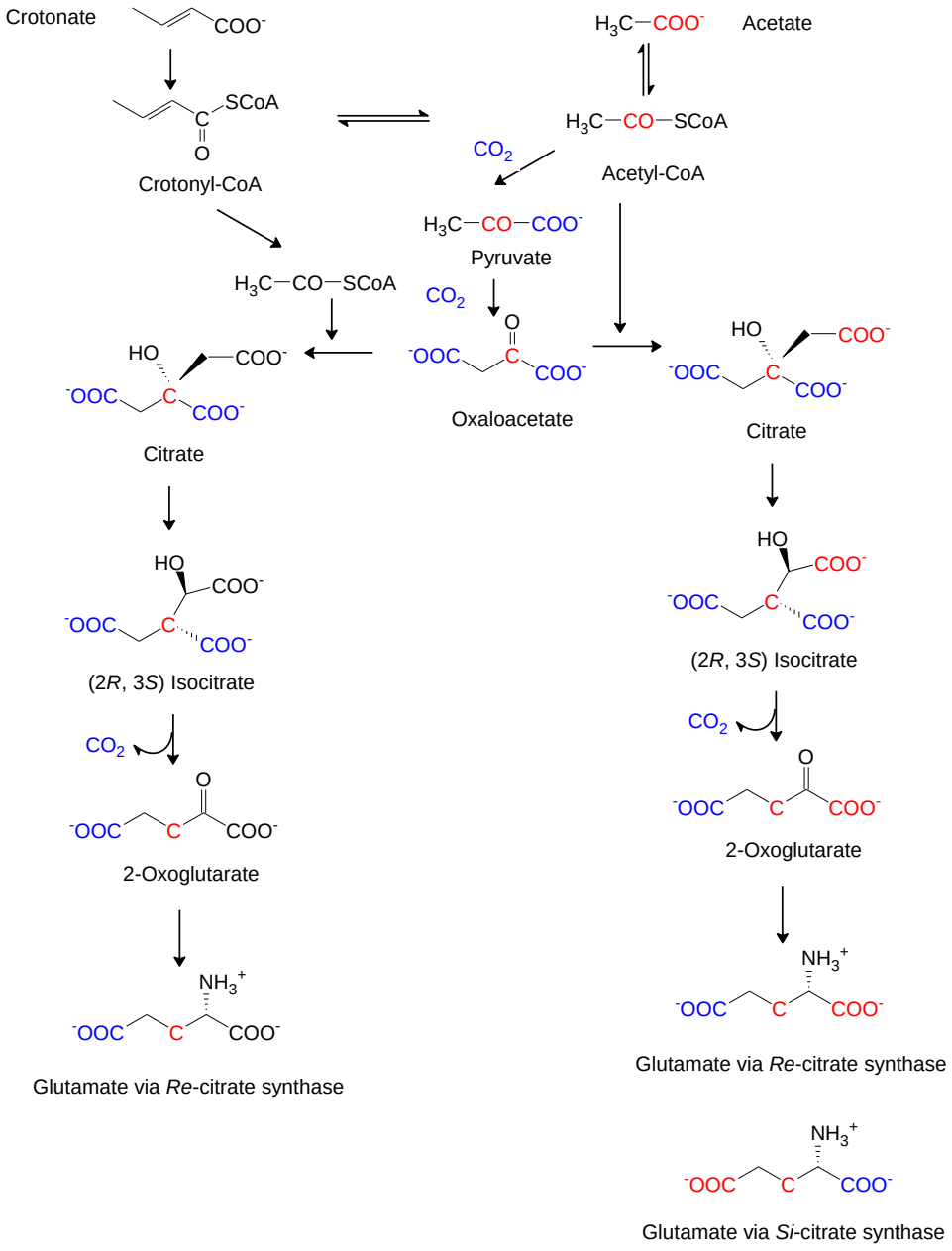

Scheme 9. Predicted labeling patterns for biosynthesis of glutamate via the oxidative branch of the TCA cycle. Pyruvate is the common source of oxaloacetate.

Depending on the sources of oxaloacetate (Scheme 9) or acetyl-CoA (Scheme 10), one may forecast mainly 4 different labeling patterns of glutamate synthesized from [1-^{14}C]acetate and unlabeled crotonate + CO_2 via *Re*-citrate synthase in the oxidative branch of the TCA cycle. These patterns differ, because acetyl-CoA required for pyruvate/oxaloacetate and citrate syntheses could be derived from unlabeled crotonate or from labeled acetate. Experiments with [1-^{13}C]acetate showed, however, that the labeling pattern of cyclohexane carboxylate

indicated a complete equilibration between acetyl-CoA originated either from crotonate or from acetate (Mouttaki et al, 2007). Therefore, we expect the pattern shown in the right pathway of Scheme 9. Furthermore, [1-^{13}C]acetyl-CoA was detected by GC-MS in cells grown on unlabeled crotonate and [1-^{13}C]acetate (Dr. Y. Tang, personal communication).

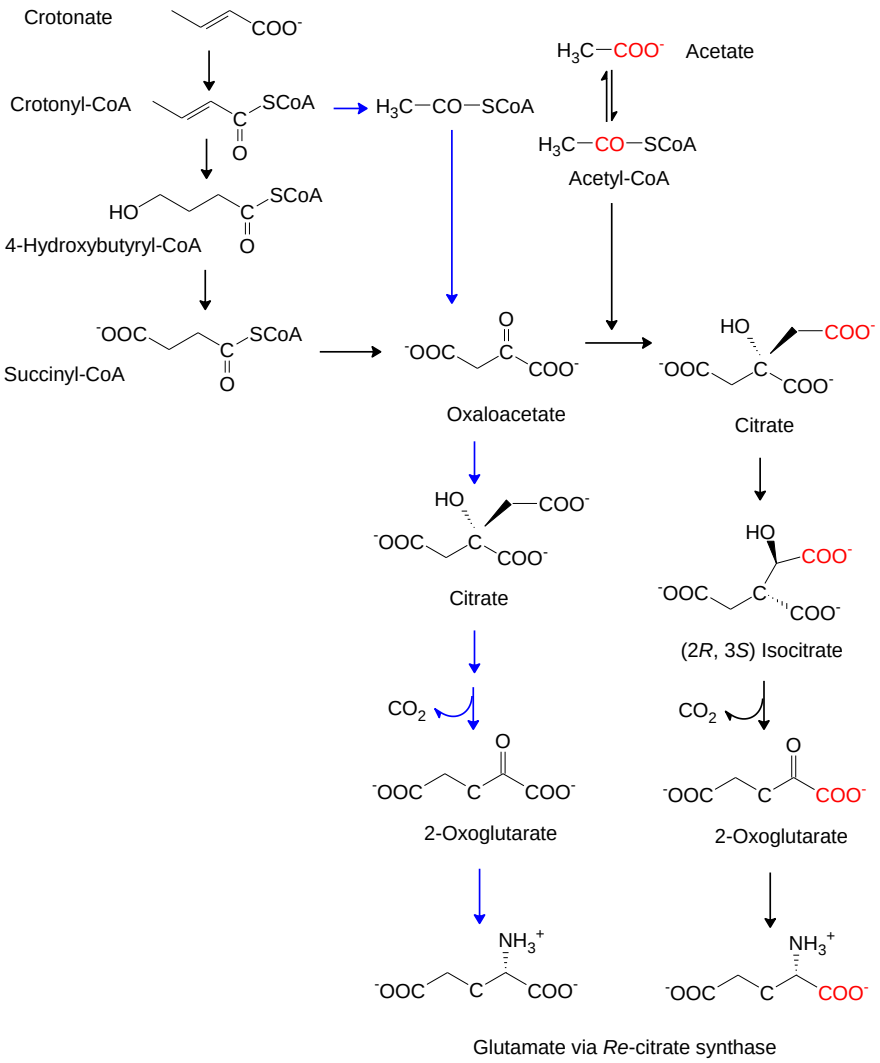

Scheme 10. Predicted labeling patterns for biosynthesis of glutamate via the oxidative branch of the TCA cycle. Oxaloacetate is derived from crotonate via 4-hydroxyglutaryl-CoA and succinyl-CoA.

2.2 Exploring glutamate biosynthesis in *S. aciditrophicus* by ^{13}C- and ^{14}C-labeling

2.2.1 The oxidative branch of TCA cycle via *Re*-citrate synthase

To elucidate the role of *Re*-citrate synthase in glutamate biosynthesis in *S. aciditrophicus*, tracer experiments with [1-^{14}C]acetate as well as ^{13}C-isotopomer-assisted metabolite analysis were applied. The predicted (Schemes 7 – 9) and observed labeling patterns are presented in Fig. 45. Dr. M. J. McInerney, Huynh Le (Uni Oklahoma, USA) prepared the cultures in presence of [1-^{13}C]acetate and Dr. Y. Tang (Washington University in St. Louis, USA) analyzed the metabolites by gas chromatography-mass spectrometry (GC-MS). Five types of charged fragments for derivatized amino acids were detected by GC-MS; the $[M-57]^+$ or $[M-15]^+$ group (unfragmented amino acids); the $[M-159]^+$ or $[M-85]^+$ group (amino acids losing the α-carboxyl group); the [f302] group (amino acids losing the R-group).

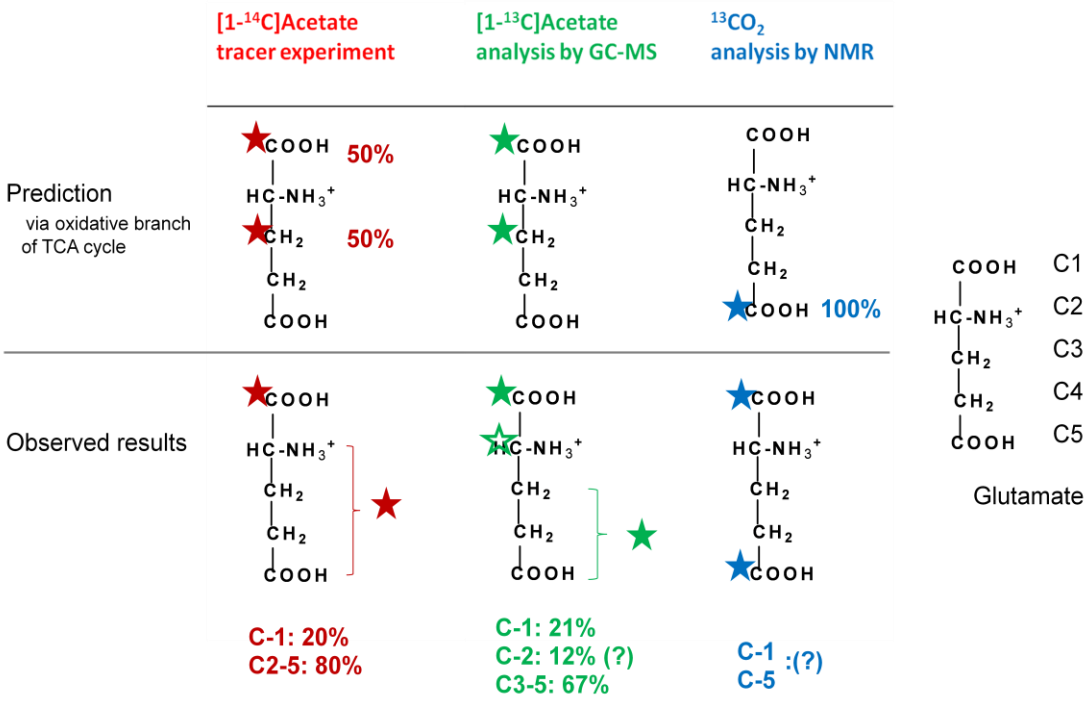

Fig. 45. Predicted and observed labeled glutamate isolated from *S. aciditrophicus* grown on crotonate with labeled [1-^{14}C]acetate (red), [1-^{13}C]acetate (green) or $^{13}CO_2$ (blue). The labeled carbons are predicted based on the oxidative branch of TCA cycle via *Re*-citrate synthase.

The labeled carbons were detected in amino acids by radioactive tracer experiments, GC-MS, and NMR, indicating a global utilization of acetate as the carbon source. The similar labeling patterns of alanine and aspartate, which are synthesized from pyruvate and oxaloacetate, respectively, suggest that these 2-oxoacids are synthesized from acetyl-CoA by carboxylations.

The predicted labeling patterns do not agree with the observed results (Fig. 45). C1 and C3 of glutamate were expected to be equally labeled from [1-^{14}/^{13}C]acetate via *Re*-citrate synthase by the oxidative branch of the TCA cycle. But the ^{14}C-tracer experiment shows that C1 of glutamate is partially labeled (20% rather than 50%) and a similar pattern is detected by GC-MS. It seems that the carbons of C2, C3, C4 or C5 are also labeled. However, it is too early to confirm that C2 is labeled. To clearly calculate the labeling pattern of C2, the mass fragment without R-group [f302], see above, is important. However, the corresponding peak was not strong enough and might not be accurate (personal communication, Dr. Y. Tang). Interestingly, the GC-MS data also showed that a 'small fraction' (10 − 20%) of glutamate was labeled with two carbons. If we assume that acetyl-CoA derived from 5 mM [1-^{13}C]acetate and 40 mM unlabeled acetyl-CoA derived from 20 mM crotonate completely mix, we should obtain 11% double labeled glutamate.

Dr. X. Xie (Philipps-Universität Marburg) helped us to evaluate the labeling patterns of aspartate and glutamate derived from $^{13}CO_2$ by NMR. The glutamate showed that not only the expected C5 but also C1 appeared to be labeled. Under the current circumstances, it is not clear whether they are labeled separately or simultaneously.

Recently, the existence of *Re*-citrate synthase has been reported by isotopomer-assisted metabolic analysis from several bacteria. The [1-^{13}C]acetate or ^{13}C-bicarbonate were added in the culture to trace the labeling patterns of metabolites. The glutamate was mainly labeled on C1 (α-carboxyl group) in *Dehalococcides ethenogens* (Tang et al, 2009) and this labeling pattern was consistent with the glutamate in *Thermoanaerobacter* sp. (Feng et al, 2009) and *Desulfovibrio vulgaris* (Tang et al, 2007). Especially, the pattern of glutamate (C1 and C3) in *D. ethenogens* is exactly in accord with the predicted pattern (50/50). It is assumed that glutamate is synthesized via *Re*-citrate synthase on the oxidative branch of TCA cycle in this organism.

2.2.2 The 2-hydroxyglutarate pathway for glutamate biosynthesis

There are three main problems to conclude that the 2-hydroxyglutarate pathway is actively present and involved in glutamate biosynthesis in *S. aciditrophicus*. First, existence of genes involved in the pathway is still disputable. Second, even if the pathway is present, the glutamate derived from unlabeled crotonate should either contain hardly any label or – assuming complete equilibration between acetyl-CoA derived from crotonate or acetate – cannot be distinguished from that via *Re*-citrate synthase. At least, the current results (Fig. 45), which reveal unequal labeling of C1 and C2-C5, do not support the predicted pattern (Scheme 7) by the 2-hydroxyglutarate pathway.

2.2.3 The reductive branch of TCA cycle

Even if there is the reductive cycle and 2-oxoglutarate is derived via it, the predicted labeling pattern (Scheme 8) does not fit to the experimental data. Especially the glutamate should not be labeled at C1. The double labeling of glutamate found with [1-^{13}C]acetate (Dr. Y. Tang, personal communication) also does not support this pathway, but is consistent with that via citrate.

2.2.4 Conclusion

The present study shows that *Re*-citrate synthase probably participates in biosynthesis of glutamate. However, several experimental observations cannot fully explain the concrete and clear biosynthetic pathway in *S. aciditrophicus* yet. To put together the pieces of a puzzle, the labeling position of each carbon should be determined.

3. Benzoate synthesis by energy conserving glutaconyl-CoA decarboxylase in *S. aciditrophicus*

S. aciditrophicus thrives syntrophically on benzoate and axenically on crotonate, which is oxidized to acetate and reduced to cyclohexane carboxylate and some benzoate. Hence, we proposed that the degradation of benzoate is reversible, whereby glutaconyl-CoA serves as a central intermediate. *S. aciditrophicus* contains three genes coding for the energy conserving

glutaconyl-CoA decarboxylase (Gcd) which could catalyse the endergonic carboxylation of crotonyl-CoA driven by an electrochemical Na^+-gradient. For the subsequent reduction of glutaconyl-CoA to glutaryl-CoA by NAD(P)H, a non-decarboxylating glutaryl-CoA dehydrogenase/electron transferring flavoprotein complex (Gdh/Etf) was identified (Djurdjevic, 2010; Wischgoll et al, 2010; Wischgoll et al, 2009). Similar to butyryl-CoA dehydrogenase/Etf from *C. kluyveri* (Li et al, 2008), Gdh/Etf could bifurcate electrons to ferredoxin (Scheme 11). In the reverse direction, the oxidation of reduced ferredoxin should drive the oxidation of glutaryl-CoA to glutaconyl-CoA by $NAD(P)^+$.

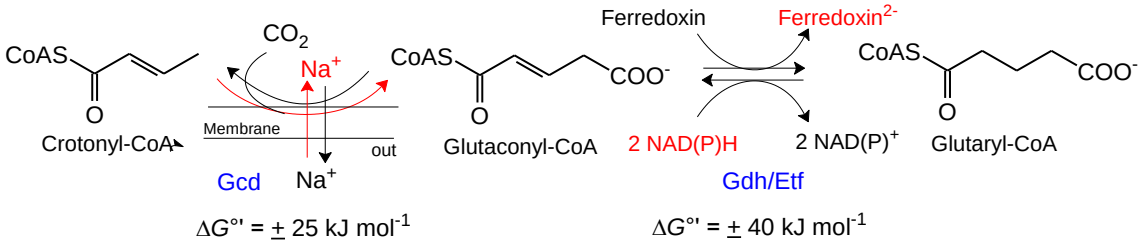

Scheme. 11. Proposed mechanism of the early step of benzoate synthesis in *S. aciditrophicus*. Gcd is glutaconyl-CoA decarboxylase; Gdh/Etf is glutaryl-CoA dehydrogenase/electron transferring flavoprotein.

The location of *gcdA* next to *gdh* (Fig. 33) also supports the behavior of Gcd and Gdh as a chain reaction in the subsequent oxidation of crotonyl-CoA to glutaryl-CoA via glutaconyl-CoA (Scheme 11). The results suggest that the energy limited *S. aciditrophicus* conserves the small energy increment of the exergonic decarboxylation by the membrane-bound, sodium ion-pumping Gcd ($\Delta G°' = -25$ kJ mol^{-1}) (Buckel, 2001a).

The sodium transport decarboxylases have a number of properties in common: (1) integral membrane proteins, (2) specific activation by Na^+ ions, and (3) the prosthetic group biotin. The enzyme bound biotin is a key factor for transferring the carboxyl group of a substrate such as glutaconyl-CoA to the subunit responsible for decarboxylation. The carboxyl transfer is completely independent from the presence of Na^+ ions and is freely reversible as shown by the exchange of substrate and product (Buckel & Liedtke, 1986; Dimroth, 1982; Dimroth & Thomer, 1983). The next step is a Na^+-dependent decarboxylation of the carboxybiotin enzyme intermediate. This apparently makes the overall decarboxylation process irreversible. It is possible that under physiological conditions the decarboxylation is reversible by coupling to Na^+ transport. Dimroth et al. reconstituted the proteoliposomes with oxaloacetate

decarboxylase and methylmalonyl-CoA decarboxylase by mediation of a Na^+ circuit catalyzed the transcarboxylations between oxaloacetate and acetyl-CoA to pyruvate and malonyl-CoA and vice versa (Dimroth & Hilpert, 1984). It is the first report that a Na^+ ion gradient rather than ATP hydrolysis is used in a biological system to overcome energetically unfavorable carboxylation reactions. We speculate that GcdB acts as a reversible catalyst either by creating an electrochemical Na^+ gradient upon decarboxylation or by CO_2 fixation to yield carboxylic acids at the expense of an already existing Na^+ gradient.

Proteomics results (unpublished data, Dr. H. Mouttaki, University of Oklahoma, USA) revealed that GcdA is abundant in crotonate-benzoate grown cells, in which it is not required[1], but was not detected in crotonate grown cells, in which it should be involved in cyclohexane carboxylate formation. GcdC, however, was present in crotonate grown cells. But the separated subunits of Gcd cannot achieve its function. For example, the 5-carboxyl group of glutaconyl-CoA is transferred by GcdA to biotin which is attached to GcdC to form N-carboxybiotin. Therefore, we conclude that Gcd is constitutively expressed both crotonate and crotonate-benzoate grown cells.

The assay of glutaconyl-CoA decarboxylase is based on the reductive carboxylation of the product crotonyl-CoA to ethylmalonyl-CoA which utilizes NADPH (Erb et al, 2007). The Gcd activity was not detected with solubilized membrane proteins from *S. aciditrophicus*. The same assay was then tried with 100,000 × *g* supernatant. But this preparation oxidized NADPH without any other components of the assay. Therefore, it cannot be said that Gcd is active in the cytoplasm. Differentiating methods to prepare the membranes and using a more concentrated membrane fraction did not help to detect the activity. The activity of recombinant GcdA was 2 mU/mg in the presence of 5 mM D-biotin in the assay. This low activity might be due to an insufficient amount of biotin to initiate the reaction so that the full-activity was not measured. For example, GcdA from *A. fermentas* requires at least 40 mM free biotin (Bendrat & Buckel, 1993) and K_m = 2.8 mM with GcdA from *C. symbiosum* (Kress et al, 2009). Even at these high biotin concentration, the specific activity is only 1% of the native complex (Buckel & Liedtke, 1986).

Attempts to crystallize the whole Gcd from *A. fermentans* and *C. symbiosum* failed (Kress et al, 2009; Wendt et al, 2003). The main problem was probably that the instability and

[1] Under these conditions crotonate is oxidized to acetate and benzoate is reduced to cyclohexane carboxylate. Therefore no C5 dicarboxylic acids are formed as intermediates.

aggregation of GcdC impeded its crystallization. Based on the crystal structure of GcdA, two hypothetical models, a symmetric and an asymmetric one were proposed. But the mechanism of transferring Na^+ and CO_2 in Gcd still remains to be elucidated. Gcd of *S. aciditrophicus* was chosen to clarify the structure and sodium translocating mechanism, because GcdC from *S. aciditrophicus* lacks the (A+P) rich domain of other GcdCs, which could interfere with crystallization. In the current study, cloning and overproduction of recombinant Gcd in *E. coli* was tried to achieve sufficient amounts of Gcd for crystallization, because the natural abundance of most membrane proteins is usually too low to isolate enough material for functional and structural studies. Moreover, even under optimal growth conditions, *S. aciditrophicus* grows slowly with low yield. Cloning of the three *gcd* genes was successful and GcdA and GcdAC were overproduced in *E. coli*. However, the expression of *gcdB* and coexpression of *gcdABC* was attempted but without success. The overproduction by using specialized *E. coli* strains did not help to solve the problem. Heterologous overexpression of membrane proteins can be hampered by different synthesis, targeting, insertion and folding characteristics in the host. Therefore, not only the 'trial and error' approaches which are mainly used to produce membrane proteins but also a more systematic approach of membrane protein overproduction should be considered in future.

References

Anstrom DM, Kallio K, Remington SJ (2003) Structure of the *Escherichia coli* malate synthase G:pyruvate:acetyl-coenzyme A abortive ternary complex at 1.95 Å resolution. *Protein Sci* **12:** 1822-1832

Auld DS (1995) [14] Removal and replacement of metal ions in metallopeptidases. In *Methods in Enzymology*, Alan JB (ed), Vol. Volume 248, pp 228-242. Academic Press

Barker H (1939) Studies upon the methane fermentation. IV. The isolation and culture of *Methanobacterium Omelianskii*. *Anton Leeuw* **6:** 201-220

Barker HA (1961) *The Bacteria, Vol 2, Gunsalus Ed. edn*, New York: Academic Press Inc.

Beatrix B, Bendrat K, Rospert S, Buckel W (1990) The biotin-dependent sodium ion pump glutaconyl-CoA decarboxylase from *Fusobacterium nucleatum* (subsp. *nucleatum*). *Arch Microbiol* **154:** 362-369

Bendrat K, Buckel W (1993) Cloning, sequencing and expression of the gene encoding the carboxytransferase subunit of the biotin-dependent Na^+ pump glutaconyl-CoA decarboxylase from *Acidaminococcus fermentans* in *Escherichia coli*. *Eur J Biochem* **211:** 697-702

Bendrat K, Müller U, Klees AG, Buckel W (1993) Identification of the gene encoding the activator of (*R*)-2-hydroxyglutaryl-CoA dehydratase from *Acidaminococcus fermentans* by gene expression in *Escherichia coli*. *FEBS Lett* **329:** 329-331

Bennett BD, Kimball EH, Gao M, Osterhout R, Van Dien SJ, Rabinowitz JD (2009) Absolute metabolite concentrations and implied enzyme active site occupancy in *Escherichia coli*. *Nat Chem Biol* **5:** 593-599

Berger S, Braun S (2004) *200 and More NMR Experiments. A Practical Course*, Weinheim: Wiley-VCH.

Boetius A, Ravenschlag K, Schubert CJ, Rickert D, Widdel F, Gieseke A, Amann R, Jorgensen BB, Witte U, Pfannkuche O (2000) A marine microbial consortium apparently mediating anaerobic oxidation of methane. *Nature* **407:** 623-626

Boiangiu CD, Jayamani E, Brügel D, Herrmann G, Kim J, Forzi L, Hedderich R, Vgenopoulou I, Pierik AJ, Steuber J, Buckel W (2005) Sodium Ion Pumps and Hydrogen Production in Glutamate Fermenting Anaerobic Bacteria. *J Mol Microb Biotech* **10:** 105-119

Bond DR, Mester T, Nesbo CL, Izquierdo-Lopez AV, Collart FL, Lovley DR (2005) Characterization of Citrate Synthase from *Geobacter sulfurreducens* and Evidence for a Family of Citrate Synthases Similar to Those of Eukaryotes throughout the *Geobacteraceae*. *Appl Environ Microbiol* **71:** 3858-3865

Boone DR, Castenholz RW, Garrity GM (2001) *Bergey's manual of systematic bacteriology*, New York: Springer.

Bott M, Pfister K, Burda P, Kalbermatter O, Woehlke G, Dimroth P (1997) Methylmalonyl-CoA Decarboxylase from *Propionigenium Modestum*. *Eur J Biochem* **250:** 590-599

Bradford MM (1976) A rapid and sensitive method for the quantitation of microgram quantities of protein utilizing the principle of protein-dye binding. *Anal Biochem* **72:** 248-254

Braune A, Bendrat K, Rospert S, Buckel W (1999) The sodium ion translocating glutaconyl-CoA decarboxylase from *Acidaminococcus fermentans*: cloning and function of the genes forming a second operon. *Mol Microbiol* **31:** 473-487

Bryant MP, Wolin EA, Wolin MJ, Wolfe RS (1967) *Methanobacillus omelianskii*, a symbiotic association of two species of bacteria. *Arch Microbiol* **59:** 20-31

Buckel W (1980a) Analysis of the fermentation pathways of clostridia using double labelled glutamade. *Arch Microbiol* **127:** 167-169

Buckel W (1980b) The Reversible Dehydration of (*R*)-2-Hydroxyglutarate to (*E*)-Glutaconate. *Eur J Biochem* **106:** 439-447

Buckel W (1986a) [42] Biotin-dependent decarboxylases as bacterial sodium pumps: Purification and reconstitution of glutaconyl-CoA decarboxylase from *Acidaminococcus fermentans*. In *Methods in Enzymology*, Sidney Fleischer BF (ed), Vol. Volume 125, pp 547-558. Academic Press

Buckel W (1986b) Substrate stereochemistry of the biotin-dependent sodium pump glutaconyl-CoA decarboxylase from *Acidaminococcus fermentans*. *Eur J Biochem* **156:** 259-263

Buckel W (2001a) Sodium ion-translocating decarboxylases. *Biochim Biophys Acta* **1505:** 15-27

Buckel W (2001b) Unusual enzymes involved in five pathways of glutamate fermentation. *Appl Microbiol Biotechnol* **57:** 263-273

Buckel W, Barker HA (1974) Two Pathways of Glutamate Fermentation by Anaerobic Bacteria. *J Bacteriol* **117:** 1248-1260

Buckel W, Dorn U, Semmler R (1981) Glutaconate CoA-Transferase from *Acidaminococcus fermentans*. *Eur J Biochem* **118:** 315-321

Buckel W, Eggerer H (1965) On the optical determination of citrate synthase and acetyl-coenzyme A. *Biochem Z* **343:** 29-43

Buckel W, Liedtke H (1986) The sodium pump glutaconyl-CoA decarboxylase from *Acidaminococcus fermentans.* Specific cleavage by n-alkanols. *Eur J Biochem* **156:** 251-257

Buckel W, Semmler R (1982) A biotin-dependent sodium pump: glutaconyl-CoA decarboxylase from *Acidaminococcus fermentans*. *FEBS Lett* **148:** 35-38

Buckel W, Semmler R (1983) Purification, characterisation and reconstitution of glutaconyl-CoA decarboxylase, a biotin-dependent sodium pump from anaerobic bacteria. *Eur J Biochem* **136:** 427-434

Cornforth J (1976) Asymmetry and enzyme action. *Science* **193:** 121-125

Cornforth JW, Redmond JW, Eggerer H, Buckel W, Gutschow C (1969) Asymmetric Methyl Groups: Asymmetric Methyl Groups, and the Mechanism of Malate Synthase. *Nature* **221:** 1212-1213

Crown SB, Indurthi DC, Ahn WS, Choi J, Papoutsakis ET, Antoniewicz MR (2011) Resolving the TCA cycle and pentose-phosphate pathway of *Clostridium acetobutylicum* ATCC 824: Isotopomer analysis, in vitro activities and expression analysis. *Biotechnol J* **6:** 300-305

Dahinden P, Auchli Y, Granjon T, Taralczak M, Wild M, Dimroth P (2005) Oxaloacetate decarboxylase of *Vibrio cholerae*: purification, characterization, and expression of the genes *Escherichia coli*. *Arch Microbiol* **183:** 121-129

de Marco A (2007) Protocol for preparing proteins with improved solubility by co-expressing with molecular chaperones in Escherichia coli. *Nat Protocols* **2:** 2632-2639

Decker K, Jungermann K, Thauer RK (1970) Energy Production in Anaerobic Organisms. *Angew Chem Int Ed Engl* **9:** 138-158

Dimroth P (1980) A new sodium-transport system energized by the decarboxylation of oxaloacetate. *FEBS Lett* **122:** 234-236

Dimroth P (1982) The Generation of an Electrochemical Gradient of Sodium Ions upon Decarboxylation of Oxaloacetate by the Membrane–Bound and Na^+–Activated Oxaloacetate Decarboxylase from *Klebsiella aerogenes*. *Eur J Biochem* **121:** 443-449

Dimroth P, Hilpert W (1984) Carboxylation of pyruvate and acetyl coenzyme A by reversal of the sodium pumps oxaloacetate decarboxylase and methylmalonyl-CoA decarboxylase. *Biochemistry* **23:** 5360-5366

Dimroth P, Thomer A (1983) Subunit composition of oxaloacetate decarboxylase and characterization of the α chain as carboxyltransferase. *Eur J Biochem* **137:** 107-112

Djurdjevic I (2010) Production of glutaconic acid in recombinant *Escherichia coli*. Fachbereich Biologie, Philipps-Universität Marburg, Marburg

Drew D, Slotboom D-J, Friso G, Reda T, Genevaux P, Rapp M, Meindl-Beinker NM, Lambert W, Lerch M, Daley DO, Van Wijk K-J, Hirst J, Kunji E, De Gier J-W (2005) A scalable, GFP-based pipeline for membrane protein overexpression screening and purification. *Protein Sci* **14:** 2011-2017

Drew DE, von Heijne G, Nordlund P, de Gier J-WL (2001) Green fluorescent protein as an indicator to monitor membrane protein overexpression in *Escherichia coli*. *FEBS Lett* **507:** 220-224

Elshahed MS, Bhupathiraju VK, Wofford NQ, Nanny MA, McInerney MJ (2001) Metabolism of Benzoate, Cyclohex-1-ene Carboxylate, and Cyclohexane Carboxylate by "*Syntrophus aciditrophicus*" Strain SB in Syntrophic Association with H_2-Using Microorganisms. *Appl Environ Microbiol* **67:** 1728-1738

Elshahed MS, McInerney MJ (2001) Benzoate Fermentation by the Anaerobic Bacterium *Syntrophus aciditrophicus* in the Absence of Hydrogen-Using Microorganisms. *Appl Environ Microbiol* **67:** 5520-5525

Erb TJ, Berg IA, Brecht V, Müller M, Fuchs G, Alber BE (2007) Synthesis of C5-dicarboxylic acids from C2-units involving crotonyl-CoA carboxylase/reductase: The ethylmalonyl-CoA pathway. *Proc Natl Acad Sci USA* **104:** 10631-10636

Erb TJ, Brecht V, Fuchs G, Müller M, Alber BE (2009) Carboxylation mechanism and stereochemistry of crotonyl-CoA carboxylase/reductase, a carboxylating enoyl-thioester reductase. *Proc Natl Acad Sci USA* **106:** 8871-8876

Evans EA, Slotin L (1940) THE UTILIZATION OF CARBON DIOXIDE IN THE SYNTHESIS OF α-KETOGLUTARIC ACID. *J Biol Chem* **136:** 301-302

Feng X, Mouttaki H, Lin L, Huang R, Wu B, Hemme CL, He Z, Zhang B, Hicks LM, Xu J, Zhou J, Tang YJ (2009) Characterization of the Central Metabolic Pathways in *Thermoanaerobacter* sp. Strain X514 via Isotopomer-Assisted Metabolite Analysis. *Appl Environ Microbiol* **75:** 5001-5008

Ferguson KA (1964) Starch-gel electrophoresis--Application to the classification of pituitary proteins and polypeptides. *Metabolism* **13:** 985-1002

Garrity G (2001) *Bergey's manual of systematic bacteriology, 2nd edition*, Berlin Heidelberg New York: Springer.

Gerike U, Hough DW, Russell NJ, Dyall-Smith ML, Danson MJ (1998) Citrate synthase and 2-methylcitrate synthase: structural, functional and evolutionary relationships. *Microbiology* **144:** 929-935

Goschalk G, Dittbrenner S (1970) Properties of (*R*)-citrate synthase from *Clostridium acici-urici*. *Hoppe-Seyler´s Zeitschrift für physiologische Chemie* **351:** 1183-1190

Gottschalk G (1968) The stereospecificity of the citrate synthase in sulfate-reducing and photosynthetic bacteria. *Eur J Biochem* **5:** 346-351

Gottschalk G (1969) Partial Purification and some Properties of the (*R*)-Citrate Synthase from *Clostridium acidi-urici*. *Eur J Biochem* **7:** 301-306

Gottschalk G, Barker HA (1966) Synthesis of Glutamate and Citrate by *Clostridium kluyveri*. A New Type of Citrate Synthase. *Biochemistry* **5:** 1125-1133

Gottschalk G, Barker HA (1967) Presence and Stereospecificity of Citrate Synthase in Anaerobic Bacteria. *Biochemistry* **6:** 1027-1034

Gottschalk G, Dittbrenner S, Lenz H, Eggerer H (1972) Studies on the *re*-Citrate Synthase Reaction. *Eur J Biochem* **26:** 455-461

Hans M, Buckel W, Bill E (2000) The iron–sulfur clusters in 2-hydroxyglutaryl-CoA dehydratase from *Acidaminococcus fermentans*. *Eur J Biochem* **267:** 7082-7093

Hans M, Sievers J, Müller U, Bill E, Vorholt JA, Linder D, Buckel W (1999) 2-Hydroxyglutaryl-CoA dehydratase from *Clostridium symbiosum*. *Eur J Biochem* **265:** 404-414

Hanson KR, Rose IA (1963) THE ABSOLUTE STEREOCHEMICAL COURSE OF CITRIC ACID BIOSYNTHESIS. *Proc Natl Acad Sci U S A* **50:** 981-988

Härtel U, Eckel E, Koch J, Fuchs G, Linder D, Buckel W (1993) Purification of glutaryl-CoA dehydrogenase from *Pseudomonas* sp., an enzyme involved in the anaerobic degradation of benzoate. *Arch Microbiol* **159:** 174-181

Herrmann G (2008) Enzymes of two clostridial amino-acid fermentation pathways. Fachbereich Biologie, Philipps-Universität Marburg, Marburg

Herrmann G, Jayamani E, Mai G, Buckel W (2008) Energy Conservation via Electron-Transferring Flavoprotein in Anaerobic Bacteria. *J Bacteriol* **190:** 784-791

Hilpert W, Dimroth P (1982) Conversion of the chemical energy of methylmalonyl-CoA decarboxylation into a Na^+gradient. *Nature* **296:** 584-585

Hopkins B, McInerney M, Warikoo V (1995) Evidence for anaerobic syntrophic benzoate degradation threshold and isolation of the syntrophic benzoate degrader. *Appl Environ Microbiol* **61:** 526-530

Huder JB, Dimroth P (1993) Sequence of the sodium ion pump methylmalonyl-CoA decarboxylase from *Veillonella parvula*. *J Biol Chem* **268:** 24564-24571

Hugler M, Wirsen CO, Fuchs G, Taylor CD, Sievert SM (2005) Evidence for Autotrophic CO_2 Fixation via the Reductive Tricarboxylic Acid Cycle by Members of the epsilon Subdivision of Proteobacteria. *J Bacteriol* **187:** 3020-3027

Huynen MA, Dandekar T, Bork P (1999) Variation and evolution of the citric-acid cycle: a genomic perspective. *Trends Microbiol* **7:** 281-291

Hwang TL, Shaka AJ (1995) Water Suppression That Works. Excitation Sculpting Using Arbitrary Wave-Forms and Pulsed-Field Gradients. *J Magn Reson* **112:** 275-279

Jackins HC, Barker HA (1951) FERMENTATIVE PROCESSES OF THE FUSIFORM BACTERIA. *J Bacteriol* **61:** 101-114

Jackson BE, Bhupathiraju VK, Tanner RS, Woese CR, McInerney MJ (1999) *Syntrophus aciditrophicus* sp. nov., a new anaerobic bacterium that degrades fatty acids and benzoate in syntrophic association with hydrogen-using microorganisms. *Arch Microbiol* **171:** 107-114

Jacob U, Mack M, Clausen T, Huber R, Buckel W, Messerschmidt A (1997) Glutaconate CoA-transferase from *Acidaminococcus fermentans*: the crystal structure reveals homology with other CoA-transferases. *Structure* **5:** 415-426

Joseph RE, Andreotti AH (2008) Bacterial expression and purification of Interleukin-2 Tyrosine kinase: Single step separation of the chaperonin impurity. *Protein Expr Purif* **60:** 194-197

Jungermann K, Thauer RK, Wenning J, Decker K (1968) Confirmation of unusual stereochemistry of glutamate biosynthesis in *Clostridium kluyveri*. *FEBS Lett* **1:** 74-76

Kalinowski H, Berger S, Braun S (1984) *13C-NMR-Spektroskopie*, Stuttgart: Thieme.

Kim J, Darley DJ, Buckel W, Pierik AJ (2008) An allylic ketyl radical intermediate in clostridial amino-acid fermentation. *Nature* **452:** 239-242

Koon N, Squire CJ, Baker EN (2004) Crystal structure of LeuA from *Mycobacterium tuberculosis*, a key enzyme in leucine biosynthesis. *Proc Natl Acad Sci USA* **101:** 8295-8300

Kosicki GW, Srere PA (1961) Deuterium isotope rate effects with citrate-condensing enzyme. *J Biol Chem* **236:** 2566-2570

Krebs HA, Johnson WA (1980) The role of citric acid in intermediate metabolism in animal tissues. *FEBS Lett* **117:** K2-K10

Kress D, Brügel D, Schall I, Linder D, Buckel W, Essen L-O (2009) An Asymmetric Model for Na^+-translocating Glutaconyl-CoA Decarboxylases. *J Biol Chem* **284:** 28401-28409

Kuntze K, Shinoda Y, Moutakki H, McInerney MJ, Vogt C, Richnow H-H, Boll M (2008) 6-Oxocyclohex-1-ene-1-carbonyl-coenzyme A hydrolases from obligately anaerobic bacteria: characterization and identification of its gene as a functional marker for aromatic compounds degrading anaerobes. *Environ Microbiol* **10:** 1547-1556

Kurz LC, Constantine CZ, Jiang H, Kappock TJ (2009) The Partial Substrate Dethiaacetyl-Coenzyme A Mimics All Critical Carbon Acid Reactions in the Condensation Half-Reaction Catalyzed by *Thermoplasma acidophilum* Citrate Synthase. *Biochemistry* **48:** 7878-7891

Lengeler JW, Drews G, Schlegel HG (1999) *Biology of the prokaryotes*: Thieme/Blackwell.

Li F, Hagemeier CH, Seedorf H, Gottschalk G, Thauer RK (2007) *Re*-Citrate Synthase from *Clostridium kluyveri* Is Phylogenetically Related to Homocitrate Synthase and Isopropylmalate Synthase Rather Than to *Si*-Citrate Synthase. *J Bacteriol* **189:** 4299-4304

Li F, Hinderberger J, Seedorf H, Zhang J, Buckel W, Thauer RK (2008) Coupled Ferredoxin and Crotonyl Coenzyme A (CoA) Reduction with NADH Catalyzed by the Butyryl-CoA Dehydrogenase/Etf Complex from *Clostridium kluyveri*. *J Bacteriol* **190:** 843-850

Mack M, Bendrat K, Zelder O, Eckel E, Linder D, Buckel W (1994) Location of the Two Genes Encoding Glutaconate Coenzyme A-Transferase at the Beginning of the Hydroxyglutarate Operon in *Acidaminococcus fermentans*. *Eur J Biochem* **226:** 41-51

Man WJ, Y Li CDOC, Wilton DC (1994) The effect of replacing the conserved active-site residues His-264, Asp-312 and Arg-314 on the binding and catalytic properties of *Escherichia coli* citrate synthase. *Biochem J* **300:** 765-770

Martins BM, Macedo-Ribeiro S, Bresser J, Buckel W, Messerschmidt A (2005) Structural basis for stereo-specific catalysis in NAD^+-dependent (*R*)-2-hydroxyglutarate dehydrogenase from *Acidaminococcus fermentans*. *FEBS J* **272:** 269-281

McInerney MJ, Rohlin L, Mouttaki H, Kim U, Krupp RS, Rios-Hernandez L, Sieber J, Struchtemeyer CG, Bhattacharyya A, Campbell JW, Gunsalus RP (2007) The genome of *Syntrophus aciditrophicus*: Life at the thermodynamic limit of microbial growth. *Proc Natl Acad Sci USA* **104:** 7600-7605

McInerney MJ, Struchtemeyer CG, Sieber J, Mouttaki H, Stams AJM, Schink B, Rohlin L, Gunsalus RP (2008) Physiology, Ecology, Phylogeny, and Genomics of Microorganisms Capable of Syntrophic Metabolism. *Ann N Y Acad Sci* **1125:** 58-72

Miles JS, Guest JR, Radford SE, Perham RN (1987) A mutant pyruvate dehydrogenase complex of *Escherichia coli* deleted in the (alanine + proline)-rich region of the acetyltransferase component. *Biochim Biophys Acta* **913:** 117-121

Miroux B, Walker JE (1996) Over-production of Proteins in *Escherichia coli*: Mutant Hosts that Allow Synthesis of some Membrane Proteins and Globular Proteins at High Levels. *J Mol Biol* **260:** 289-298

Moore JT, Uppal A, Maley F, Maley GF (1993) Overcoming Inclusion Body Formation in a High-Level Expression System. *Protein Expr Purif* **4:** 160-163

Mouttaki H, Nanny MA, McInerney MJ (2007) Cyclohexane Carboxylate and Benzoate Formation from Crotonate in *Syntrophus aciditrophicus*. *Appl Environ Microbiol* **73:** 930-938

Mouttaki H, Nanny MA, McInerney MJ (2008) Use of benzoate as an electron acceptor by *Syntrophus aciditrophicus* grown in pure culture with crotonate. *Environ Microbiol* **10:** 3265-3274

Müller U, Buckel W (1995) Activation of (*R*)-2-hydroxyglutaryl-CoA Dehydratase from *Acidaminococcus fermentans*. *Eur J Biochem* **230:** 698-704

Ogston AG (1948) Interpretation of Experiments on Metabolic processes, using Isotopic Tracer Elements. *Nature* **162:** 962-963

Peters F, Shinoda Y, McInerney MJ, Boll M (2007) Cyclohexa-1,5-Diene-1-Carbonyl-Coenzyme A (CoA) Hydratases of *Geobacter metallireducens* and *Syntrophus aciditrophicus*: Evidence for a Common Benzoyl-CoA Degradation Pathway in Facultative and Strict Anaerobes. *J Bacteriol* **189:** 1055-1060

Petterson G, Lill U, Eggerer H (1989) Mechanism of interaction of citrate synthase with citryl-CoA. *Eur J Biochem* **182:** 119-124

Peyraud R, Kiefer P, Christen P, Massou S, Portais J-C, Vorholt JA (2009) Demonstration of the ethylmalonyl-CoA pathway by using ^{13}C metabolomics. *Proc Natl Acad Sci USA* **106:** 4846-4851

Riddles PW, Blakeley RL, Zerner B (1983) Reassessment of Ellman's reagent. *Methods Enzymol* **91:** 49-60

Rose IA, O'Connell EL (1967) Mechanism of Aconitase Action. *J Biol Chem* **242:** 1870-1879

Schaarschmidt J, Wischgoll S, Hofmann H-J, Boll M (2011) Conversion of a decarboxylating to a non-decarboxylating glutaryl-coenzyme A dehydrogenase by site-directed mutagenesis. *FEBS Lett* **In Press, Corrected Proof**

Schweiger G, Dutscho R, Buckel W (1987) Purification of 2-hydroxyglutaryl-CoA dehydratase from *Acidaminococcus fermentans*. *Eur J Biochem* **169:** 441-448

Scott I, Roessner C, Santander P (1999) *B_{12} biosynthesis: the anaerobic pathway. In: Banerjee R (ed) Chemistry and biochemistry of B_{12},* New York: Wiley.

Simon EJ, Shemin D (1953) The Preparation of S-Succinyl Coenzyme A. *J Am Chem Soc* **75:** 2520-2520

Smith DM, Buckel W, Zipse H (2003) Deprotonation of Enoxy Radicals: Theoretical Validation of a 50-Year-Old Mechanistic Proposal. *Angew Chem Int Ed Engl* **42:** 1867-1870

Smith PK, Krohn RI, Hermanson GT, Mallia AK, Gartner FH, Provenzano MD, Fujimoto EK, Goeke NM, Olson BJ, Klenk DC (1985) Measurement of protein using bicinchoninic acid. *Anal Biochem* **150:** 76-85

Srere PA, Kosicki GW (1961) The Purification of Citrate-condensing Enzyme. *J Biol Chem* **236:** 2557-2559

Tang K-H, Feng X, Zhuang W-Q, Alvarez-Cohen L, Blankenship RE, Tang YJ (2010) Carbon Flow of Heliobacteria Is Related More to Clostridia than to the Green Sulfur Bacteria. *J Biol Chem* **285:** 35104-35112

Tang Y, Pingitore F, Mukhopadhyay A, Phan R, Hazen TC, Keasling JD (2007) Pathway Confirmation and Flux Analysis of Central Metabolic Pathways in *Desulfovibrio vulgaris* Hildenborough using Gas Chromatography-Mass Spectrometry and Fourier Transform-Ion Cyclotron Resonance Mass Spectrometry. *J Bacteriol* **189:** 940-949

Tang YJ, Yi S, Zhuang W-Q, Zinder SH, Keasling JD, Alvarez-Cohen L (2009) Investigation of Carbon Metabolism in "*Dehalococcoides ethenogenes*" Strain 195 by Use of Isotopomer and Transcriptomic Analyses. *J Bacteriol* **191:** 5224-5231

Texter FL, Radford SE, Laue ED, Perham RN, Miles JS, Guest JR (1988) Site-directed mutagenesis and proton NMR spectroscopy of an interdomain segment in the pyruvate dehydrogenase multienzyme complex of *Escherichia coli*. *Biochemistry* **27:** 289-296

Thauer RK (1988) Citric-acid cycle, 50 years on. *Eur J Biochem* **176:** 497-508

Thauer RK, Jungermann K, Decker K (1977) Energy conservation in chemotrophic anaerobic bacteria. *Microbiol Mol Biol Rev* **41:** 100-180

Wagner S, Bader ML, Drew D, de Gier J-W (2006) Rationalizing membrane protein overexpression. *Trends Biotechnol* **24:** 364-371

Wagner S, Klepsch MM, Schlegel S, Appel A, Draheim R, Tarry M, Högbom M, van Wijk KJ, Slotboom DJ, Persson JO, de Gier J-W (2008) Tuning *Escherichia coli for* membrane protein overexpression. *Proc Natl Acad Sci USA* **105:** 14371-14376

Wendt KS, Schall I, Huber R, Buckel W, Jacob U (2003) Crystal structure of the carboxyltransferase subunit of the bacterial sodium ion pump glutaconyl-coenzyme A decarboxylase. *EMBO J* **22:** 3493-3502

Wiegand G, Remington SJ (1986) Citrate Synthase: Structure, Control, and Mechanism. *Annu Rev Biophys Biophys Chem* **15:** 97-117

Wifling K, Dimroth P (1989) Isolation and characterization of oxaloacetate decarboxylase of *Salmonella typhimurium*, a sodium ion pump. *Arch Microbiol* **152:** 584-588

Wilson K (2001) *Preparation of Genomic DNA from Bacteria*: John Wiley & Sons, Inc.

Wischgoll S, Demmer U, Warkentin E, Günther R, Boll M, Ermler U (2010) Structural Basis for Promoting and Preventing Decarboxylation in Glutaryl-Coenzyme A Dehydrogenases. *Biochemistry* **49:** 5350-5357

Wischgoll S, Heintz D, Peters F, Erxleben A, Sarnighausen E, Reski R, Van Dorsselaer A, Boll M (2005) Gene clusters involved in anaerobic benzoate degradation of *Geobacter metallireducens*. *Mol Microbiol* **58:** 1238-1252

Wischgoll S, Taubert M, Peters F, Jehmlich N, von Bergen M, Boll M (2009) Decarboxylating and Nondecarboxylating Glutaryl-Coenzyme A Dehydrogenases in the Aromatic Metabolism of Obligately Anaerobic Bacteria. *J Bacteriol* **191:** 4401-4409

Wunderwald P, Buckel W, Lenz H, Buschmeier V, Eggerer H, Gottschalk G, Cornforth JW, Redmond JW, Mallaby R (1971) Stereochemistry of the *re*-Citrate-Synthase Reaction. *Eur J Biochem* **24:** 216-221

Wüthrich K (1986) *NMR of Proteins and Nucleic Acids*, New York: Wiley-VCH.

Zhi W, Srere PA, Evans CT (1991) Conformational stability of pig citrate synthase and some active-site mutants. *Biochemistry* **30:** 9281-9286

Acknowledgements

Above all things, I would like to thank Prof. Wolfgang Buckel for the opportunity to work in his group and for the very interesting research projects. His inspirational ideas, generous support, and encouragement became the reliable cornerstone for me throughout my study period. I also thank Frau Buckel for her warm-hearted kindness.

I appreciate my collaborators from University of Oklahoma, Prof. Michael J. McInerney for providing the *S. aciditrophicus* strain as a kind gift and for his helpful suggestions about glutamate biosynthetic pathway; Jessica Sieber for teaching me handling *S. aciditrophicus* and for preliminary tests of Rnf, glutaconyl-CoA decarboxylase, and glutaconyl-CoA dehydrogenase; Dr. Housna Mouttaki for proteomics; Huynh Le for preparation of *S. aciditrophicus* cells grown on crotonate with [1-^{13}C]acetate for analysis by GC-MS.

Many thanks to:

Prof. Yinjie Tang from Washington University for analysis of ^{13}C-labeled metabolites from *S. aciditrophicus* by GC-MS and his fruitful comments.

Prof. Matthias Boll and Kevin Kuntze from Universität Leipzig for large-scale fermentation of *S. aciditrophicus*.

Prof. Albrecht Messerschmidt and Milko Velarde from MPI Martinsried for attempts on crystallization of *Re*-citrate synthase.

Dr. Seigo Shima and Dr. Haruka Tamura from MPI Marburg for allowing me to use their facilities for crystallization.

Dr. Xiulan Xie for her patient guidance and analysis of NMR data.

Dr. Peter Friedrich for his great helps in chemistry work, especially studies on stereochemistry.

Jörg Kahnt from MPI Marburg for measuring the MALDI-TOF spectra and the Nano-LC-MS.

Iris Schall for purification of auxiliary enzyme pool and glutaconyl-CoA decarboxylase from *Acidaminococcus fermentans*.

I am indebted to all present and past lab members for their helps and friendships, which leaded to cheerful atmosphere and made my stay and work very pleasant.

I am grateful to Patricia Wagner, Jutta Seip, and Susanne Rommel for wholehearted and administrative helps.

I appreciate Deutscher Akademischer Austausch Dienst (DAAD) and Deutsche Forschungsgemeinschaft (DFG) as well as MPI for funding.

I would like to thank my family and friends for their LOVE and support throughout my studies.

Curriculum vitae

Personal data

Name, Vorname:	Kim, Marie
Geburtsdatum:	17. 06. 1983
Geburtsort:	Daegu, South Korea
Nationalität:	South Korea

Education

1999.03 – 2002.02	Daegu Hyehwa Girls' High School
2002.03 – 2005.02	B.Sc. in Life Science and Biotechnology, Kyungpook National University, Korea
2005.03 – 2007.08	M.Sc. in Microbiology, Kyungpook National University, Korea
2007.09 –	PhD candidate, Philipps-Universität Marburg, Germany
2008.10 –	Association student, International Max Planck Research School (IMPRS) for Environmental, cellular and Molecular Microbiology
2009.01 – 2011.03	Deutscher Akademischer Austausch Dienst (DAAD) scholarship

Erklärung

Ich versichere, dass ich meine Dissertation

Exploring the biosynthetic pathways of

glutamate and benzoate in *Syntrophus aciditrophicus*

selbstständig, ohne unerlaubte Hilfe angefertigt und mich dabei keiner anderen als der von mir ausdrücklich bezeichneten Quellen und Hilfen bedient habe.

Die Dissertation wurde in der jetzigen oder einer ähnlichen Form noch bei keiner anderen Hochschule eingereicht und hat noch keinen sonstigen Prüfungszwecken gedient.

_____ _____

(Ort/Datum) (Unterschrift mit Vor- und Zuname)